TAMPEREEN TEKNILLINEN YLIOPISTO
TAMPERE UNIVERSITY OF TECHNOLOGY

DTU Technical University of Denmark

NUR-E-HABIBA
Student ID # 245194

DEVELOPMENT OF PH-SENSITIVE AND ADJUVANT-BASED POLYMER LIDS FOR MICROCONTAINERS LEADING TO TARGETED DELIVERY OF ORAL VACCINES

Master of Science Thesis

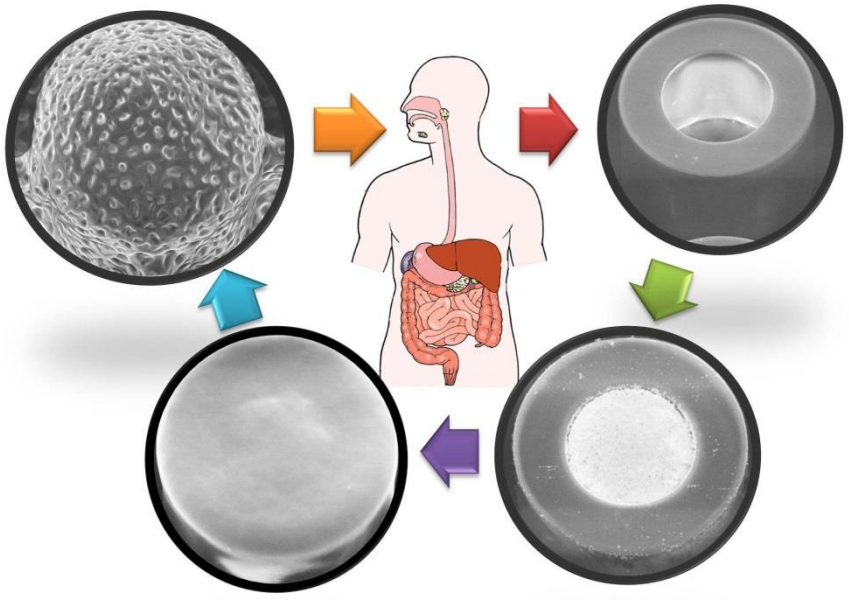

Examiner: Prof. Matti Karp
Department of Chemistry and Bioengineering,
Tampere University of Technology, Finland

Supervisors: Prof. Anja Boisen and Post-Doc. Line Hagner Nielsen
Department of Micro- and Nanotechnology,
Technical University of Denmark, Denmark

Submission Date: 02nd March, 2017

ABSTRACT

NUR-E-HABIBA: Development of pH-Sensitive and Adjuvant-Based Polymer Lids for Microcontainers Leading to Targeted Delivery of Oral Vaccines
TAMPERE UNIVERSITY OF TECHNOLOGY
Masters of Science Thesis, 99 pages, 9 appendix pages
March 02, 2017
Master's Degree Program in Bioengineering
Department of Chemistry and Bioengineering
Major Subject: Bioengineering
Examiner: Professor Matti Karp

Keywords: Oral Vaccination, Drug Delivery, Polymer Lid, Microcontainer, Spray Coating

Oral vaccination, one of the prominent ongoing research areas of drug delivery and immunology, requires effective targeted drug delivery method as well as triggered immune responses. In this thesis project, polymeric microcontainers (MCs) formed on silicon substrate were used as drug carriers. The focus of the thesis was on the development and optimization of pH-sensitive and adjuvant-based polymer lids on the drug-loaded MCs in order to facilitate the drug release at the desired area (small intestine) and to trigger immune response. In this study, the development of double-layered lids on top of the MCs was achieved by establishing a pH-sensitive outer lid made of Eudragit L100-55 polymer and an inner lid made of chitosan polymer incorporated with an adjuvant - MPLA (mono phosphoryl lipid A). The chitosan-MPLA lid is a novel polymeric lid which has not been in any literature yet for targeted oral drug delivery studies. The purpose of the outer lid was to protect the inner lid from dissolving in a gastric pH value (e.g. at pH 3.5); whereas, the adjuvant-based inner lid was needed to facilitate the drug release from the MCs in the small intestinal pH value (e.g. at pH 6.0) followed by triggering immune response.

The model drug used in these studies was amorphous sodium salt of furosemide (ASSF), prepared in a spray dryer followed by loading the drug into the MCs using an embossing method. Next, different polymer solutions were spray-coated on the drug-loaded MCs to form single or double layer lids. To determine the most optimized lid formation, detailed lid morphology was analyzed using scanning electron microscope (SEM) and stylus profiler. The results show that both the inner and outer lids were homogenously formed where the inner lid had very smooth surface with an average thickness of 6.2 +/- 0.3 µm and the outer lid had porous texture with an average thickness of 31.4 +/- 2.8 µm. To investigate the pH-sensitivity of the lids, *in vitro* drug release experiments were performed in buffer media with different pH values (pH of rat's gastric and intestinal media) using a micro dissolution apparatus. Finally, x-ray photoelectron spectroscopy (XPS) analysis was performed to detect the presence of MPLA in the inner lid.

Both the release studies and lid morphology analysis exhibit that the optimized double-lids remains intact with a negligible drug release percentage at a pH value corresponding to the stomach, whereas it degrades and releases above 84% of the model drug in the medium corresponding to an intestinal pH value. Thus, the pH-sensitive and adjuvant-based double-lids development demonstrates the future potential to be used for different vaccine formulations in targeted oral drug delivery in *in vivo* and animal studies.

PREFACE

This master's thesis project in bioengineering was carried out in the IDUN (Intelligent Drug Delivery and Sensing Using Microcontainers and Nanomechanics) research center at the Department of Micro- and Nanotechnology (DTU Nanotech), Technical University of Denmark (DTU), Copenhagen, Denmark. The thesis topic and the examiner were approved in the Faculty of Natural Sciences at Tampere University of Technology (TUT) on September 07, 2016. The duration of this thesis project was five and half months, fulltime laboratory based research work.

First and foremost, I am very much grateful to the most merciful God (Allah) for giving the opportunity and intelligence for conducting this project work. I owe many thanks to the head of my Degree Program and the Professor of my home university, Matti Karp for his approval on conducting my thesis project in Denmark. I express my sincere gratitude to my practical supervisor Line Hagner Nielsen, a Post-Doctoral researcher at DTU Nanotech for her guidance, supervision and encouragement throughout the project. I also thank Professor Anja Boisen of DTU Nanotech who gave me the opportunity to join her highly motivated and international research team. I am grateful to my colleagues who have been cooperating with me in the laboratories and sharing their knowledge. This auspicious opportunity of the master's thesis project has allowed me to connect with other researchers within and outside the group.

Lastly, I am indebted to my family for their prayers, inspiration and emotional supports for my success.

Copenhagen, Denmark
March 02, 2017
Nur-E-Habiba

CONTENTS

ABBREVIATIONS AND DEFINITIONS

µDiss	Micro Dissolution
AA	Acetic Acid
ASSF	Amorphous sodium salt of furosemide
Avg	Average
BCS	Biopharmaceutical classification system
Chi	Chitosan
CNTR	Counter number of passes
DBS	Di butyl sebacate
DC	Dendritic cells
EHT	Extra high tension
EL	Eudragit L
GI	Gastro intestinal
HCL	Hydrochloric acid
HP	High pressure
IDR	Intrinsic dissolution rate
IgA	Immunoglobulin A
IgG	Immunoglobulin G
IPA	Isopropyl alcohol
KH_2PO_4	Potassium phosphate monobasic
LC-MS	Liquid chromatography-mass spectrometry
LMW	Low molecular weight
LPS	Lipopolysachharide
Mag	Magnification
MC	Microcontainer
M-cells	Microfold cells
MiliQ water	Ultrapure water
MPLA	Mono phosphoryl lipid A
NaOH	Sodium hydro oxide
PBS	Phosphate buffered saline
PEG	Polyethylene glycol
PLGA	Poly (D,L-lactide-co-glycolide)
SD	Standard deviation
SE2	In chamber secondary electron
SEM	Supra scanning electron microscope
Si	Silicon
SU-8	A negative photoresist containing 8-epoxy groups
TEC	Tri ethyl citrate
VP	Variable pressure
VPSE	Variable pressure secondary electron
w/v	Weight in relation to total volume
w/w	Weight in relation to total weight
WD	Working distance
XPS	X-ray electron spectroscopy

1. INTRODUCTION

This chapter briefly introduces the thesis project and its significance. It also presents the project overview, objectives and the scopes of the thesis.

1.1 Vaccination and its Significance

Vaccines often consist of biological material (e.g. virus, or bacteria) (1) stimulating the immune system to produce adaptive immunity towards certain infections or pathogens (2,3). A vaccine formulation typically consists of an antigen and an adjuvant, but sometimes it has additional preservatives, stabilizers or antibiotics added to its composition to protect the formulation from either bacterial contamination, or from losing its effectiveness during storage (4). Vaccination is the most effective and widely used methods of preventing infectious diseases worldwide. Its significant contribution to public health and disease prevention has made it an enormous focus of study (3).

There are different types of vaccines such as inactive vaccine, attenuated vaccine, virus-like particle vaccine and subunit vaccine (5). In addition, the DNA vaccines and dendritic cell-based vaccines are emerging new generation of vaccines (6). The vaccine formulation can be administered in various routes, such as oral, injection, transdermal or intranasal. (5). However, most vaccines are injected into the body, but it would be easier and more beneficial if the vaccine formulation could be made suitable for oral administration.

Oral vaccination is a non-invasive drug administration and has several advantages (7). Delivering drugs by the oral routes is in general cost-effective, easy to administer and does not require any skilled person for administration. Nevertheless, there are several challenges in oral administration of vaccines; for example, the low pH and the presence of degradation enzymes in the stomach often destroy the antigen and inactivate the vaccine formulation. As a result, the antigen cannot generate immune response when it reaches the small intestinal tract at its target area (8).

1.2 Project Overview

For protecting the oral vaccines from degrading in the gastric medium, one of the solutions is to modify the actual drug formulation in such a way that it can survive the extreme gastric environment (9). Another possible solution can be to encapsulate the formulated vaccines into micro-fabricated drug delivery devices or microcontainers that are made of biocompatible and biodegradable polymeric materials (10,11) which would be capable of targeted drug release (7,12). The IDUN Drug research group at DTU Nanotech is working on a project for developing microcontainers as an oral drug delivery system for vaccines (13), The research group has already developed particulates intended for oral vaccine delivery, and now is trying to come up with potential approaches to ensure the effectiveness of targeted oral drug delivery using the microcontainers. The microcontainers aim to protect the vaccine formulation through the gastric medium or stomach, and then release the formulation into the small intestine near the M-cells (micro-fold cells). Therefore, the microcontainers require suitable lid coated over them with desired properties (e.g. pH sensitivity and drug release capacity) to ensure targeted drug delivery to specific cells along the intestinal lining. The thesis is a part of this project to develop polymeric lids on microcontainers.

1.3 Aim of the Thesis

This thesis project is aimed to develop double-layered polymeric lids on microcontainers (MCs) containing specific drug formulation. The inner layer consisted of chitosan incorporated with an adjuvant – MPLA (Monophosphoryl Lipid A) for pre-activation of the immune cells. The outer layer consisted of a pH sensitive polymer, Eudragit L100-55 to provide protection to the inner lid as well as the drug from degrading in the gastric medium. In addition, the outer lid contained such properties that it would get dissolved inside the small intestine while making the inner lid exposed. On the other hand, the purpose of the inner polymeric lid was to carry the incorporated adjuvant to the small intestinal immune cells and let the drug to be released at the targeted site. The objective of incorporating the adjuvant was to provide a targeted drug delivery to the small intestinal immune cells by triggering the specific cells. Fig. 1.1 illustrates the placement of the double lids on the microcontainers loaded with vaccine formulation, and Fig. 1.2 summaries the steps towards polymeric double-lids development.

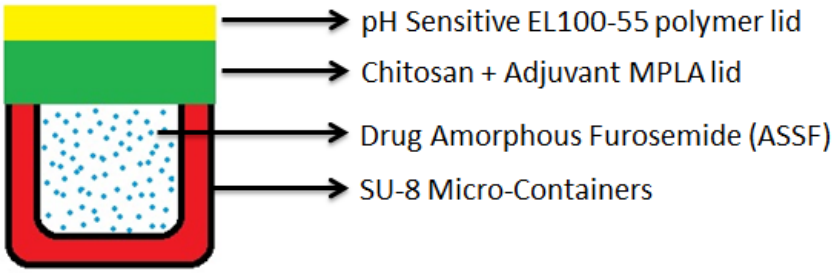

Fig. 1.1: *Placement of the polymeric double lids on top of the drug-loaded MC*

Fig. 1.2: *Major steps of developing pH-sensitive and adjuvant-based polymeric double-lids*

List of the thesis objectives:

The objectives of the study are listed below:

i. Successfully loading the model drug (ASSF) into the MCs
ii. Development of MPLA-chitosan lid
iii. Development of Eudragit L100-55 lid
iv. Studying the lid morphology
v. Investigating the pH sensitivity of the lids by *in vitro* drug release study in different pH media
vi. Optimization of the double-lids development

1.4 Scope of the Thesis

The entire thesis report can be divided into three main parts where, 1) Theory, 2) Laboratory experiments and 3) Future implications. The report is organized as below.

Chapter 1 of the report introduces the subject matters, gives an overview of the project and states the project objectives. Chapter 2 discusses the thesis background and commonly used terms, while the Chapter 3 of this report explains the techniques used in this study; for example, scanning electron microscope imaging, x-ray photoelectron spectroscopy and micro dissolution profiling. In Chapter 4, the methodologies of different experiments performed during this study are illustrated. The methodology starts with ASSF drug formulation and loading it into microcontainers. Following the drug loading process, a polymer solution (chitosan) incorporated with an adjuvant (e.g. MPLA) was spray coated on the loaded microcontainers, which were then further spray coated with a pH sensitive polymer (Eudragit) to form a pH sensitive and adjuvant based double-layered lid. After forming the polymeric double lids, *in vitro* drug release tests were performed to test the behavior of the lids in gastric medium and small intestine medium. However, there were some limitations to some of the experiments which are described in this chapter.

In Chapter 5, the results of the drug release test, the lid thickness measurement using stylus profiler and the lid morphology analysis using SEM are discussed in detail. This chapter also includes the MPLA detection results from x-ray photoelectron spectroscopy (XPS). However, due to the limit of detection of the XPS, the small amount of MPLA incorporated into chitosan lid could not be detected. Therefore, for future studies other detection methods such as liquid chromatography-mass spectrometry (LC-MS) could be used for MPLA detection if convenient. Lastly, the report concludes with some future implications and potentials of this project in Chapter 6. The successful development of the double-lids from this *in vitro* study needs further investigation in cell study and in animal studies as the next step of the thesis project.

2. BACKGROUND

This chapter discusses the basic aspects of oral drug delivery, important components of vaccine, and the chemical and mechanical properties of different polymers, plasticizers and the model drug.

2.1 Oral Administration of Vaccines

Oral administration of vaccines involves immunization through a mucosal route (14). Since pathogenic infiltrations from the mucosal tract are responsible for most of the infectious diseases, therefore, when vaccines are delivered to the tissues of this tract, they can actually mimic natural infections. Hence, vaccination to the mucosal tissues can provide protection during the very initial infection attack and that is why oral delivery of vaccines has become the most preferable route of administration (15). Nevertheless, depending on the location of the mucosal tissues, the mucosal surfaces are exposed to different environments such as gastric environment and mucus barrier that pose challenges towards oral vaccine formulations (7). Some of the challenges to overcome are the extremely low pH condition in stomach, the presence of proteolytic enzymes and bile salts and the low permeability of the drug in the intestinal cells (15). Nevertheless, comparing with the injectable vaccines, the oral vaccines are more promising and more efficient. Studies have shown that injectable vaccines produce insufficient specific mucosal immune responses and are therefore ineffective in preventing infections at the sites of mucosal entry. On the contrary, both the antigenic specific systemic antibodies (IgG) in blood and mucosal antigen specific antibodies (IgA) can be produced by oral vaccines. In addition, oral vaccines are proven to be effective for both the aged and young M-cells (15).

2.2 Antigen

Antigens are molecules that can induce immune response in the host organisms by binding to the product of the immune response (16); however, some antigens are themselves the parts of the host organisms. Antigens can be any substrates from the environment including chemicals, pollens, virus and bacteria, that enter the body, or are already parts of the body, and they trigger the immune system to produce antibodies against the anti-

gens (17). Therefore, each antibody is antigen specific so that the antigen binding site of the antibody can be bound with the specific antigen (Fig. 2.1) (18,19).

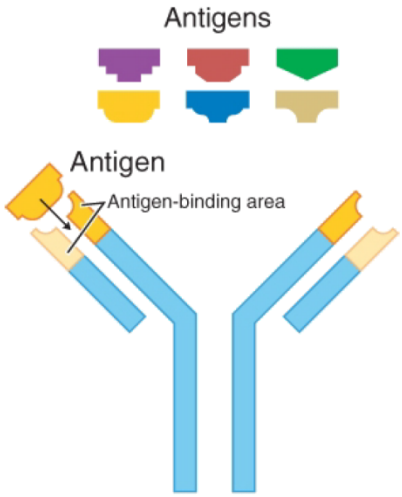

Fig. 2.1: *Interactions between antigen and antibody at the antigen binding site* (18)

2.3 Adjuvant

Adjuvants are immunostimulants or immune-potentiators widely used in protein vaccines in order to improve the humoral, cellular and mucosal immune responses. Adjuvants help minimizing the amount of foreign materials of vaccines (e.g. virus, or bacteria), by enhancing the immune response to produce higher amount of antibodies and to provide longer lasting protection (20–22).

Adjuvants can also modify the immune response in such a way that it would extend the presence of antigens in blood. Furthermore, adjuvants can act as stabilizing agents to absorb the antigen presenting cells, to activate macrophages and lymphocytes, and to provide support to cytokines production (4).

2.4 MPLA

Monophosphoryl lipid A (MPLA), is a synthetic adjuvant derived from lipopolysachharide (LPS) (23) and it has been proven very effective in terms of inducing Th-1 type immune responses to heterologous proteins in both human and animal vaccines. The molecular formula of MPLA is $C_{96}H_{184}N_3O_{22}P$ and its molecular weight is

1763.469 g/mol (24,25). The suggested storage temperature for MPLA is -20ºC (24). The chemical structure of MPLA is presented in Fig. 2.2.

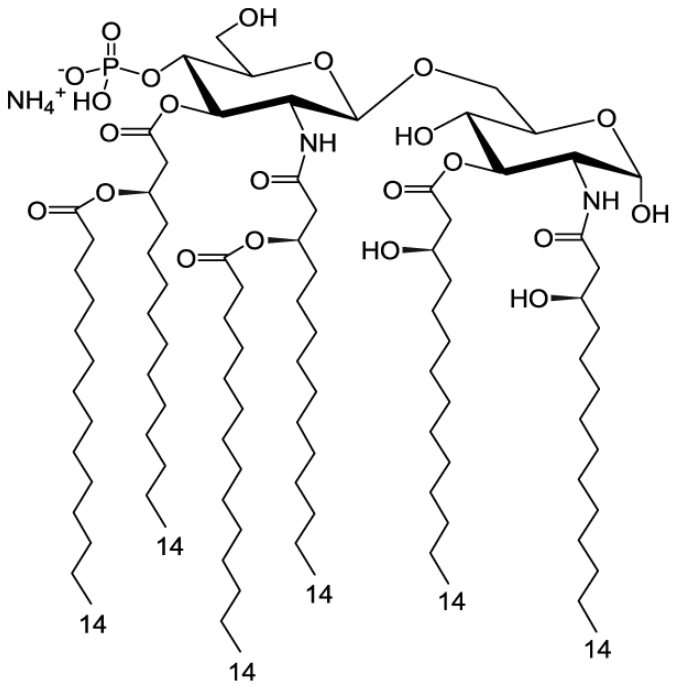

Fig. 2.2: *Chemical structure of the adjuvant, MPLA* (Adapted from (24))

Studies have addressed MPLA as one of the most promising adjuvants for animal and human vaccines (26–30) and it has already been approved for the Hepatitis B vaccine in Europe (26,27). Also, it has been used for anti-cancer vaccine research in the USA (28). In addition to that, orally administrated nanoparticles, such as poly(D,L-lactide-co-glycolide) or PLGA, with incorporated adjuvant MPLA (31) and model antigen OVA (ovalbumin) have shown potentials in both systematic and mucosal immune responses in mice (23). Another recent study has proven that the coating with MPLA evokes a strong cellular immune response and the functionalized hydroxyethyl starch nanocapsules with MPLA significantly enhance the uptake of nanocapsule by the dendritic cells (DCs) (32). MPLA functionalized microcapsules are also being tested *in vivo* for targeted drug delivery to combat infectious liver diseases with promising results (33). Therefore, MPLA has been chosen as an adjuvant to be incorporated into the polymeric lid of this study, so that the adjuvant-based lid can enhance immune response at the targeted drug delivery site.

2.5 Microcontainers

Microcontainers or MCs are micro size polymeric carriers or devices of drug for oral drug delivery (10,12,34). They have been previously used as oral drug delivery system, especially where the poorly water soluble drugs are involved, biodegradable polymeric MCs are used in order to improve the bioavailability of the drug (9-11). A study published in 2016 has shown that compared to ASSF (amorphous sodium salt of furosemide) in capsule, ASSF in polymeric MCs has a relative bioavailability of 220% (35). Microcontainers vary from micro and nanoparticles. The MCs used in this study were a model system and they were fabricated in-house in the epoxy (30) polymer SU-8 by a two-step photolithography process and silicon was used as the substrate . Each small squared cut of silicon had an area of 12.8×12.8 mm, and it contained 25×25 = 625 microcontainers. The outer diameter of the MCs was 300 µm with an inner diameter of 220 µm. The total height of each microcontainer was 305 µm with the actual container depth of 270 µm. (Fig. 2.3)

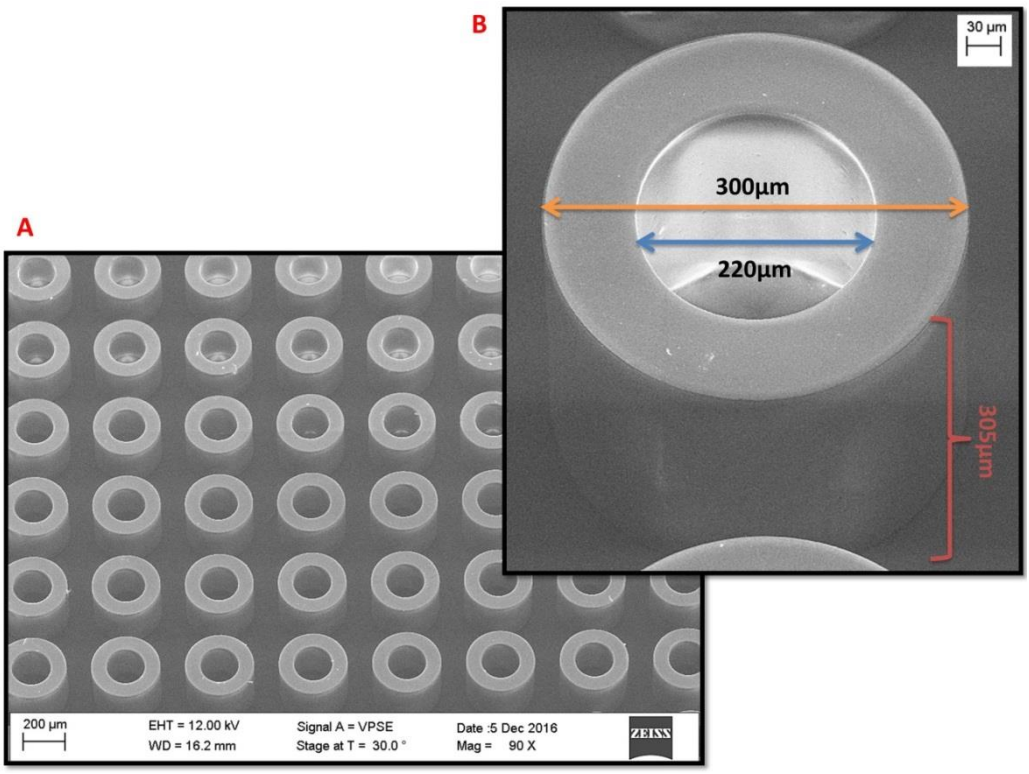

Fig. 2.3: *Supra SEM images of* ***A.*** *SU-8 microcontainers on silicon substrate;* ***B.*** *of a single microcontainer stating the dimensions*

MCs are designed for unidirectional drug delivery with only one side of the microcontainer open and the other side has a flat base with a walled reservoir (36). The middle cavity of the microcontainers is filled with drug and can then be coated with a lid to protect the drug from undesirable environments and to ensure targeted drug delivery (9).

2.6 Furosemide

Furosemide is a diuretic drug that prevents body from absorbing too much salt, and thus letting the salt to be passed through urine (37). It is a poorly soluble drug, which has been widely utilized in different drug dissolution studies (38). According to the Biopharmaceutics Classification System (BCS) standard, furosemide falls into Class IV which refers to low solubility and low permeability (39). The oral bioavailability in humans is stated to be very variable from person to person and is found to be in the range of 43-69%. The chemical formula of furosemide is $C_{12}H_{11}ClN_2O_5S$ and molecular mass is 330.75 g/mol. The chemical structure of furosemide is given below (Fig. 2.4). (40).

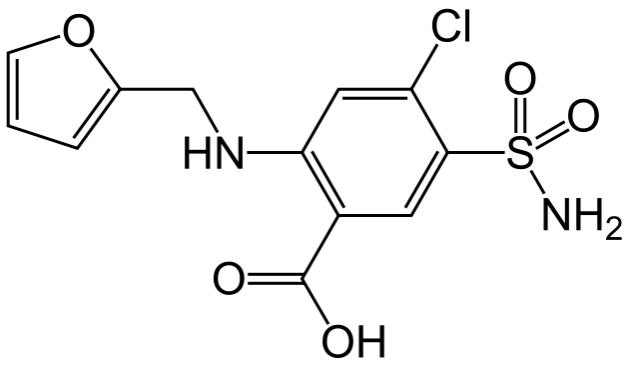

Fig. 2.4: *Chemical structure of furosemide* (40)

Furosemide is used to treat edema by reducing extra fluid in the body for the patients with heart failure, kidney disease and liver disease. It also can lessen the symptoms of shortness of breath and swelling of limbs such as arms and legs. Moreover, it can also treat high blood pressure, or hypertension. (37). Common side effects of furosemide include numbness, tingling, headache, dizziness and blurred vision (40). Therefore, it is important to wear safety mask and gloves during working with Furosemide in laboratory.

2.6.1 ASSF

ASSF or amorphous sodium salt of furosemide is formed from a sodium hydroxide containing aqueous solvent (41). In this study, the ASSF utilized was prepared in house by spray drying pure furosemide powder and the detailed process is provided in the Materials and Methods section later in this report. The prepared ASSF has a glass transition temperature of 101.2 ºC and it exhibits 291 days of physical stability at 22 ºC. Studies have shown that storing the amorphous form of furosemide at 40 ºC and 75% relative humidity, converts the amorphous form into crystalline form after 2 days. The apparent solubility of ASSF in different gastric and intestinal stimulated media is proven to be much higher compared to other forms of furosemide, such as furosemide free acid and other amorphous forms. In addition, the ASSF demonstrates good biorelevant dissolution behaviors in micro dissolution experiments and stable conversion of salt into polymorph (42). Comparison studies have been done in rats using pure furosemide and ASSF, and the results show that ASSF is more suitable and advantageous over pure furosemide in terms of biorelevant dissolution, and solubility in oral drug delivery (32,33, 34). Thus, the promising properties of ASSF especially its high intrinsic dissolution rate (IDR) and apparent solubility in *in vitro* and *in vivo* studies for oral vaccination (32–36), have made ASSF to be chosen as the model drug for this study.

2.7 Eudragit

Eudragit polymers are derived from esters of acrylic and methacrylic acid and their physiochemical properties largely vary depending on their functional groups. (45). Fig. 2.5 provides an example of different functional groups in Eudragit polymers and their varying behavior. Eudragit polymers are well known to be utilized as coating on oral solid dosage forms since 1954 (46).

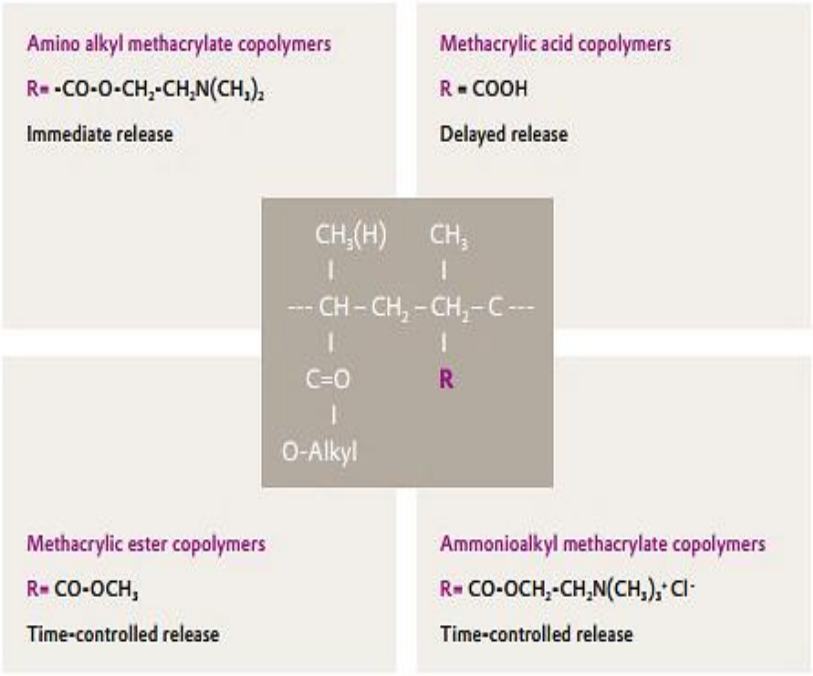

Fig. 2.5: *Different functional groups of Eudragit polymers leading varying drug release behaviors* (46)

There are many different grades of Eudragit polymers with different physical and chemical properties including glass transition temperature, solubility, physical appearance and field of application. (46), (47). For example, the glass transition temperature of Eudragit L100-55 is 110 ºC, whereas it is only 9ºC in Eudragit NE 30D (47). Table 2.1 represents availability, solubility and application of some widely used Eudragit polymers in drug delivery studies.

Table 2.1: *Dissolution properties of different commonly used Eudragit polymers for drug release* (46-48)

Eudragit Polymer	Availability	Dissolution Properties	Applications
L 30 D-55	30% aqueous dispersion	Soluble in intestinal fluid above pH 5.5	Enteric coatings
L 100-55	Powder	Soluble in intestinal fluid above pH 5.5	Enteric coatings
L 100	Powder	Soluble in intestinal fluid above pH 6	Enteric coatings
L 12,5	12.5% organic solution	Soluble in intestinal fluid above pH 6	Enteric coatings
S 100	Powder	Soluble in intestinal fluid above pH 7	Enteric coatings
S 12,5	12.5% organic solution	Soluble in intestinal fluid above pH 7	Enteric coatings
FS 30 D	30% aqueous dispersion	Soluble in intestinal fluid above pH 7	Enteric coatings
NE 30 D	Cationic, yellow	Swellable, permeable	Sustained release
E 100	Cationic, yellow granules	Soluble in gastric fluid up to pH 5	Film coatings

2.7.1 Eudragit L100-55

Eudragit L100-55 is a white powder and has faint characteristic odor. It has an average molecular weight of 320 000 g/mol. This giant polymer contains an anionic copolymer based on methacrylic acid and ethyl acrylate with a ratio of 1:1 free carboxyl group: ester group as shown in Fig. 2.6 (49).

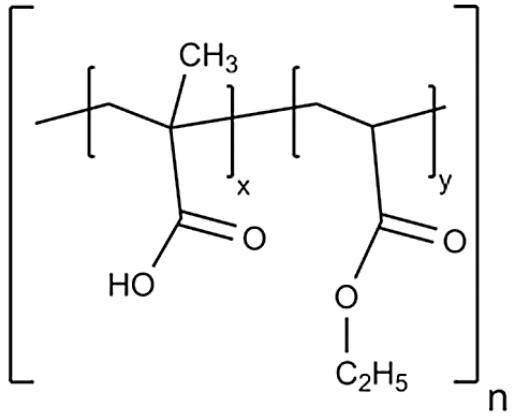

Fig. 2.6: *Chemical structure of Eudragit L100-55* (49)

Eudragit L100-55 is soluble in methanol, ethanol, isopropanol, acetone and sodium hydroxide and the solution gives clear to cloudy color depending on the solvent. However, this polymer is practically insoluble in water, petroleum ether, ethyl acetate and methylene chloride. For storage, Eudragit L100-55 should be kept away from moisture and in between 8-25ºC. (49).

2.8 Plasticizer

Plasticizers, also known as dispersants, are the chemicals that are added to polymeric substances to enhance their flexibility, workability and viscosity, and also in some cases, to aid the polymers' processing. Adding plasticizers to polymers lowers their modulus, reduces glass transition temperature and decreases tensile strength. (50,51). Adding plasticizer to the polymer induces greater mobility by disturbing polymer-polymer interactions in the polymer chain and establishing polymer-plasticizer interactions (52). There are more than 30, 000 substances that have plasticizing properties and, in 2014 the total global plasticizers consumption was about 8.4 million metric tons (53,54). Majority of plasticizers are organic esters and the choice of plasticizer depends on the properties desired in the final product and its applications. Toxicity, compatibility, hydrophobicity or hydrophilicity, ease of mixing, stability in processing and service condition are some important criteria in choosing the convenient plasticizer (50).

2.8.1 TEC

Tri ethyl citrate (TEC) is the most common plasticizer used with Eudragit polymers (47). It is an ester of citric acid (55), whose chemical formula is $CH_3COOC(COOCH_2CH_3)(CH_2COOCH_2CH_3)_2$ (Fig. 2.7) and the molecular weight is 318.32 g/mol (56).

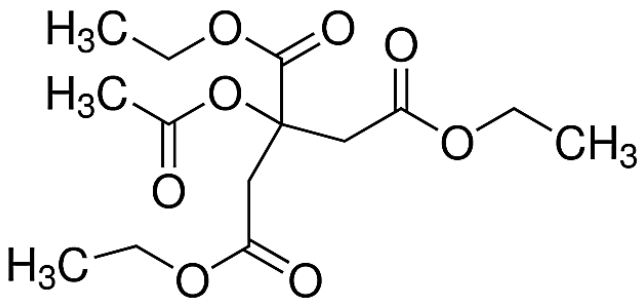

Fig. 2.7: *Chemical structure of TEC* (56)

It is a colorless and odorless liquid (55). The TEC used in this study had a purity of 99%, with the density of 1.136 g/ml at 25ºC. The boiling point of TEC is 228-229ºC/100mmHg (lit.) and it has hydrophilic properties (56).

2.8.2 DBS

Di butyl sebacate (DBS) is a bio-based di butyl ester of sebacic acid (57). It is usually produced from cracking of castor oil, resulting into colorless and odorless transparent oily DBS liquid (58). Its chemical formula is $[-(CH_2)_4CO_2(CH_2)_3CH_3]_2$ and molecular weight is 314.46 g/mol (59). Fig. 2.8 shows its chemical structure below.

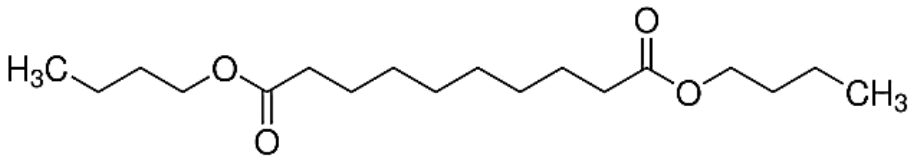

Fig. 2.8: *Chemical structure of DBS* (59)

The boiling point of DBS is 178-179ºC/3 mmHg (lit.) and its density at 25ºC is 0.936 g/ml (59). It is highly pure, cold resistance, hydrophobic and easily biodegradable plasticizer (58). The water solubility of this plasticizer is only 0.04 g/L (60). DBS is soluble

in hexane, toluene, ethanol and acetone but insoluble in water and propylene glycol (59).

2.8.3 TEC versus DBS

Both the TEC, a hydrophilic plasticizer, and the DBS, a hydrophobic plasticizer, are widely utilized in Eudragit L polymers. Studies have shown previously that TEC and DBS, the both plasticizers affect the water absorption behavior, adhesive properties of Eudragit polymer coating, drug permeability and other mechanical properties including tensile strength, modulus of elasticity and glass transition temperature of the polymer coating (52,61–65). Therefore, in this study, both plasticizers were incorporated with EL100-55 polymer solution in separate experiments prior to lid formation to see their effects on the lid stability as well as the capacity of targeted drug release. In the beginning of the lid development study, the TEC was chosen as the plasticizer for EL100-55 because it is the most common plasticizer used in this polymer (66). Due to higher water solubility of TEC, polymer pellets incorporated with this plasticizer seem to have much faster drug release compared to DBS incorporation (65). TEC incorporated polymeric films take up water more rapidly and thus render an increase in the permeability of the polymer films. On the other hand, TEC was found to be rapidly leached out of polymeric coatings, in contrast to DBS. This phenomenon resulted in decreased mechanical resistances of the film as well as facilitated crack formation (63). Studies have shown that theophylline pellets coated with TEC has an approximate zero-order release rate, whereas, it is a two-phase release profile if the pellets are coated with DBS, in contrast (64). Studies done both *in vitro* and *in vivo* have shown that DBS is a good choice as a hydrophobic plasticizer for Eudragit polymer in terms of controlled drug release (67). Therefore, both TEC and DBS are chosen as plasticizers to be used in this lid development study.

2.9 Chitosan

Chitosan is a linear polysaccharide often obtained from the outer skeleton of shellfish such as shrimp, crab and lobster. (68, 69). Chitosan is derived from chitin, the second most significant natural polymer, upon deacetylation (Fig. 2.9).

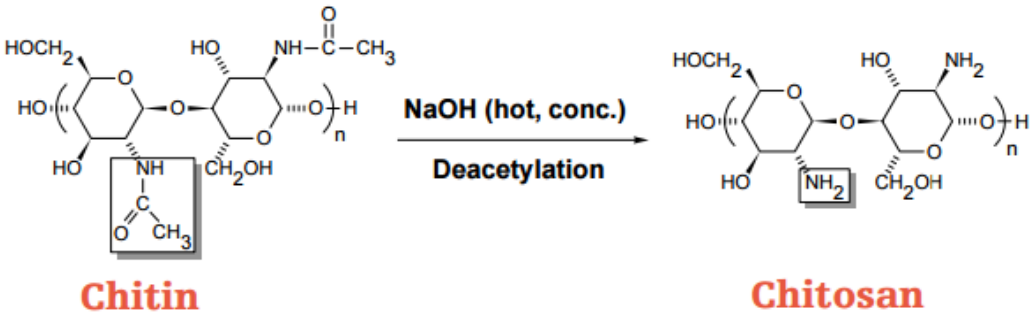

Fig. 2.9: *Deacetylation of chitin polymer to derive chitosan* (Adapted from (69))

It can have varying degree of acetylation, thus different numbers of acetyl groups along its chain and therefore, chitosan can have varying molecular weights (68,70). Chitosan is biocompatible, hydrophobic, nontoxic, pseudo-natural cationic polymer with pH sensitivity (68). About its physical properties, chitosan has high surface area, porosity, tensile strength and conductivity (71). Moreover, its hydrated form shows good mucoadhesive properties, so it supposes the facilitation of transmucosal absorption of, especially some polar drugs, at the intestinal epithelial cells (71,72). Chitosan has been widely used in immunization vaccine research and development, however it has poor immune response in terms of mucosal application and therefore, chitosan often requires an adjuvant for boosting an immune response (73).

In this study, the chitosan was used to carry the adjuvant, MPLA to the targeted drug delivery site. The chitosan used in this study, is called low molecular weight chitosan (LMW Chi), purchased from Sigma-Aldrich. According to the information provided by its manufacturer, the LMW Chi has (71) a molecular weight between 50,000-190,000 Da, depending on its viscosity. The viscosity of this polymer is 20-300 cP and deacetylation percentage is 75-85%. The LMW Chi is soluble in dilute aqueous acids. (74). Though chitosan has its optimum solubility at pH 4.0, or even lower (71), the solubility of chitosan polymer largely varies depending on its different percentage weight in relation to the volume of solvent (% w/v), as well as on the type of solvent (e.g. acetic acid (AA), melic acid, and citric acid) (75). In this study, 0.5% w/v of LMW Chi in 0.1M AA was used which has a pH value of approximately 3.4 (75).

3. TECHNIQUES

This chapter introduces and then illustrates the techniques and their usages. For example, loading microcontainer technique, spray coating technique, lid morphology and analysis techniques are discussed with images.

3.1 Spray Drying Technique

Spray drying is a technique that transforms liquid into dry powder by atomization through an atomizer in a hot drying gas medium (Fig. 3.1). It is a rapid, cost effective, scalable and reproducible technique which is often considered as a dehydration process. However, spray dryer is also utilized in encapsulation process of hydrophilic and hydrophobic active compounds (76,77). It is a very scalable process for producing dry pharmaceutical powders without substantial thermal degradation and with high percentage yield. Spray drying is suitable even for heat sensitive substances due to its fast drying process and relatively short heat exposure. It has, thus, become a key player in producing different inhalable drugs (77).

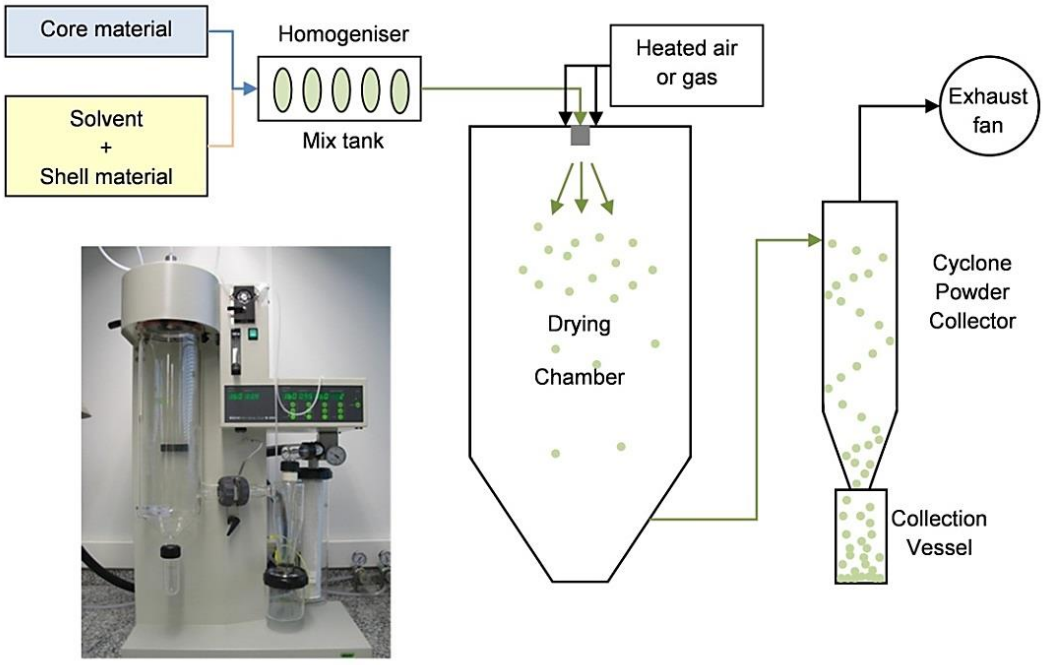

Fig. 3.1: *Schematic diagram of a spray drying process and an image of a real spray dryer* (Adapted from (78))

In Fig. 3.1, during the process of spray drying, the equipment has to be heated in the first step at a desired temperature. It has a two-fluid nozzle which has high cavitation with durable and precise reproducible capacity. The double nozzle system works for droplet formation and in the drying chamber, the conductive heat exchange between drying gas and the sample droplets takes place. The aspirator delivers the drying gas and the cyclone powder collector made of glass and electrically conductive layer prevents product losses in the cyclone, and thus particles get collected with high yield. As shown in Fig. 3.1, there is an outlet filter or collection vessel which collects the finest particles, at the end of the process (77,79).

3.2 Powder Embossing Method

Powder embossing method is a novel method recently introduced in order to ease and enhance loading efficiency of MCs with drug. Different drugs including pure drug, lipid-based microparticles and pure polymer have been successfully loaded into MCs using this method. In this method, as shown in Fig. 3.2, a shadow mask is used conforming to the dimensions of sample MCs to align the shadow mask on top of the sample. The shadow mask helps to load the cavities of the empty MCs precisely and prevents deposition of drug between the MCs. Following the alignment, the desired powder drug is embossed into the MCs applying specific pressure under the bonding press equipment. Thus, this is an easy-going drug loading process which can simultaneously load many MCs in a single step. In this study, the powder embossing method was used to load 625 MCs at a time. However, further research is ongoing to ensure the scalability and reproducibility of this method in terms of homogenous loading (80).

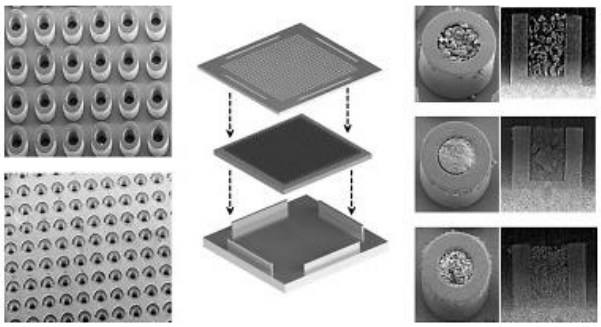

Fig. 3.2: *Powder embossing method- overview of empty MCs and a shadow mask (left); alignment of empty sample and shadow mask (middle); loaded MCs (right, top-to-bottom: pure drug-lipid based microparticles-pure polymer)* (Adapted from (80)).

3.3 Spray Coating Technique

Spray coating is a widely performed conventional coating approach for achieving micro and milimeter thickness of coating. This coating technique undergoes three consecutive steps- i) formation of microdroplets of the desired solution (e.g. Eudragit solution, and chitosan solution) from the spray coater through atomization; ii) deposition and adherence of the droplets onto the sample (e.g. drug loaded MCs) placed on the spray coater's hotplate; iii) coalescence of those droplets on the substrate and formation of intact coating (81,82). Fig.3.3 depicts a diagram of spray coater's configuration which basically consists of a spray nozzle (e.g. accumist, micromist, impact nozzles), connected to a compressed air pump and a coating solution.

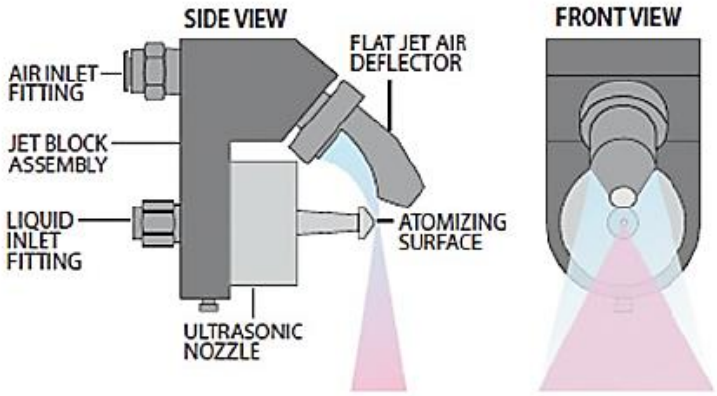

Fig. 3.3: *Schematic view of spray coating configuration* (Adapted from (83))

The coating solution inlet fitting is connected to a syringe driver where the solution filled syringe is clamped on and the solution is injected into the nozzle for atomization. Once the sample or substrate for coating is placed on the hotplate, the spray coating parameters such as atomization air pressure, gun-to-surface distance, spray area, infuse rate and temperature, are optimized based on the solution specific coating requirements. The quality of coating is highly affected by the spray coating parameters and the physio-chemical properties of the coating solution (82).

3.4 µDissolution Technique

The µDiss profiling is a miniaturized dissolution method that requires very small amount of active pharmaceutical ingredient (API) and dissolution medium (84,85), and therefore, is widely used in drug release or dissolution studies (86). Besides continuous monitoring of drug absorbance, the µDiss apparatus can measure the IDR, with the help

of additional mini-IDR^{TM} disc. Thus, the µDiss profiler has been used to evaluate dissolution behavior and obtain drug dissolution rate, even for poorly soluble drugs such as furosemide. As shown in Fig. 3.4, this versatile instrument has fiber optic UV spectroscopy that collects the real time drug concentration in the release medium. The attached dip probes along with the mirror and optical path slit are immersed into the release medium in the temperature and stirring controlled glass vials. The light beam is directed to the liquid through the optical path slit and then gets reflected by the mirror. Thus, the absorption spectra of the solute are collected in real time (84,87).

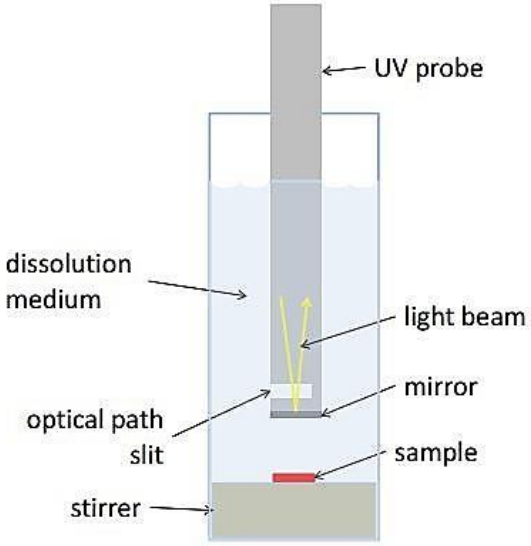

Fig. 3.4: *Schematic view of a µDiss vial with the sample and an immersed measuring probe* (Adapted from (88))

3.5 Surface Profiling using Stylus Profiler

The stylus profiler is a high-sensitive surface analyzer that is used to measure thickness and roughness of a surface. An overview of a Tecnor Alpha-step IQ stylus profiler hardware and its software (Alpha-step IQ) is shown in Fig. 3.5. The upper part of the software window consists of different scanning parameters that can be set for controlling the stage and stylus movement as well as data analysis.

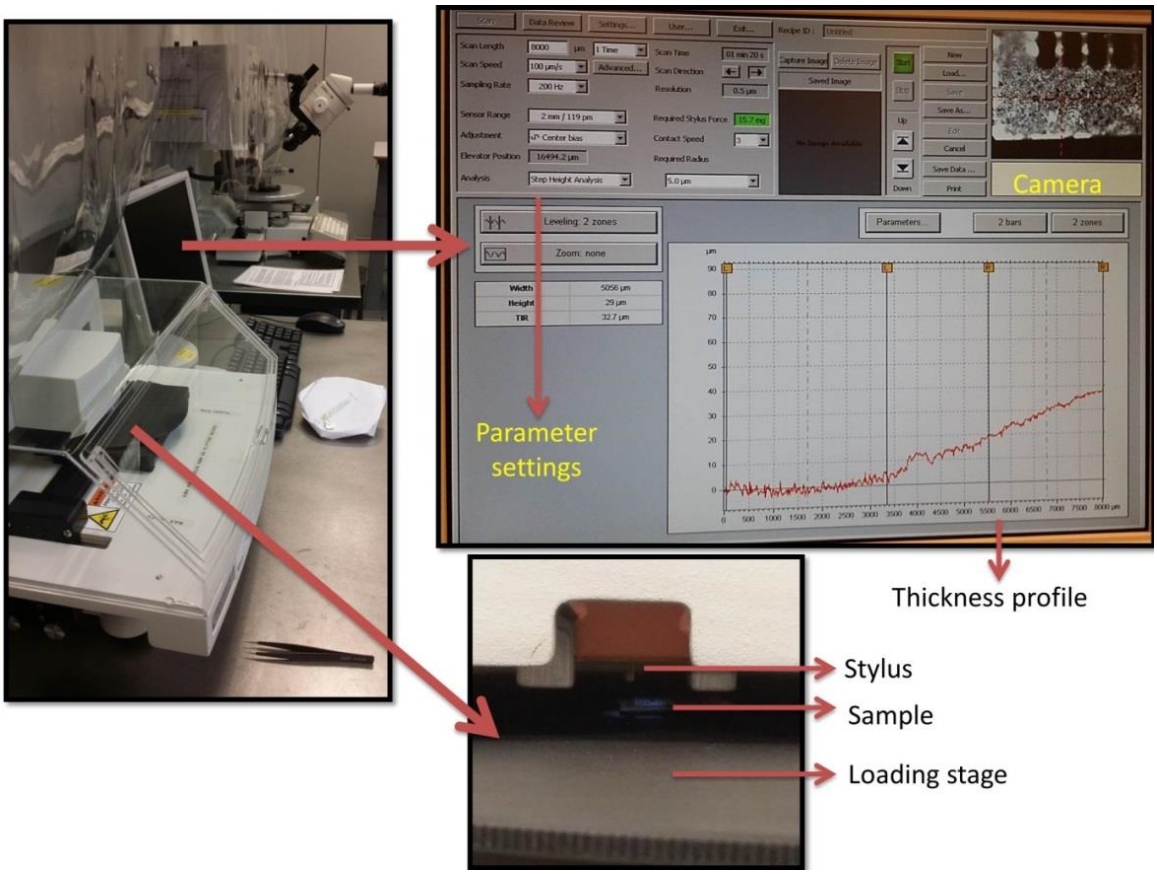

Fig. 3.5: *Tencor Alpha Step Stylus Profiler, sample loading and scanning of sample surface for thickness measurement*

This instrument is equipped with a video camera that shows the surface of the substrate and the red crosshair stylus apex as it keeps moving along the measuring surface. The stylus' apex or curvature has a radius of 5 μm only. On the other hand, lower part of the window is for measurement display as the scan is performed. For loading the sample, the stage is put down as shown in Fig. 3.5 where the parameters used during the thickness measurement are also displayed. If the sample seems to be too light and small, it is better to attach the sample to the loading stage, using lightly sticky double sided tape in order to avoid movement of the sample itself while the stylus is passing across it (Fig. 3.5). The movement of loading stage in x, y directions is controlled by the knobs located on the left side of the equipment. The equipment can measure samples with 150 mm diameter max and up to 15 mm of thickness. It can scan up to 10 mm horizontal and 2 mm vertical surface. (Tencor Alpha Step).

3.6 Scanning Electron Microscopy

The scanning electron microscope (SEM) produces images by generating a variety of signals at the solid specimens' surface utilizing focused beam of high energy electrons. These electron-sample interactions driven signals provide information regarding the surface morphology, chemical composition, structure and orientation of materials of the scanned sample (89). Compared to other conventional optical microscope, SEM has higher magnification with exceptionally good resolution. It also offers larger depth of field and requires minimal specimen preparation (90).

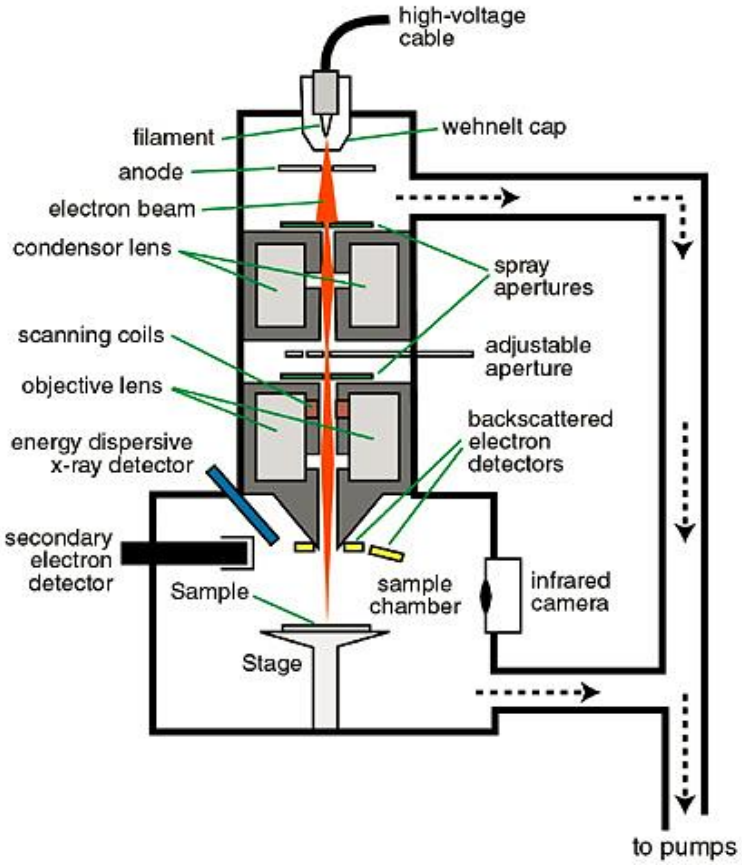

Fig. 3.6: *Schematic overview of a scanning electron microscope*
(Adapted from (91))

The fundamental principle of SEM lies in accelerated electrons that carry significant kinetic energy which is subsequently dissipated as variety of signals by electron-sample interactions. Signal specific detectors then detect the scattered electrons and amplify them to be projected in the display. Essential components of SEM include electron gun or source, electron lenses, sample stage, detectors of signals, display or data output device and other infrastructure requirements such as vacuum system, pump and power

supply (Fig. 3.6). Most SEM has more than one detector for capturing signals (89). Further details regarding the SEM used in this study are provided later.

3.7 X-ray Photoelectron Spectroscopy

The x-ray photoelectron spectroscopy (XPS), also known as electron spectroscopy for chemical analysis (ESCA), is a surface-sensitive, quantitative, non-destructive technique that can measure the elemental compositions including empirical formula, electronic state, and chemical state in a compound. This instrument requires high vacuum or ultra-high vacuum conditions and it can detect all atomic elements except hydrogen and helium. The average depth analysis of XPS is about 5 nm (92,93).

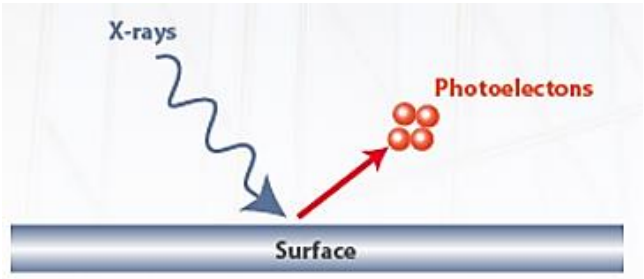

Fig. 3.7: *Emission of photoelectron by x-ray beams* (Adapted from (92))

The fundamental principle of XPS is to excite sample surface with mono-energetic Al kα x-rays, while simultaneously measuring the emitted electrons and kinetic energy (Fig. 3.7). Thus, by counting the emitted electrons over a range of kinetic energy, a photoelectron spectrum is obtained. Analyzing the binding energy and the intensity of a photoelectron peak, the identity of the particular component, its chemical state and the quantity of the detected element can be determined. Fig. 3.8 presents a diagram of the essential components of a XPS which includes x-ray source, detector, camera, ion gun, flood gun, lamp, sample holder, and analyzer. (93).

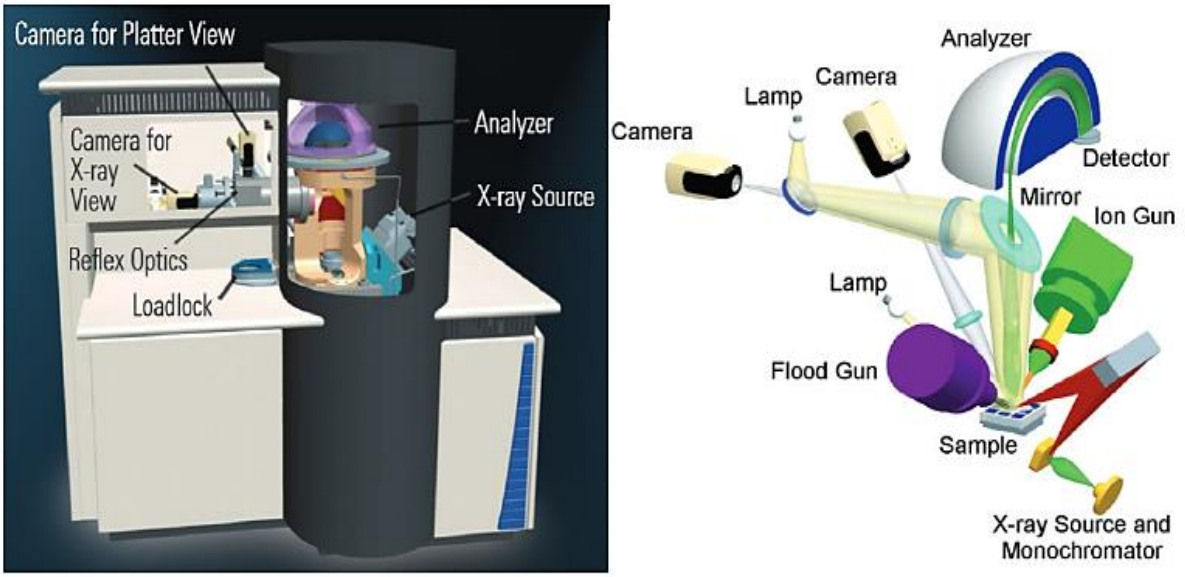

Fig. 3.8: *Schematic view of XPS equipment showing the location of the major components* (Adapted from DTU Danchip Manual for XPS-ThermoScientific 2015)

4. MATERIALS AND METHODS

This chapter mentions the materials and explains the stepwise methodology of developing polymeric lids of microcontainers leading to targeted drug delivery. In addition, this section illustrates the lid stability tests and validation experiments. The study was divided into six major parts. The parts are shown in **Chart 4.1** below:

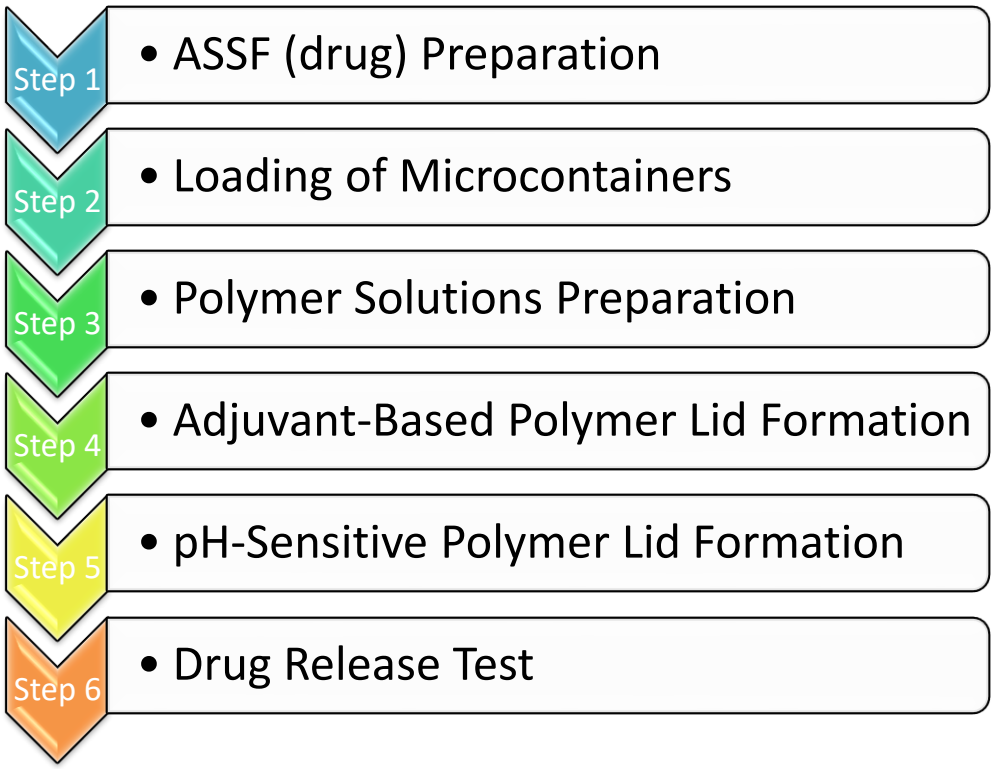

Chart 4.1: *Major experimental steps of the study*

4.1 Preparation of Amorphous Sodium Salt of Furosemide

Amorphous sodium salt of furosemide (ASSF) was prepared using a Mini Spray Dryer (B-290 No. 1, Büchi, Germany). For the ASSF preparation, 4.0 g of furosemide (Sigma Aldrich) was mixed with 100 ml of 96% Ethanol and 2.5 ml of 5M NaOH. Finally, 897.5 ml of miliQ water was added to the solution to obtain 4 g/L (12.085 mM) of final drug concentration. The solution was protected from light and was stirred on a magnetic stirrer at a temperature of 55^{o} C for about 45 minutes followed by spray drying the solu-

tion using spray dryer. The parameters of the spray dryer settings were identical to studies published in literature (39,41) are given below in Table 4.1.

Table 4.1: *Parameter settings of the spray dryer for preparation of ASSF*

Parameters	Values
Inlet temperature (° C)	200
Aspirator (%)	80
Pump (%)	10
Atomizer (mm)	40

A de-humidifier (Buchi B-290) was used with the spray dryer equipment for drying the drug solution during the process. Fig. 4.1 shows the setup of spray dryer, parameter settings and the preparation of ASSF drug.

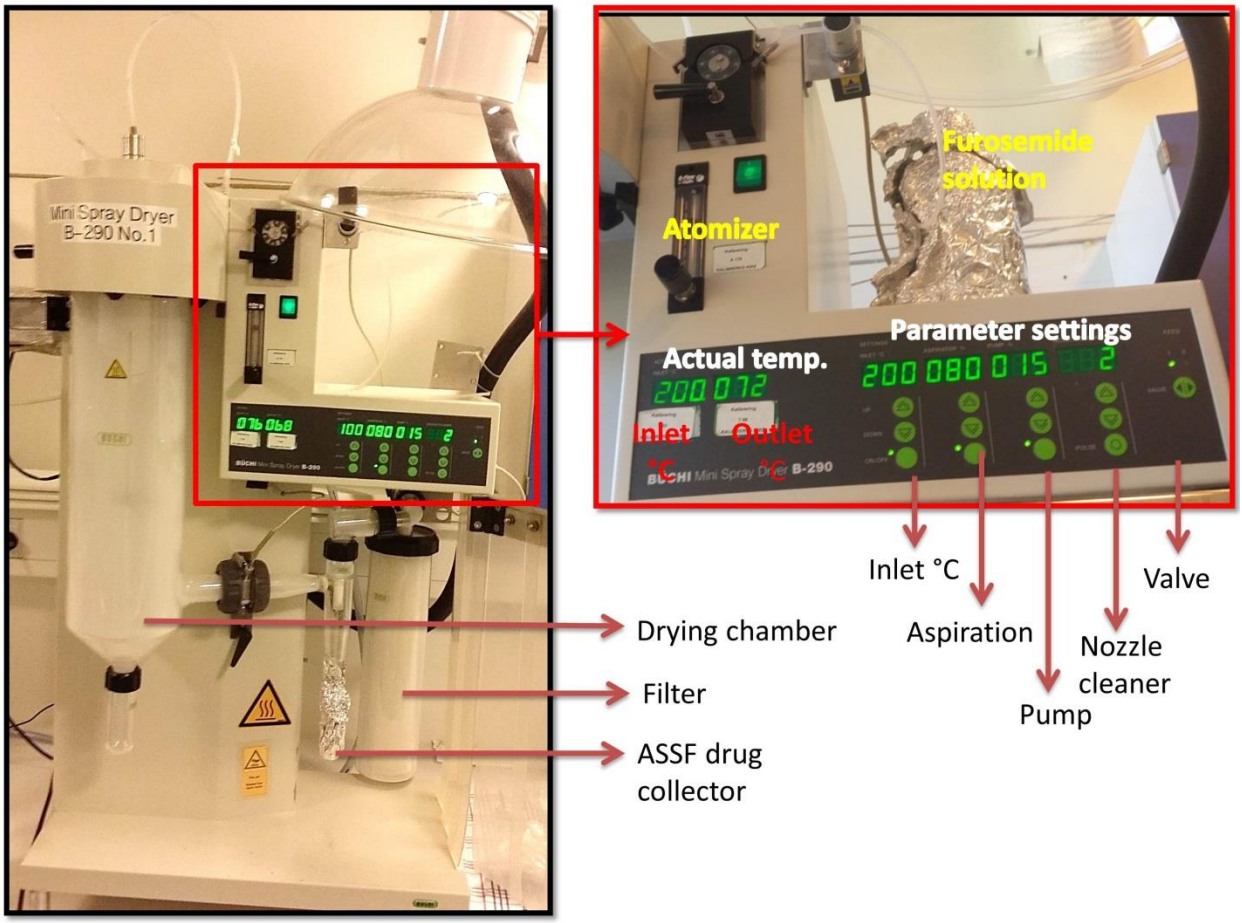

Fig. 4.1: *Spray dryer setup and preparation of Amorphous Sodium Salt of Furosemide (ASSF)*

After the spray drying, the ASSF drug was extracted from the collection chamber and transferred to another vial. The ASSF vial was then wrapped with aluminum foil and placed inside a desiccator to avoid contact with outside air.

In order to calculate the yield, the empty collection chamber was weighted prior to using the spray dryer. After the spray drying process, the spray dried ASSF and the collection chamber were weighted. Thus, the yield calculation was done using the following formula.

$$Yield = \frac{Actual\ weight\ of\ Produced\ ASSF}{Initial\ weight\ of\ Furosemide\ powder} * 100$$

4.2 Loading of Microcontainers (MCs) with ASSF

ASSF was loaded into the microcontainers by the powder embossing method. Fig. 4.2 below shows SU-8 microcontainers on silicon chips which were fabricated in the cleanroom (DTU Danchip, Denmark).

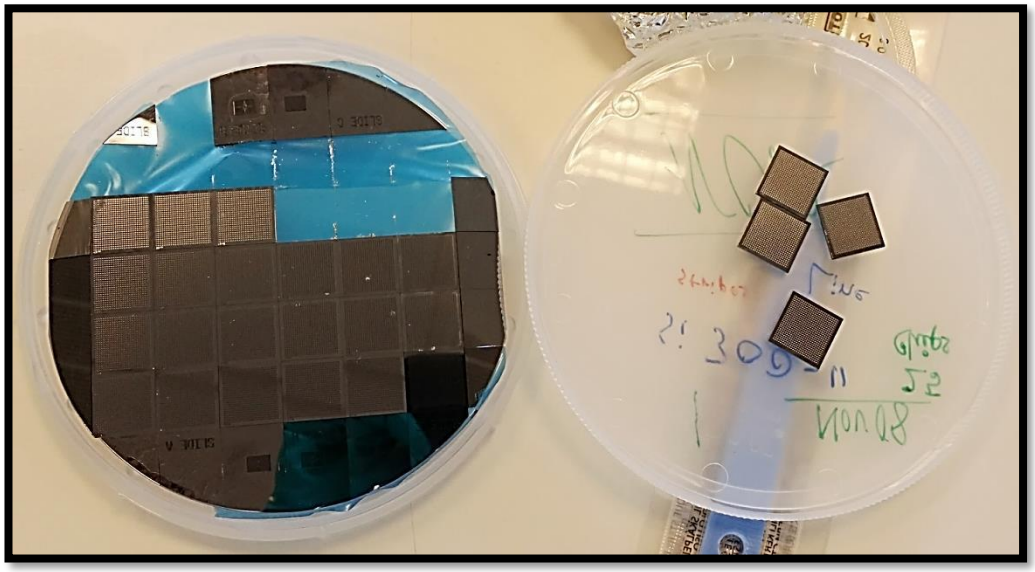

Fig. 4.2: *SU-8 microcontainers on silicon chips*

In the beginning of loading, the desired amount of ASSF was taken onto the shadow mask drug holder (Fig. 4.3). Next, the shadow mask was placed on top of the sample chip followed by placing both into the shadow mask frame.

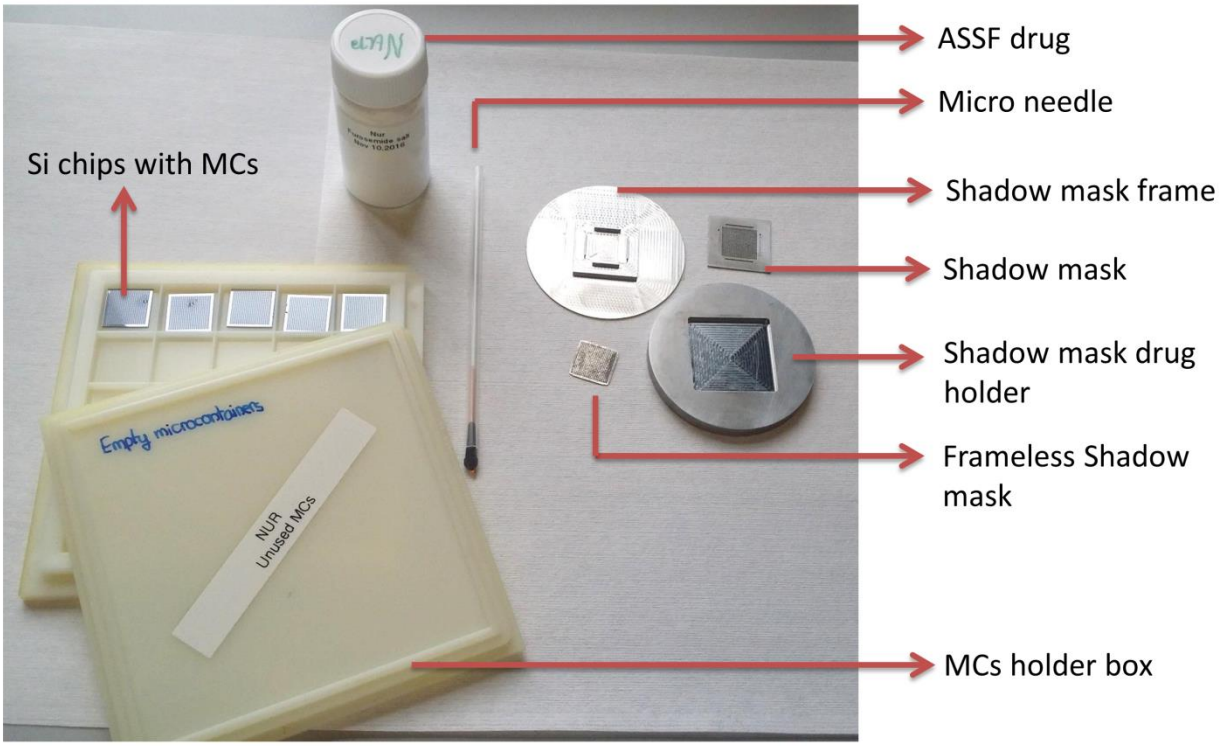

Fig. 4.3: *The various parts of shadow mask for loading the MCs using an embossing method*

Finally, the shadow mask-fitted sample chip is placed on top of the drug at the drug holder. After proper placement, 2kN of pressure is applied at room temperature and thus the drug gets loaded inside the MCs of the silicon chip. Fig. 4.4 below shows the placement of the silicon chip containing MCs and the orientation of the shadow mask on top of the bonding press metal plate for loading.

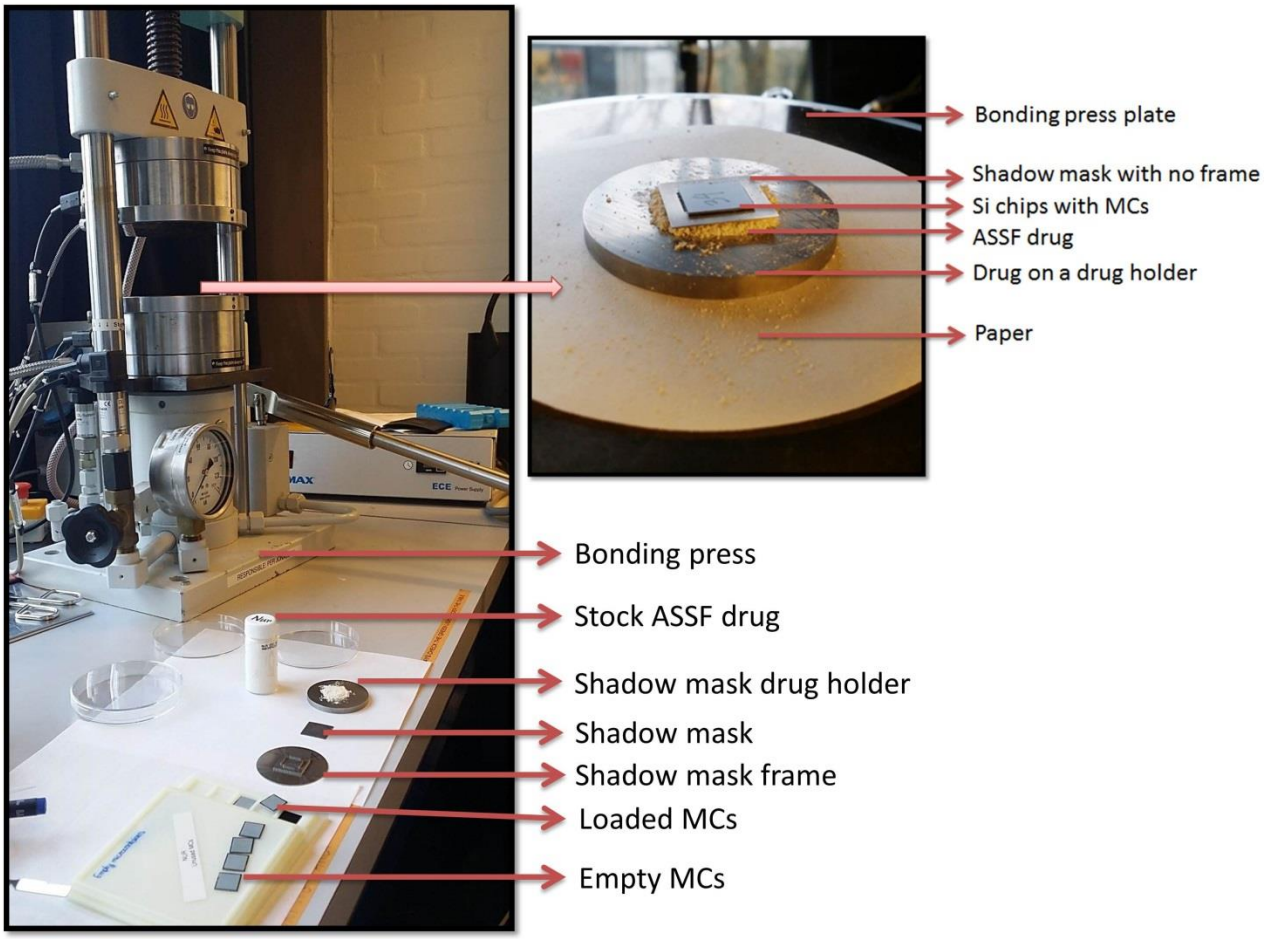

Fig. 4.4: *Loading of ASSF drug using a shadow mask in bonding press*

Each chip was assigned a number and the weights of the chips had been recorded using a microbalance before and after loading in order to calculate the amount of drug loaded into each specific chip. It is important to know the weight of loaded drug into each chip, so that during the release test in micro dissolution apparatus, the concentration and dissolution percentage of the drug from each chip can be calculated.

Amount of loaded drug = (Weight of chip after loading – Weight of chip before loading)

$$\textit{Drug concentration} = \frac{Amount\ of\ loaded\ drug\ (mg)}{Volume\ of\ medium\ (mL)}$$

4.3 SEM Imaging of Loaded Microcontainers

After sample loading, the quality of loading was analyzed using SEM imaging. Here, the loading quality refers to the number of MCs loaded with drug, quantity of loaded drug in the MCs, number of MCs broken or fallen off during the powder embossing process using the bonding press.

Fig. 4.5 shows the drug loading analysis under a tabletop SEM (Phenom Pro), whereas the Fig. 4.6 presents an overview of a supra SEM (Zeiss).

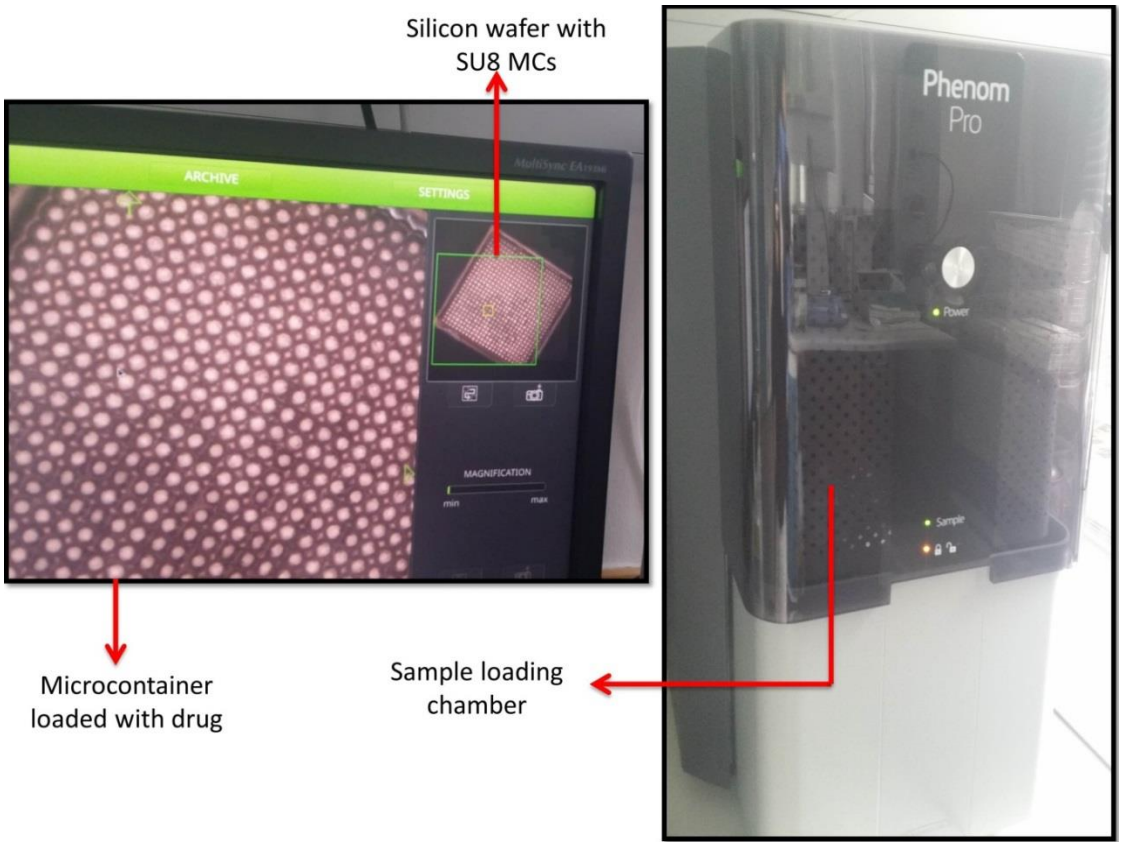

Fig. 4.5: *Sample analysis under a Tabletop SEM*

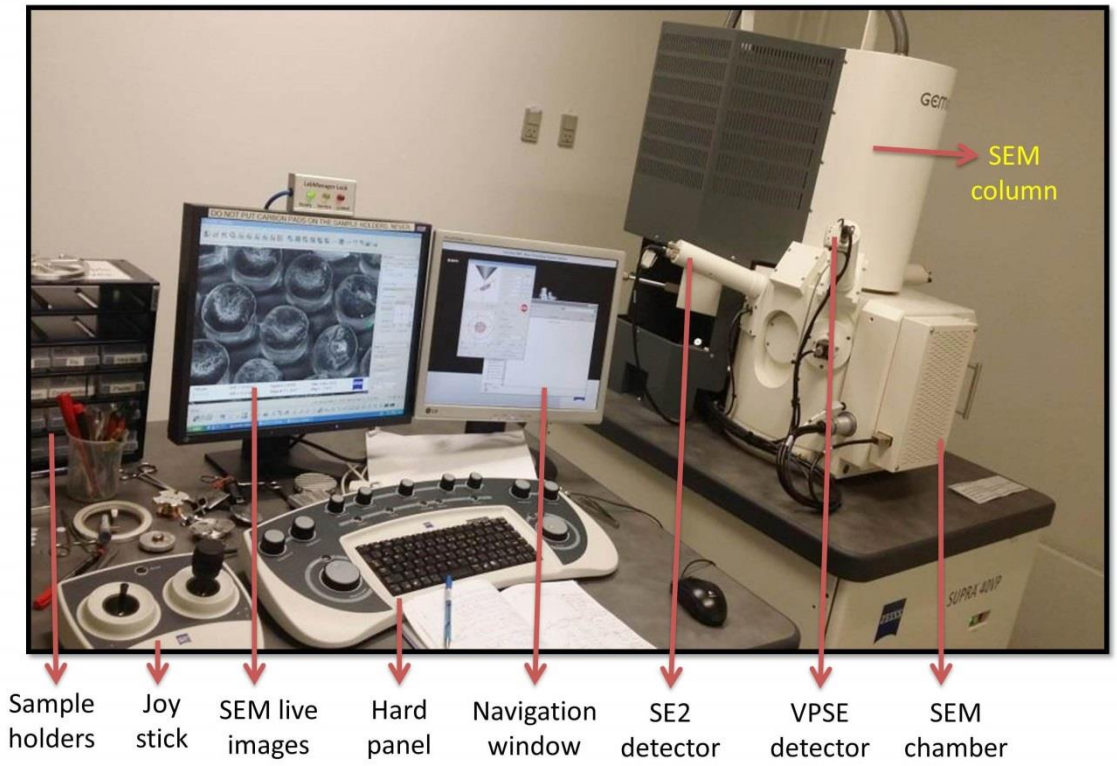

Fig. 4.6: *Overview of a Supra SEM and sample analysis*

Since most of the (almost 98% of the) sample analysis was performed using supra SEM, therefore, this section describes the methodology of supra SEM imaging. The analysis began with sample mounting on the SEM sample holder. After mounting the samples, the instrument was vent and pumped down. Then the sample holder with the samples on top of it was mounted inside the SEM. In case of blank sample (e.g. empty SU8 micro-containers on silicon wafer), the sample was coated with thin gold layer using Sputter Coater 03 (Cressington 208HR) in order to reduce problems with charging on sample during SEM analysis. After the samples were inside the SEM, the stage was pumped down and the high voltage extra high tension (EHT) was turned on. Depending on the sample type and the analysis, different parameters such as working distance (WD), aperture alignment, stigmation, EHT and type of detection lens were optimized. Table 4.2 below shows some of the important parametric values that were used for analyzing the MCs in the supra SEM.

Table 4.2: *Some important parameters of SEM imaging*

Parameters	Values
Vacuum mode	Both HP & VP
Detectors	Both SE2 & VPSE
Tilt	30°
EHT	8-18 kV
WD	8-12 mm

Once the image was optimized enough to be captured, it was saved for further analysis. The same procedure was followed for lid morphology investigation throughout this study.

4.4 Preparation of Polymer Solutions

In this section, the preparation of different polymer solutions for developing different lids on the drug-loaded MCs is presented. During this study, three types of Eudragit solutions and two types of chitosan solutions were prepared for different lids formation.

4.4.1 Eudragit Solution with TEC

This Eudragit solution contained 1% (w/v) Eudragit L100-55 (Evonic, Essen, Germany) with 15% TEC (Sigma Aldrich) and 6% mol of NaOH pellets in isopropanol (IPA). To prepare the solution, 2.0 g of Eudragit was first mixed with 150 ml IPA and 264 µl TEC and the mixture was stirred overnight at 700 rpm and at 45-50°C. After the solution turned transparent, 24 mg of NaOH was added to the solution and was let to solubilize for another day. The final volume of the solution was adjusted at 200 ml using additional IPA to obtain a Eudragit solution with a concentration of 1%.

4.4.2 Eudragit Solutions with DBS

Two different Eudragit solutions were prepared using a plasticizer called DBS (Sigma Aldrich). The first type of Eudragit solution contained 1% (w/v) EL100-55, 6% mol of aqueous NaOH and 5% DBS. The process of preparing this solution was the same as that of the previous of EL solution which took about two days for the solution preparation.

The second type of Eudragit solution contained 1% EL100-55 with 5% DBS, without any NaOH. It took only about 6 hours of magnetic stirring to have a homogenous transparent solution with a final concentration of 1% Eudragit.

4.4.3 Chitosan Solution

0.5% (w/v) chitosan solution was prepared in 0.1M acetic acid (AA). To prepare this solution, 0.5 g of low molecular weight (LMW) chitosan (Sigma Aldrich) was added to 0.6 ml of pure AA. Finally, total volume of the solution was adjusted to 100 ml to obtain a chitosan solution of 0.5% concentration. The solution was stirred at 350 rpm using 50-55°C overnight. After a homogeneous solution was obtained, the solution was filtered at least 5 times using syringe filters with different pore sizes of 0.80, 0.45 and 0.20 µm (Advantec) due to high impurity (about 18-20%), and it was then preserved in a glass bottle sealed with parafilm.

4.4.4 Chitosan Solution with MPLA

Unlike the previous chitosan solution, this solution contains an adjuvant, called MPLA (Avanti, 699800P). This solution contained 0.5% (w/v) of LMW chitosan with 3% (w/w) MPLA in 0.1M AA. To prepare this solution, 1.8 mg of MPLA was dissolved in 180 µl of 1:4 methanol:chloroform solution. It took approximately 3 hours to completely dissolve the MPLA in the methanol-chloroform solution. Next, the MPLA solution was added to 12 ml of the 0.5% (w/v) chitosan dissolved in 0.1M AA. It took approximately 3 days to obtain a homogenous solution of MPLA and chitosan. The solution, however, contained negligible amount of impurities and therefore, was filtered twice using 0.80 and 0.45 µm pore sized syringe filters. Fig. 4.7 shows the chitosan-MPLA solution below.

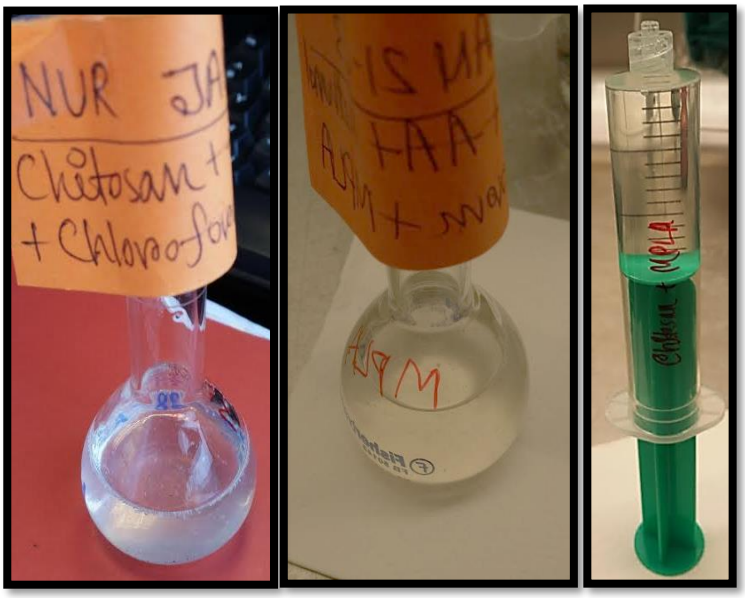

Fig. 4.7: *Chitosan-MPLA with impurities (left); Chitosan-MPLA after vortexing and further stirring (middle); Chitosan-MPLA after twice filtration (right)*

4.5 Adjuvant-Based Polymer Lid Formation

The purpose of developing chitosan lid was to incorporate an adjuvant (e.g. MPLA) into it. Since MPLA is an expensive adjuvant, in the beginning of the study, only chitosan lid was spray coated in order to test its stability and ability to permeate drug at targeted pH medium.

A spray coater (Exactacoat, Sono-Tek Corporation, NY, USA) equipped with a AccuMist™ ultrasonic mini-spray atomizing nozzle (94) was used to spray the prepared chitosan solution on top of ASSF loaded SU-8 microcontainers fabricated on silicon chips (section 4.2). The spray coater has three main parts (Fig. 4.8)- i) Syringe Pump, ii) Spray Chamber, iii) Spray coater connecting computer, which has three particular softwares (i.e. Generator control; Syringe pump; and Exactacoat portal version 1.0.3, build 10/2009). The necessary parameters for spray coating are set by using these softwares (Table 4.3).

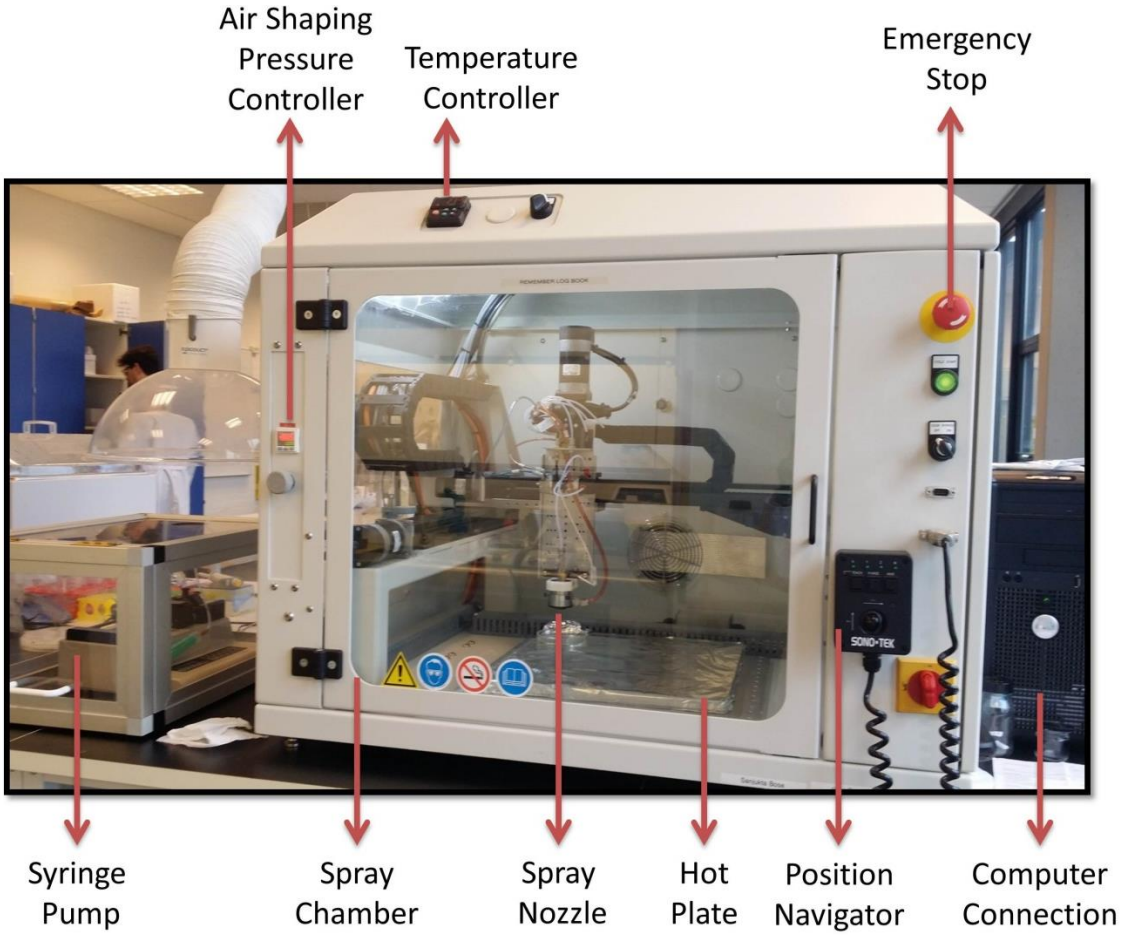

Fig. 4.8: *Spray Coater for formation of the polymeric lids*

In this polymeric lid formation process, following the cleaning and optimization steps, a 20mL luer lock syringe (Braun) was filled with chitosan solution and clamped at the syringe pump which has a connected motor to pump the solution from the syringe into the spraying tube inside the spray chamber. The ASSF loaded samples were placed inside the spray chamber on its hot plate. The spray chamber's temperature, air shaping pressure and position of the spraying nozzle were adjusted prior to spraying the polymer solution. Table 4.3 represents the spray coating parameters used for chitosan lid formation.

Table 4.3: *Parameters for spray coating 0.5% w/v Chitosan solution in 0.1M Acetic Acid*

Spray Coater Manual Controllers			
Temperature	40 °C	**Air Shaping Pressure**	0.01 kPa
Exactacoat Portal			
Wait Time	0.04 sec	**Area**	X2
Stall Point	0.5	**CNTR**	60 (x2)
Z	25	**Path Speed**	25 mm/sec
Generator			
Run Power	1.5 watts	**Idle Power**	0 watts
Syringe Pump			
Infuse Rate	0.100 ml/min	**Syringe Diameter**	20 mm

In this study, 4 silicon chips containing MCs and 2 control chips without MCs were spray coated simultaneously and about 7 ml of chitosan solution was used for the given parameters and the coating area.

The total spray duration for the chitosan coating completion was 1 hour and 15 minutes. The same protocol and parameters were used to spray coat both chitosan solutions, with and without the adjuvant MPLA. SEM images were taken to analyze the lid morphology following the lid formation.

4.6 pH-Sensitive Polymer Lid Formation

A pH-sensitive polymer solution, EL100-55 was spray coated on top of the above-mentioned chitosan lid, so that the chitosan lid can be protected in gastric medium but be exposed at the small intestine medium in order to ensure targeted drug delivery. As described in the polymer solution preparation Subsection 4.4.1-4.4.2, three types of EL100-55 solutions were prepared to form pH-sensitive lid. Despite the differences in the chemical types and amounts and process of solution preparations, the spray coating parameters and method were the same for all the EL100-55 solutions. However, different counter numbers of passes (CNTR) of the nozzle of the spray coater were tested to determine an effective thickness of the spray coated EL lids. It is worth-mentioning that 1 CNTR refers to1 full coverage of the nozzle movement from one end of the spray coating area (or sample area) to the other end. The parameters used in this process are presented in Table 4.4.

Table 4.4: *Parameters for spray coating 1% w/v Eudragit L100-55 solution and Isopropanol solvent*

Spray Coater Manual Controllers			
Temperature	40 °C	**Air Shaping Pressure**	0.02 kPa
Exactacoat Portal			
Wait Time	0.04 sec	**Area**	X2
Stall Point	0.5	**CNTR ***	60 (x2)
Z	35	**Path Speed**	5 mm/sec
Generator			
Run Power	2.2 watts	**Idle Power**	0 watts
Syringe Pump			
Infuse Rate	0.100 ml/min	**Syringe Diameter**	20 mm

**CNTR 60 and 20 were used during the EL100-55 which gave different thicknesses in the lids*

Likewise the chitosan lid formation, 4 silicon chips containing MCs and 2 control chips without MCs were spray coated simultaneously with EL solution. For the given parameters and the coating area, 11 ml of EL solution was needed during the 2 hours of spraying. Fig. 4.9 presents the optical microscopic view of the samples before and after spray coating with EL100-55.

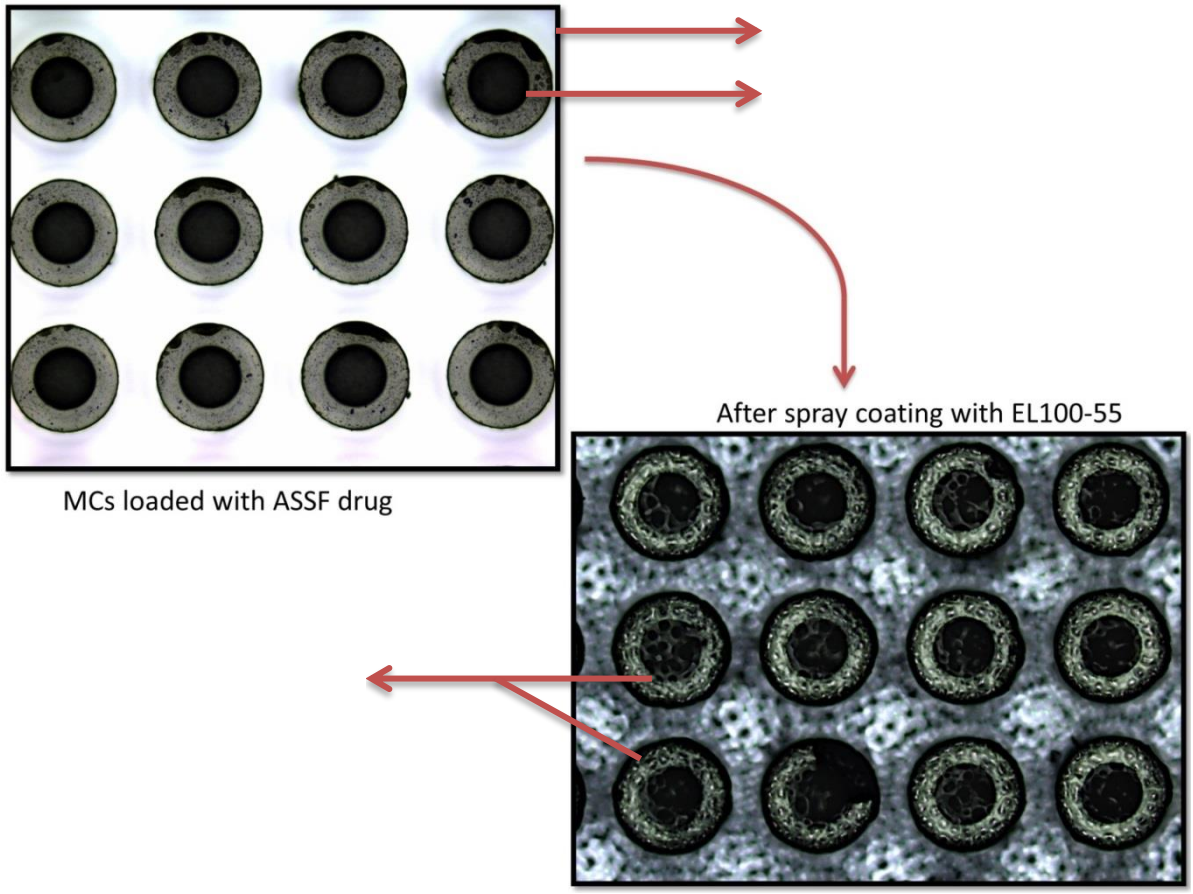

Fig. 4.9: *Optical microscopic view of MCs after loaded with ASSF and then, again after spray coated with 1% Eudragit L100-55 solution*

Following the lid formation, the lid morphology analysis was performed in supra SEM (Zeiss). The drug-loaded samples with polymeric lids were then carefully preserved in a sample holder box, kept inside a desiccator away from light for the release study in µDiss profiler, as the next step. On the other hand, the spray-coated plane silicon wafers without MCs were utilized for thickness measurement.

4.7 Lid Thickness Measurement in Stylus Profiler

A stylus profiler (Tecnor, Alpha-step IQ surface profiler) was used to measure the thickness of the lid for all the samples throughout this study. The sample or the polymer lid was spray coated in the middle part of a plane silicon wafer (Fig. 4.10 A) so that the stylus runs from one side of the silicon wedge to the other wedge where plane silicon would be present (Fig. 4.10 B and C). Thus considering both wedges of the plane silicon wafer as zero height level or ground, the measurement profile would calculate the

height or the thickness of the lid spray coated in the middle part of the wafer. Therefore, a center bias adjustment was chosen in the parameter settings, as presented in Table 4.5.

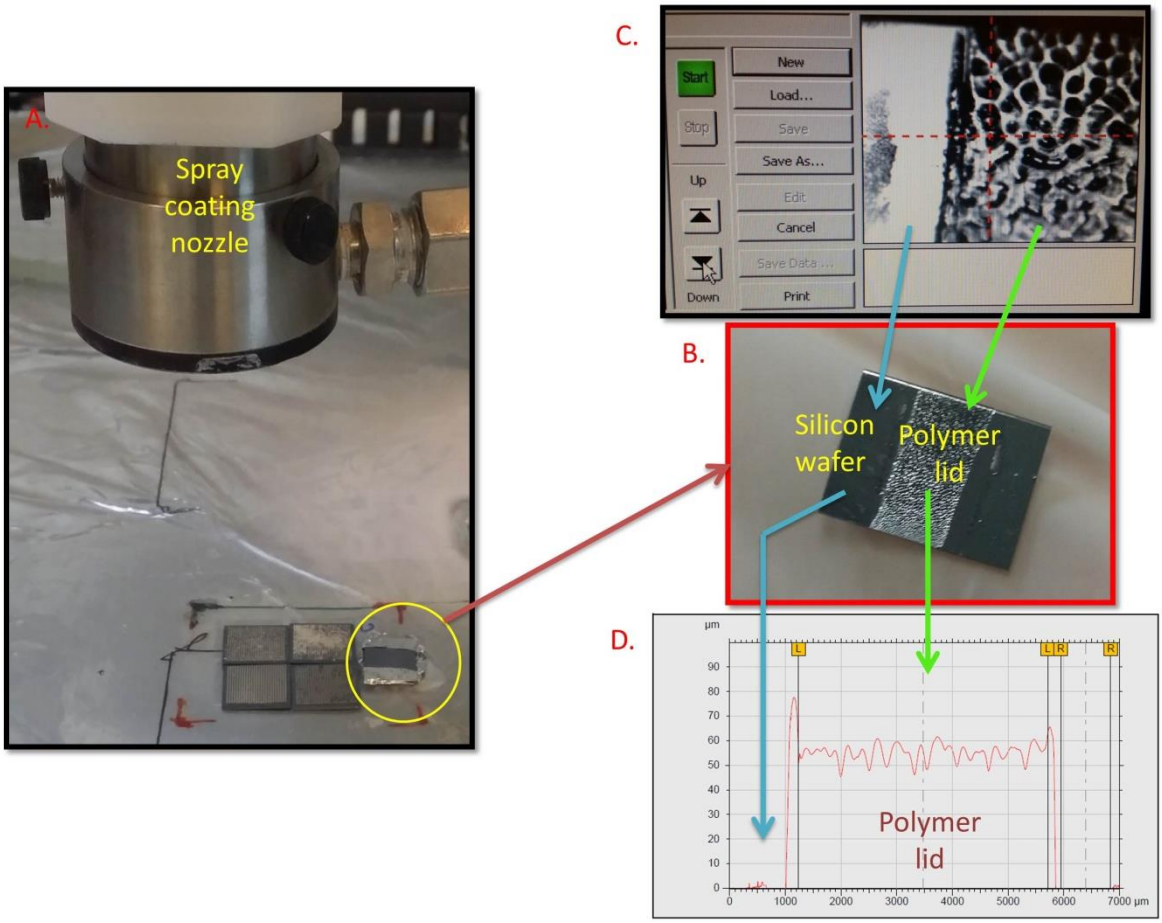

Fig. 4.10: A. *Sample (polymer lid) for thickness measurement has been prepared using spray coater;* ***B.*** *Sample for thickness measurement is ready to go into the stylus profiler;* ***C.*** *Video camera showing the movement of the stylus on the polymeric lid surface as indicated by a red crosshair;* ***D.*** *Thickness profile in the measurement window*

Table 4.5: *Parameter settings for thickness measurement of polymeric lids*

Parameters	Values
Scan length	5000-7000 µm
Scan speed	100 µm/s
Sampling rate	50 Hz
Resolution	2 µm
Sensor range	550 µm / 32.8 pm
Contact speed	3
Adjustment	Central bias

4.8 Lid Stability Test

Prior to performing the actual release study, the lid stability tests were done three times using glass slides, plane silicon chip with no MC and lastly, silicon chips containing SU-8 MCs with and without drug, in two separate pilot studies.

In the 1st pilot study, the lid stability tests were performed with glass slides in standing buffer solutions. When the results turned out positive, then in the 2nd pilot study, the lid stability was tested on magnetic stirring plate mimicking the actual release test parameters, such as rotation, temperature and volume of the release medium, in order to determine whether the polymeric lids of the ASSF-loaded MCs are stable and thus ready to go through the actual release test in a µDiss profiler.

4.8.1 Lid Stability Test in Standing Buffer Solutions

In the 1st pilot study, glass slides were spray coated with EL100-55 solution. In this test, firstly100 mM of phosphate buffer was prepared with pH 3.5 and pH 5.0, separately. The glass slide spray-coated with polymer lid was dipped into the phosphate buffer of pH 3.5 (pH of mice stomach (95)) for 2 hours and then the lid was analysed under an optical microscope (Zeiss). Next, the same sample was dipped into another phosphate buffer of pH 5.0 (pH of mice small intestine (95)) for 4-5 hours and was analysed again under the same microscope as shown in Fig. 4.11. Unlike the 2nd pilot study, the thickness measurement under the stylus profiler was not done during the 1st pilot study.

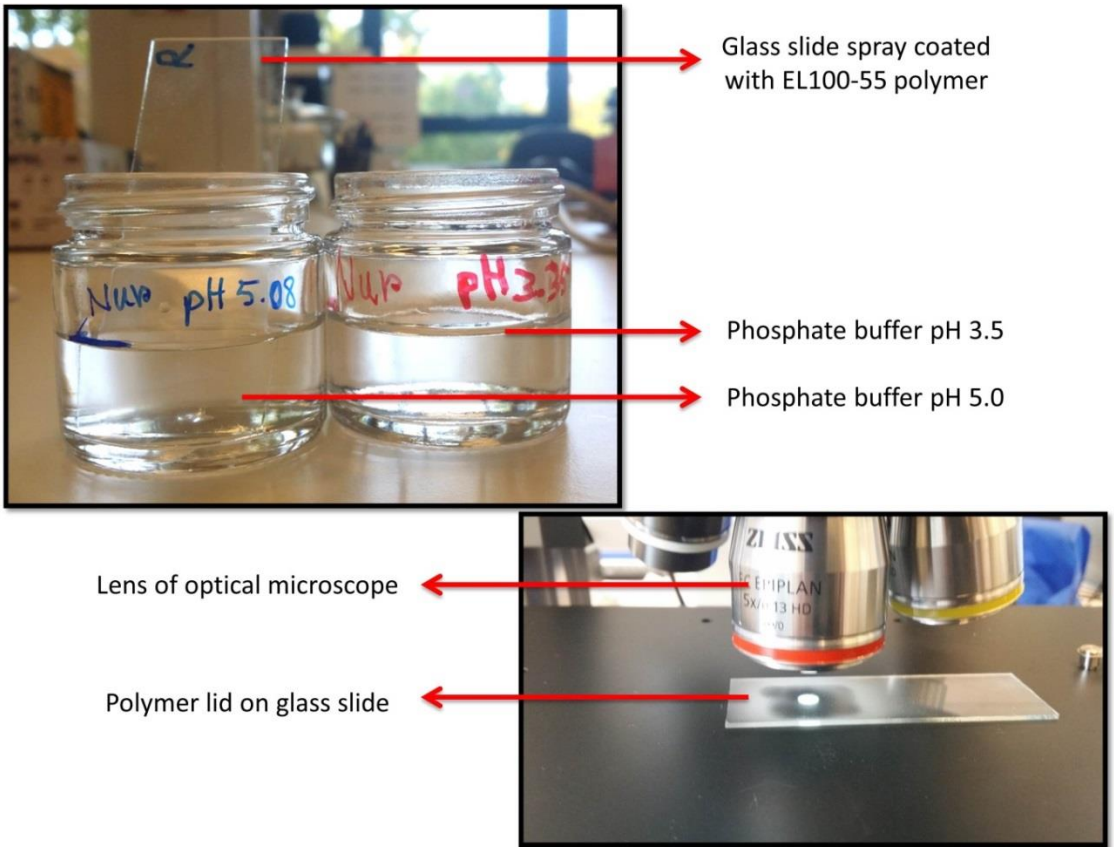

Fig. 4.11: *Lid stability test using glass slide in standing buffer solutions and then, the lid morphology analysis under an optical microscope*

In another stability test in standing buffer solutions, plane silicon wafer was used instead of glass slides. Also, double lids – both EL and chitosan polymers, were spray coated during this experiment as shown in Fig. 4.12. First of all, a part of the silicon wafer was covered with aluminum foil and then the wafer was spray-coated with chitosan solution. Then the aluminum foil cover was extended further to cover up half of the spray-coated chitosan lid. Once the half of the chitosan lid and the plane silicon wedge were secured, then the EL100-55 was spray coated. At the end of double spray coating, thus there were three different sections or surfaces on a single silicon wafer- 1. plane silicon surface; 2. chitosan lid surface; and 3. EL100-55 lid surface (Fig. 4.12).

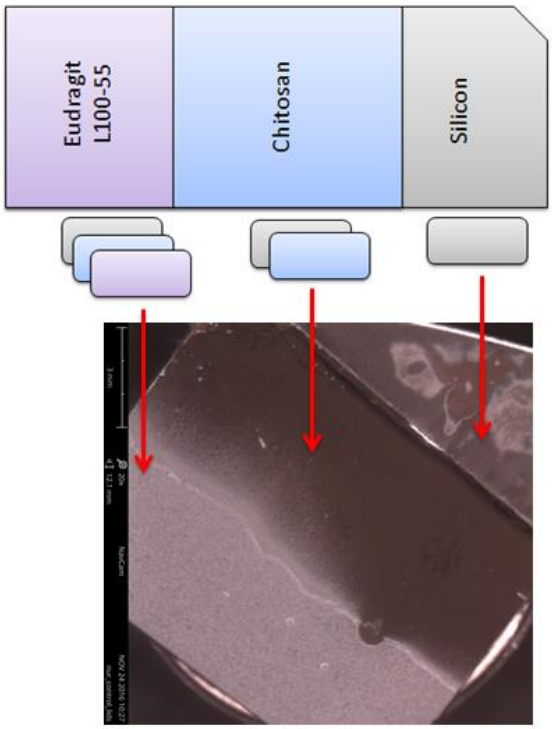

Fig. 4.12: *Spray coated double lids (EL and Chi polymers) on silicon wafer for lid stability analysis*

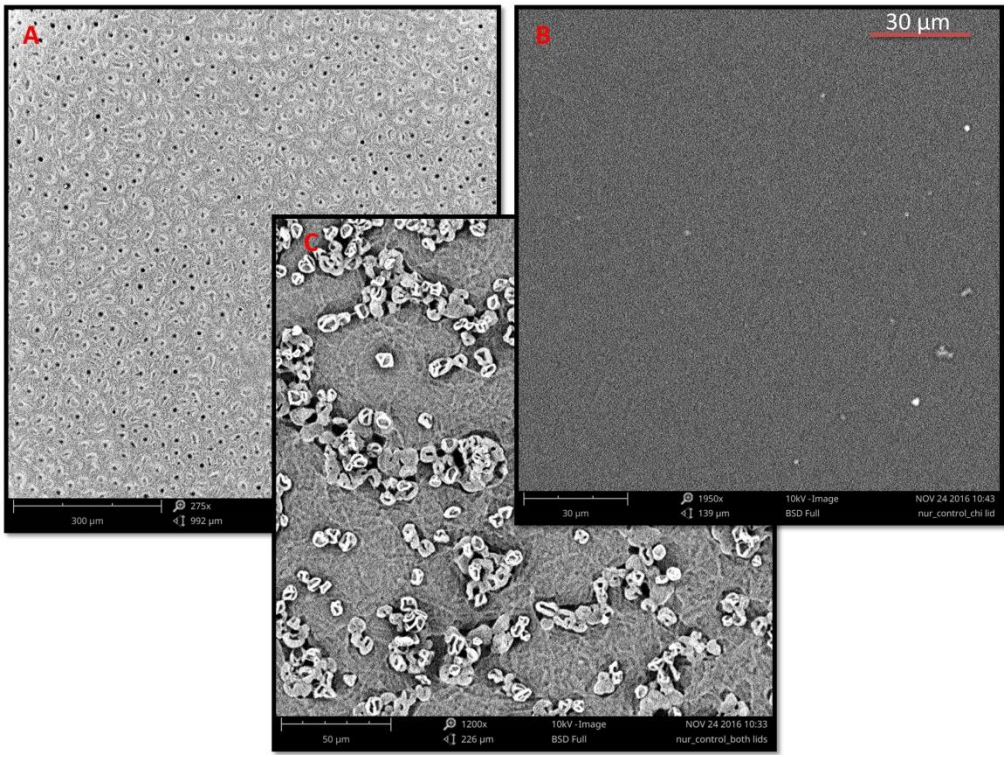

Fig. 4.13: *A. Eudragit L100-55 lid; B. Chitosan lid; C. A mixture of both EL and Chitosan lids on silicon wafer under a table top SEM view*

The lids were analyzed under table top SEM for morphology study. The SEM images presented in Fig. 4.13 show that the EL100-55 lid has many porous structures or shapes; whereas the chitosan lid looks very smooth and plain. The differences between these lids are more obvious and comparable in Fig. 4.13 C where both polymers mixed together during spray coating. The lid stability tests were run in both pH 3.5 and pH 5.0 similar to the samples on glass slides.

4.8.2 Lid Stability Test on Magnetic Stirrer

The 2nd pilot study of the lid stability test was quite similar to the Section 4.8.1. However, the difference with the previous pilot study was that instead of standing buffer solutions, magnetic stirrer was used mimicking some of the parameters of the real release study. In addition, the thickness of the stable EL lid and Chi lid were measured in a stylus profiler and their surface texture and smoothness were noted.

Following the lid formation and thickness measurements, the samples were exposed to 100 mM phosphate buffer at pH 3.5 for 2 hours and then at pH 5.0 for 5-7 hours. Similar to the actual release test in µDiss Profiler (Section 4.9), 37°C temperature, 100 rpm stirring speed and round µDiss stirring magnets were used during this study (Fig. 4.14).

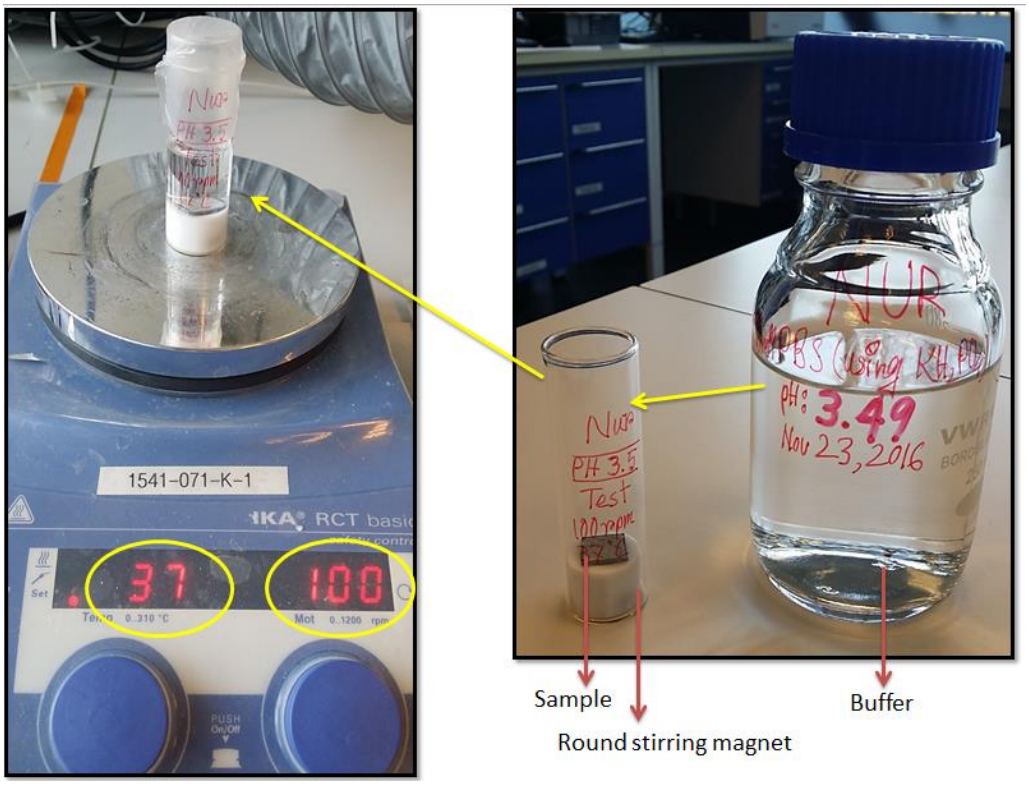

Fig. 4.14: *Lid stability test on magnetic stirrer with a rotation of 100 rpm and at 37 °C*

After the lid stability experiment, the samples were analyzed under an optical microscope (Zeiss) (Fig. 4.15). This experiment was repeated three times in order to confirm the stability of both the EL polymer lid and the chitosan lid.

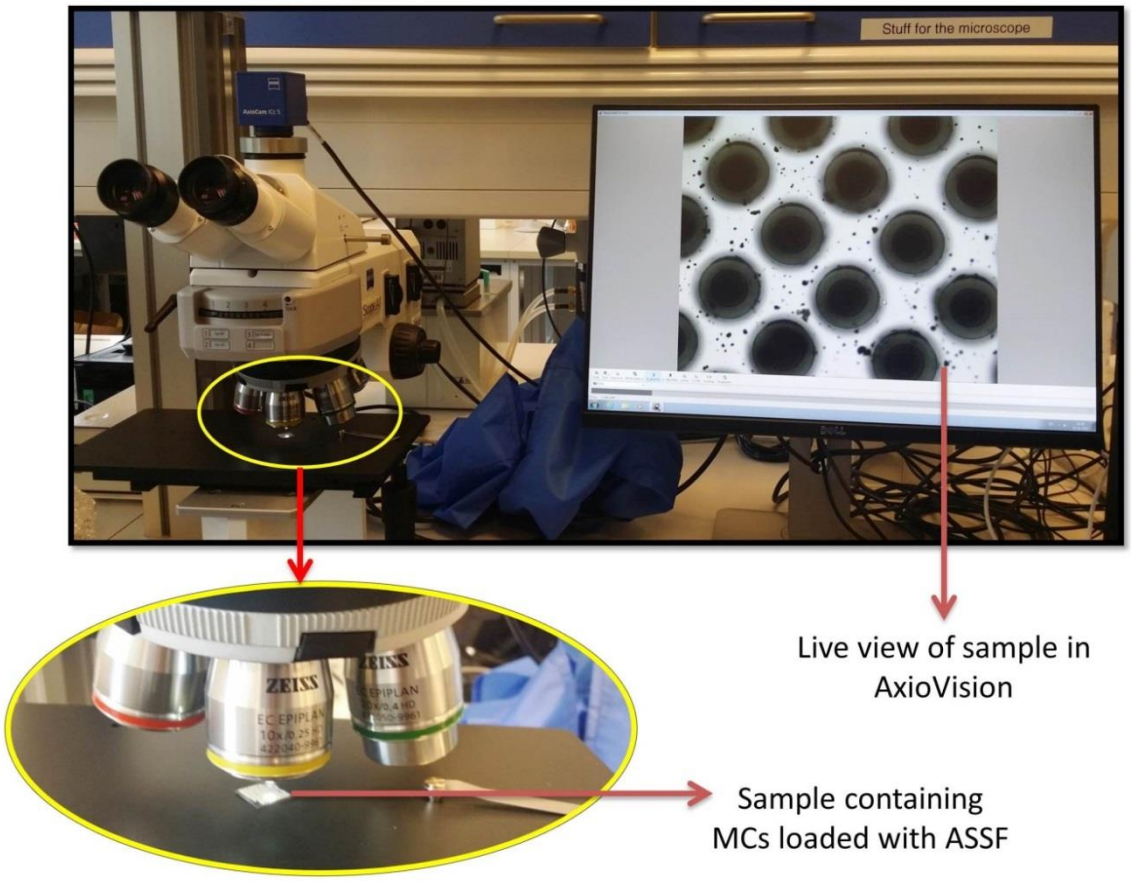

Fig. 4.15: *Sample analysis for lid stability test under optical microscope*

4.9 Drug Release in a µDiss Profiler

Following the lid formation and the successful lid stability pilot studies, the ASSF-loaded samples with polymeric lids were ready for the drug release test in a micro dissolution apparatus. The instrument consisted of a µDiss Profiler (Pion Inc), a UV spectrophotometer (Rainbow Dynamic Monitor System) and a mini batch (Struers KEBO Lab Julabo). The temperature of mini batch should be adjusted according to the requirement of the experiment and for this study, it was set as 37 °C. Fig. 4.16 shows the µDiss Profiler apparatus used during the entire study.

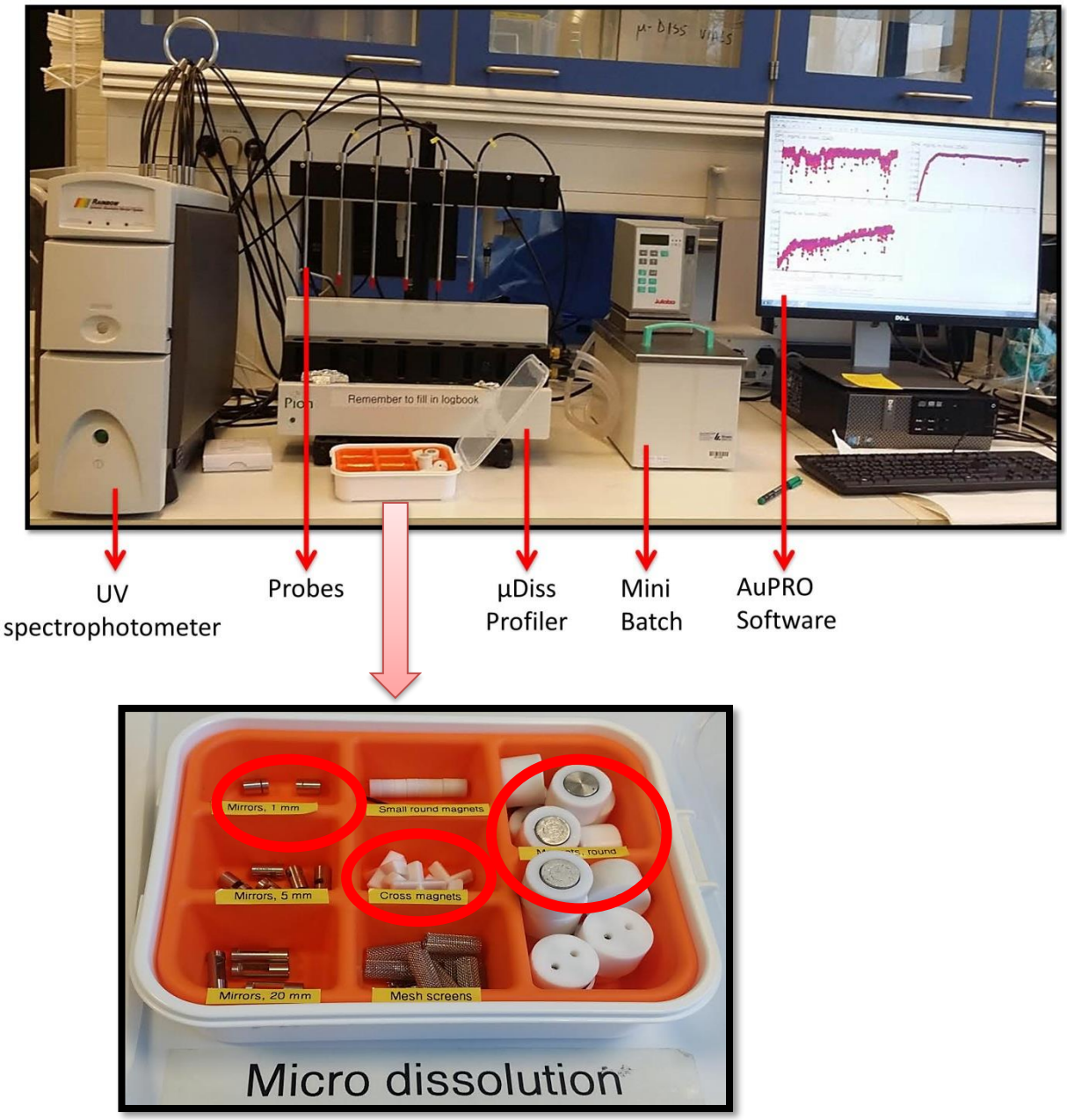

Fig. 4.16: *Micro Dissolution profiler and its parts for drug release test*

Cross magnets were used during making standard curves and round magnets were used in release test percentage dissolution curves. However, 1 mm mirrors were used for all of the release tests during both standard and dissolution curves.

Chemicals needed for the release test were Furosemide (Fagron), Potassium Phosphate Monobasic or KH_2PO_4 (Sigma), PBS tablet (Sigma-Aldrich), 5M NaOH, 1M HCL and MiliQ water. The methods for preparing the buffer and standard solutions are described below.

4.9.1 Preparation of Phosphate Buffers

2.72 g of KH_2PO_4 was used in miliQ water to prepare 200 ml of 100 mM phosphate buffers (Fig. 4.17). The appropriate pH value was adjusted by using either 1M HCL for or 5M NaOH.

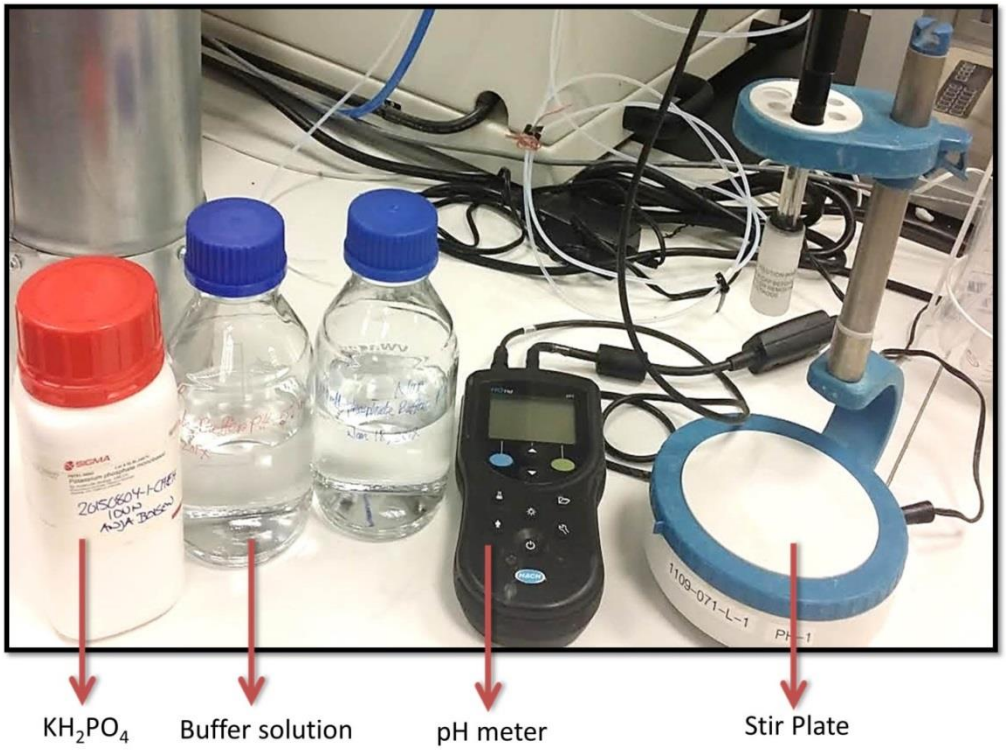

Fig. 4.17: *Preparation of phosphate buffer and pH adjustment*

4.9.2 Preparation of Furosemide Standard Solution

250 mg of furosemide was weighed using a micro-balance and then a glass volumetric flask of 25 ml was used to dissolve the furosemide in miliQ water with a final volume of 25 ml. In this procedure, few drops of 5M NaOH were added to the solution to dissolve the furosemide prior to volume adjustment. Thus, 30.2 mM final concentration of the furosemide standard solution with a pH of approximately 10 was achieved.

4.9.3 Preparation of Standard Curves

Before the drug release experiment, standard curves were prepared in order to construct reference data points for UV absorbance spectra of the actual drug release. In this process, 10 ml of buffer solution (either pH 3.5, or 5, or 6.0) was added into each µDiss

vial with star magnet, followed by placing them into the µDiss profiler. After the probes were connected and placed in the buffer medium, the instrumental software (Au PRO 5.1) was run for setting the necessary parameters as presented below in Table 4.6.

Table 4.6: *Parameter settings for µDiss profiler*

Parameters	Values
Volume in Vials	10 ml
Temperature	37 °C
Detection Range	310-350 nm
Baseline	710 nm
Mirror or Path Length	1 mm
Stirring Speed	100 rpm
Molecular weight	331.0 g/mol
Units of spectra	mg/ml

Next, a blank data point and then the standard data points were collected by adding furosemide standard solution into the buffer medium stepwise to collect spectrum for varying concentration and volume. For the standard curve in pH3.5, a range of concentration from 0.01 mg/ml to 0.2 mg/ml was chosen; whereas it was 0.04975 mg/ml to 1.6667 mg/ml for pH 5, or pH 6 (APPENDIX A).

4.9.4 Release of ASSF from MCs and Preparation of Dissolution Curves

For the drug release experiments, similar setup as described in (39, 41) were used. Five different protocols (Table 4.7) were used in order to test the efficacy of different lids. For the different protocols the required pH specific standard curve was used for preparing the dissolution curves.

Table 4.7: *List of six different protocols for drug release test used multiple times to test both the stability of the polymer lids and the release of drug at targeted pH*

Protocol	Purpose	Polymer Lid	Duration	pH	Buffer
1	ASSF drug release from SU8 MCs	No Lid	21 hours	6.5 (e.g human small intestine)	Phosphate buffer
2	pH sensitivity of EL lid in mice stomach	Eudragit L100-55 (plasticizer: TEC)	2 hours	3.5 (e.g mice stomach)	PBS
			5 hours	5.0 (e.g mice small intestine)	
3	pH sensitivity of EL lid in wild mice intestine	Eudragit L100-55 (plasticizer: DBS)	2 hours	3.5 (e.g rat stomach)	Phosphate buffer
			5 hours	6.0 (e.g rat small intestine)	
4	Capability of chitosan lid to disperse drug in mice intestine	Chitosan	5-10 hours	5.0 (e.g mice small intestine)	Phosphate buffer
5	pH sensitivity and lid stability test of EL-Chitosan double layer lids	Eudragit L100-55 (plasticizer: DBS) and Chitosan	2 hours	3.5 (e.g rat stomach)	Phosphate buffer
			13 hours	6.0 (e.g rat small intestine)	
6	Development of pH sensitive (EL lid) adjuvant based polymer lid (Chitosan-MPLA)	Eudragit L100-55 (plasticizer: DBS) and Chitosan-MPLA	2 hours	3.5 (e.g rat stomach)	Phosphate buffer
			19 hours	6.0 (e.g rat small intestine)	

Following the parameter settings, the samples were loaded into the µDiss profiler. As shown in Fig. 4.18, the drug-samples with polymeric lids were attached to the µDiss round magnets with the help of carbon pad and then were put in each vial and the vials were placed inside the µDiss profiler. 10 ml of 100 mM phosphate buffer were poured into each vial and then were airtight with parafilm and wrapped with aluminum foil in order to avoid light exposure during the release test. After the data point collection of

the drug release concentration was done, the drug dissolution % or percentage release was calculated in excel using the formula below.

$$Drug\ Dissolution\ \% = \frac{Drug\ concentration\ in\ release\ medium\ over\ time\ (mg/mL)}{Drug\ Concentration\ (mg/mL)} * 100$$

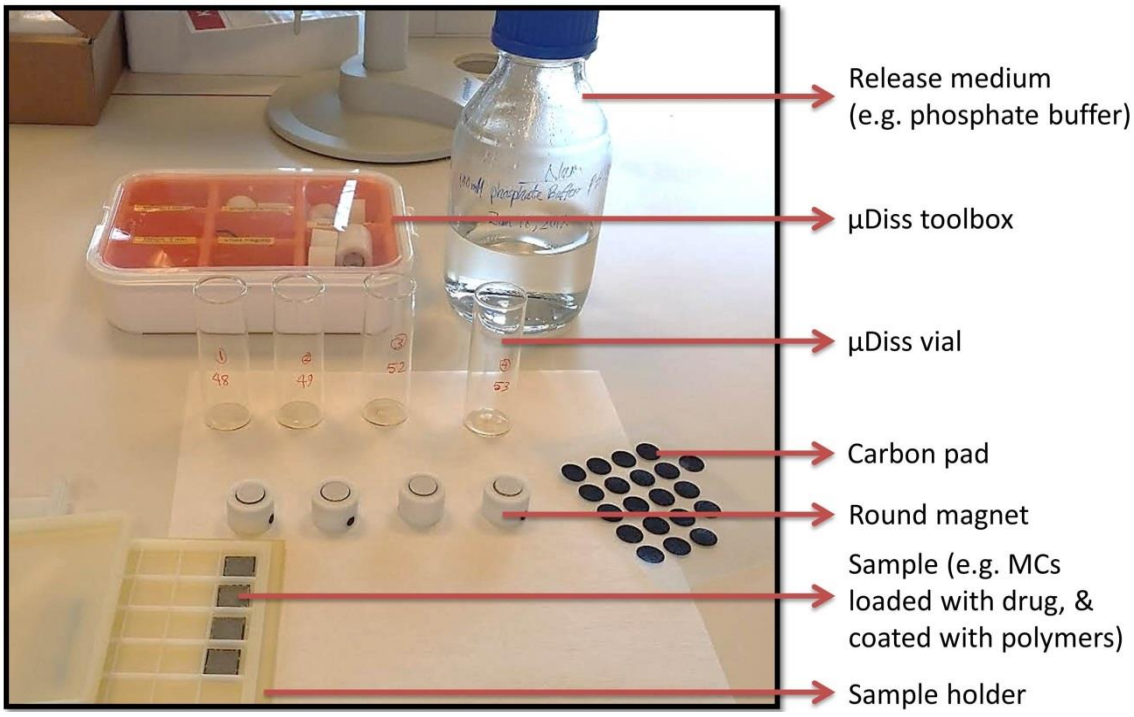

Fig. 4.18: *µDiss experimental setup for sample placement*

After each release test, the lid morphology and stability of the samples were analysed in SEM (Supra 40VP Gimini). In cases of those experiments involved in more than one pH medium as indicated in Table 4.7, after each release test it was highly important to perform the lid morphology study in order to determine if the experiment should further proceed for another pH medium. For example, if the lid was dissolved in gastric pH of 3.5, then it would be pointless to run the release test further in the small intestine pH medium (pH 6.0).

4.10 MPLA Detection in XPS

For detecting the presence of adjuvant MPLA incorporated into the chitosan polymer lid, x-ray photoelectron spectroscopy (XPS, K-Alpha, Thermoscientific) was used. Three types of samples were prepared for the XPS detection. i. Piece of plain silicon wafer as a blank sample; ii. Silicon wafer spray coated with chitosan solution (Subsec-

tion 4.4.3) as a control; and iii. Silicon wafer spray coated with chitosan-MPLA adjuvant solution (Subsection 4.4.4).

XPS samples have to be completely dry and stick to the sample holder tightly using small clips as shown in Fig. 4.19. Likewise SEM, the analysis chamber was vent prior to sample loading in the load-lock and the stage was pumped down after the loading using the instrumental software (Avantage; version 5.948). After the stage is pumped down to base pressure, the position is called the parking position. Next, the sample holder gets transferred to the stage inside the analysis chamber. The software window shows a platter view of the sample holder displaying the attached samples on it, and below that, a magnified live view of the analysis points. Once the experiment was run, the "Current Data View" showed the spectrum that was being recorded.

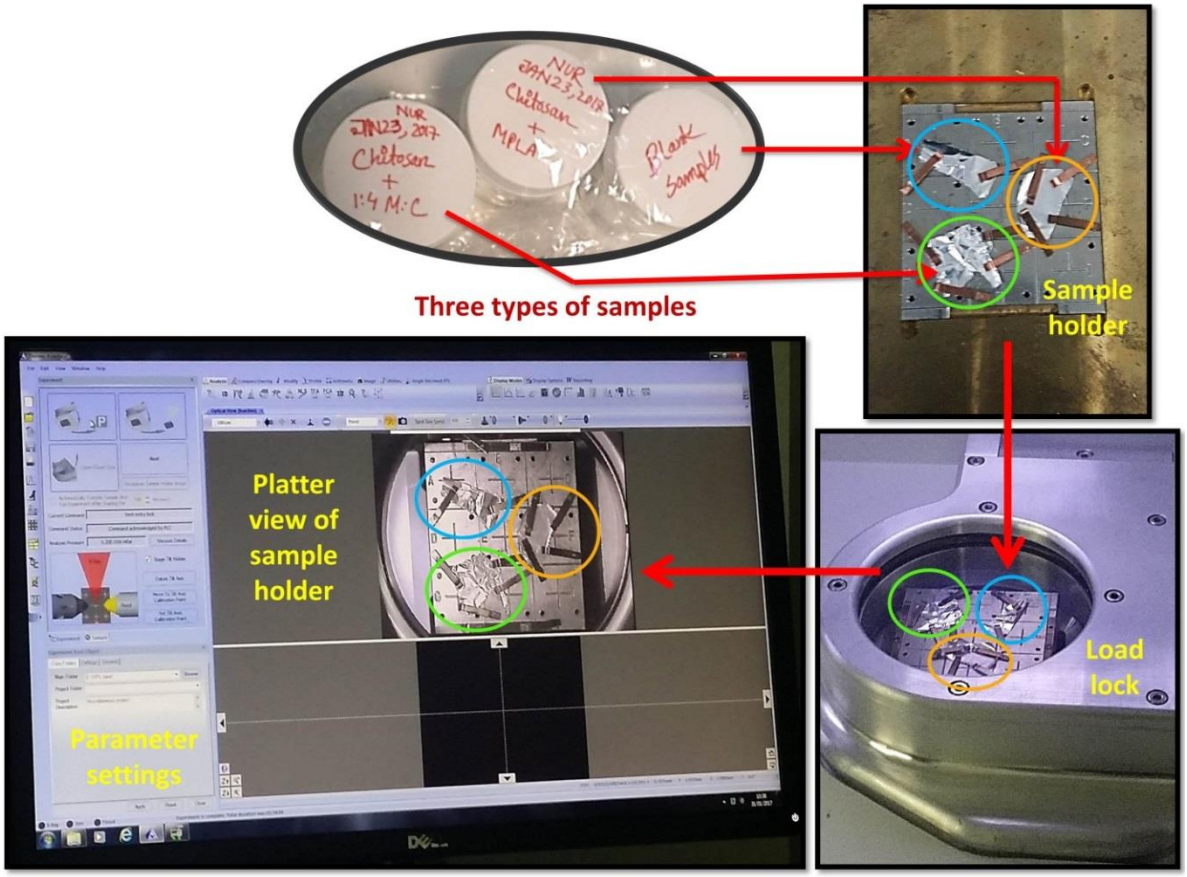

Fig. 4.19: *Samples loading and viewing in XPS equipment*

After the analysis, the samples were transferred back to the load-lock and the equipment was vent. After taking the samples out of the holder, the empty sample holder was put back into the load lock in order to minimize degassing from the sample holder followed by pumping down the stage.

5. RESULTS AND DISCUSSIONS

5.1 ASSF Drug Production Yield

ASSF was produced by spray drying using two different protocols where the optimized protocol contained 25% larger amount of each chemical. Table 5.1 below presents the percentage yield of ASSF using the two protocols for a total of 4 batches of production. The yield from the various batches of ASSF was approximately between 62% and 74 %.

Table 5.1: *%Yield of ASSF during different experiments*

Protocol#	Experiment#	Date of Production	Yield %	Average % yield	Standard Deviation
1	1-a	05-10-2016	61.5	63.75	3.18
	1-b	26-10-2016	66		
2	2-a	10-11-2016	73	73.4	0.56
	2-b	06-12-2016	73.8		

The results in Table 5.1 show that the new optimized protocol is more efficient since it has 73.4 +/- 0.56 % yield on average which is much higher in compared to the previous protocol.

5.2 Loading of Microcontainers

Loading of microcontainers with the embossing method was successful and the loading resulted in a load of about 4.2 µg of ASSF per MC on average. Using shadow mask for loading MCs, prevented deposition of drug in the empty space between MCs and thus, ensured precise loading. As shown in Fig. 5.1, SEM images were taken after the loading to ensure proper loading and notes were made regarding the loading quality.

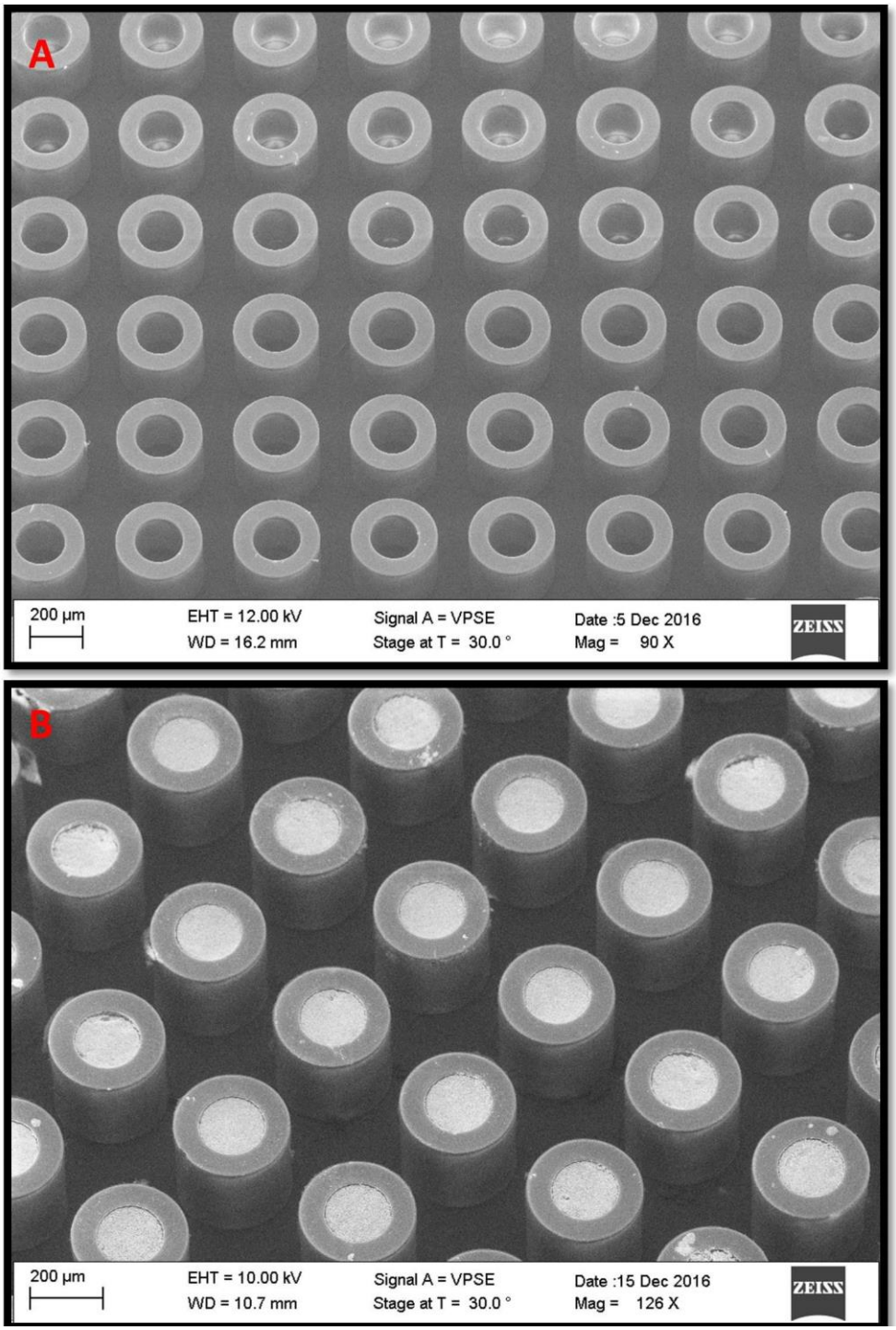

Fig. 5.1: A. *SEM images of empty MC;* ***B.*** *MCs loaded with ASSF using shadow mask*

Nevertheless, the loading was variable, due to several factors. For example, if the shadow mask is not properly clipped on the sample, then the loading would not be precise and there would be drug deposition in between MCs and some MCs would be partially loaded, or completely unloaded. Also, some MCs might fall off, or even the silicon chip

might get broken due to misalignment of the shadow mask and the MCs. As a result, it would give a wrong estimation of amount of drug loaded into each MC, as well as a biased drug release curve in the µDiss experiment.

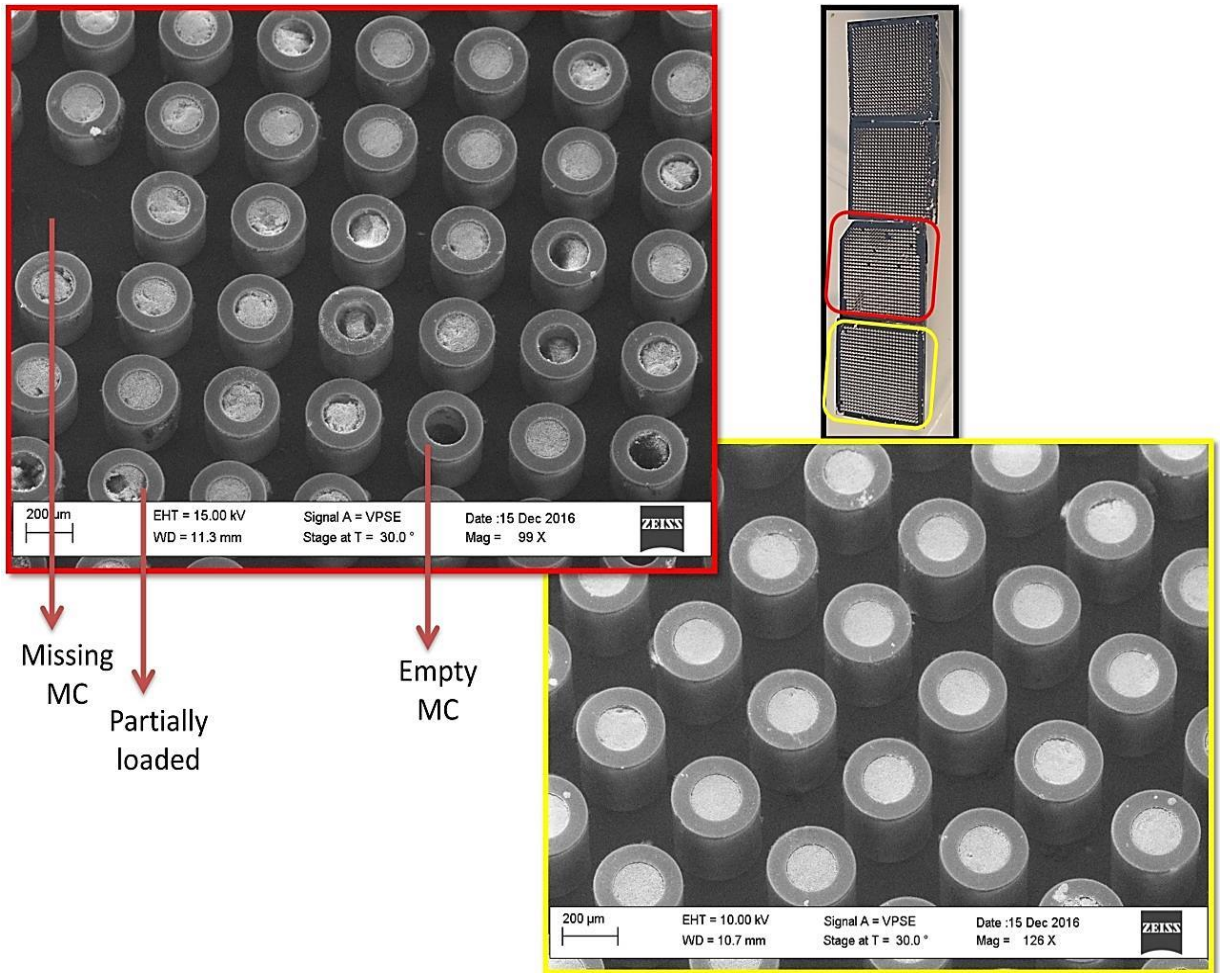

Fig. 5.2: *SEM images showing improper sample loading (red) and properly loaded sample (yellow)*

Another factor was the surface condition of the shadow mask. Sometimes, due to using the same shadow mask for a long time, the shadow mask surface becomes rugged which also results in the above unfavorable circumstances, and thus biased release test results. Fig. 5.2 presents the SEM images of both a properly loaded and a poorly loaded samples. APPENDIX B contains more images of ASSF loading using powder embossing method and APPENDIX C presents different shadow masks.

Nonetheless, using shadow mask in powder embossing method has been proven effective in a recent literature (80), where other drugs such as cubosomes and PVP were loaded successfully for vaccine delivery.

5.3 Drug Release from MCs without Lid

ASSF release from MCs without lid was performed to investigate if the drug can be released from the SU-8 microcontainers into the medium of pH 6.5 for 21 hours. In this study, phosphate buffer of pH 6.5 was chosen as the release medium in order to mimic the drug release in human small intestine. Fig. 5.3 shows the drug release over time from five different µDiss channels for five individal samples and the gray curve represents the average of these five release curves.

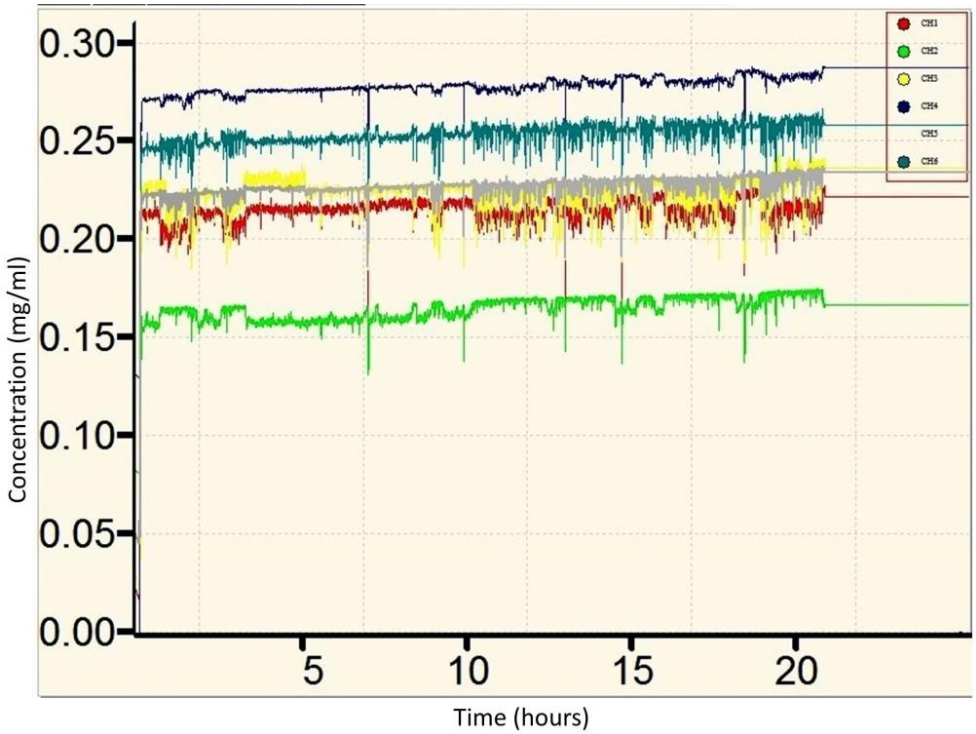

Fig. 5.3: *Release Test of ASSF drug from SU-8 MCs in 100mM phosphate buffer of pH6.5 medium*

Except channel 2 (green curve), the other channels show very good drug release in pH 6.5 medium. The reason of this exception might be an improper loading of the sample which ends up with less loaded drug and thus less release (APPENDIX B). Since there is no lid used on top of the MCs, therefore immediate and very fast drug release was observed from the all the samples. These results replicate the results of similar literature in (43).

Unlike this experiment, in the following release tests with lids, the amount/weight of loaded drug in each sample was recorded prior to spray coating, so that the percentage dissolution of drug release can be calculated after the release test.

5.4 pH-Sensitivity and Drug Release Test with Chitosan Lid

After the chitosan lid formation on the ASSF-loaded MCs, SEM investigation was done to analyze and record the lid morphology. The SEM images in Fig. 5.4 show that the chitosan lid was very smooth and homogenously formed over the MCs.

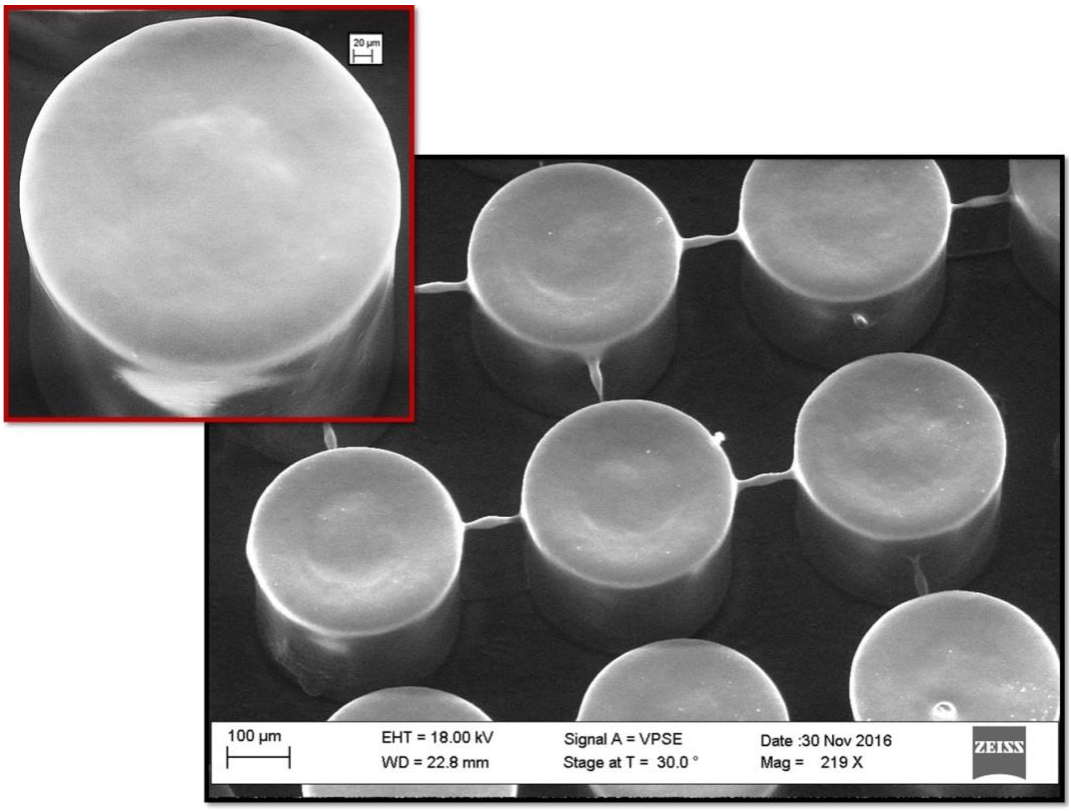

Fig. 5.4: *Chitosan lid morphology analysis under SEM*

Following the morphology analysis, the lid thickness was measured using stylus profiler (Fig. 5.5). The average thickness of the chitosan lid was found 6.62 +/- 0.29 µm in this experiment which is reproducible. This experiment was repeated three times with 5 samples in each, and the average thickness of chitosan lid was recorded as 6.20 +/- 0.3 µm.

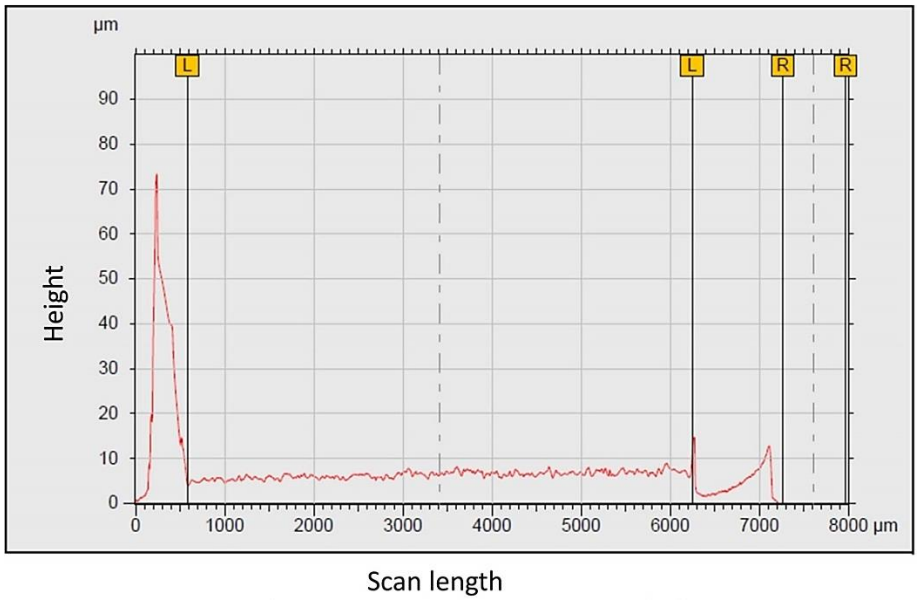

Fig. 5.5: *Thickness measurement of chitosan lid on average*

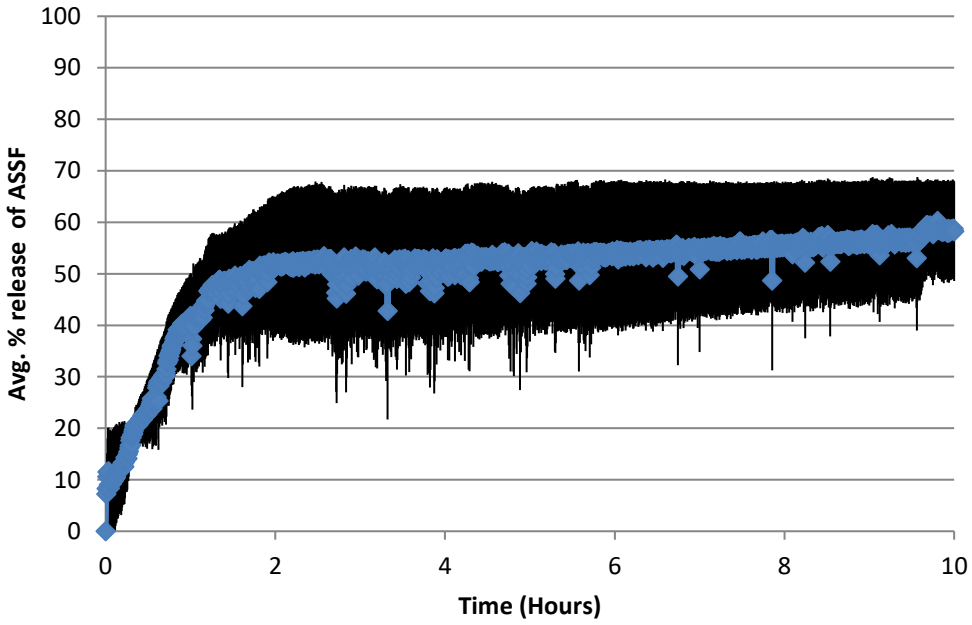

Fig. 5.6: *Release of ASSF from MCs coated with chitosan lid in phosphate buffer pH5.0 for 10 hours. The data represents the mean of 5measuremets±SD.*

After the thickness measurement, the samples with chitosan lid were tested in the release medium of pH 5.0 for the drug release in a µDiss profiler over 10 hours. The average dissolution results are plotted in Fig. 5.6 which shows that the avg. % of drug release almost saturates after 2 hours, and then there is a negligible increase in the release trend between 7 and 10 hours. This experiment however had issues like APPENDIX D

(Fig. D: A), and therefore it showed a lower release % compared to the other chitosan lid experiments. Similar release test performed in pH 6.0 medium, demonstrated above 85% of release over 7 hours (Section 5.8).

Chitosan lid morphology was analyzed after 5 and 10 hours of drug release in phosphate buffer of pH 5.0 which are depicted in Fig. 5.7 below.

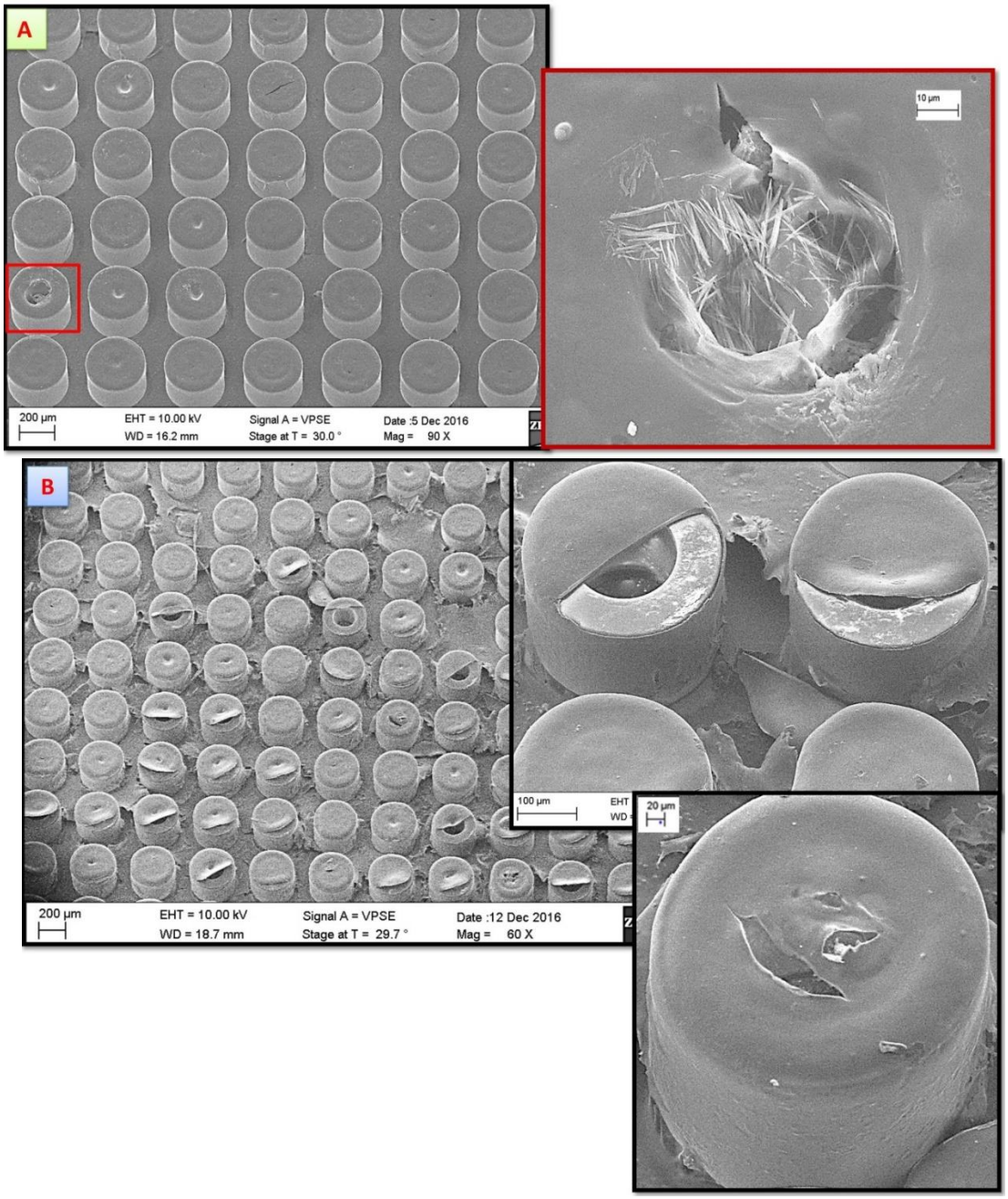

Fig. 5.7: A. *Morphology of Chitosan lid after 5 hours of release test in phosphate buffer of pH 5.0;* ***B.*** *Chitosan lid after 10 hours of release test in phosphate buffer of pH5.0.*

In comparison to the chitosan lid in pH 5.0 after 5 hours in Fig. 5.7A, the lid morphology in Fig. 5.7B after 10 hours of release seems to be more lifted off the samples and also there are more holes and scars in the chitosan lid. In addition, some crystalline furosemide can be seen through the holes of MCs after the 5 hours of release test, whereas, after 10 hours, almost no furosemide was found. This phenomenon complies with the average % release curve in Fig. 5.6 showing slight increase in the drug release. However, since the release of the drug after 10 hours experiment is not significantly different from the drug release after 5 hours, therefore, it suggests that most drug was released into the medium by 5 hours. Therefore, for the next chitosan release test, 5-7 hours of duration was chosen, instead of a 10 hours long experiment.

5.5 pH-Sensitivity and Drug Release Test with Eudragit Lid

This section is divided into three subsections, where in the 1st subsection, the major results of the two pilot studies from Section 4.8 conducted to determine lid stability are shared. In this subsection, the EL100-55 lid morphology analysis after and before pH-sensitivity test on standing buffer media from the 1st pilot study is discussed. Here, the pH-sensitivity of the EL100-55 lid was determined based on its stability in gastric medium (e.g. pH 3.5) and dissolution in small intestinal medium (e.g. pH 5.0 and pH 6.0). In addition, this subsection also presents the average thickness measurements of EL100-55 lid from the 2nd pilot study of the lid stability test.

In the 2nd subsection, the pH-sensitivity and the drug release capacity of EL100-55 lids with 15%TEC plasticizer are analyzed, where different CNTR of coating and thus different lid thicknesses are examined. On the other hand, the 3rd subsection of Section 5.5 discusses the efficiency of the pH-sensitive EL100-55 lid with 5% DBS plasticizer in terms of its drug release capacity in pH 6.0 medium.

Lastly, the Section 5.5 ends with a summarized comparison table of different EL100-55 lids in terms of their plasticizer, thickness, stability in gastric medium and drug dissolution capacity in small intestinal medium.

5.5.1 Analysis of EL Lid on Glass Slide and its pH-Sensitivity Test Results

This section analyzes the results from the lid stability tests mentioned in Section 4.8.1, performed using glass slides on standing buffer media of pH 3.5 and pH 5.0, respectively.

After spray coating the EL100-55 solution on glass slide, half of the slide was dipped into the 100mM phosphate buffer solution of pH 3.5 for 2 hours first and then it was analysed under the optical microscope (Zeiss) as shown below in Fig. 5.8.

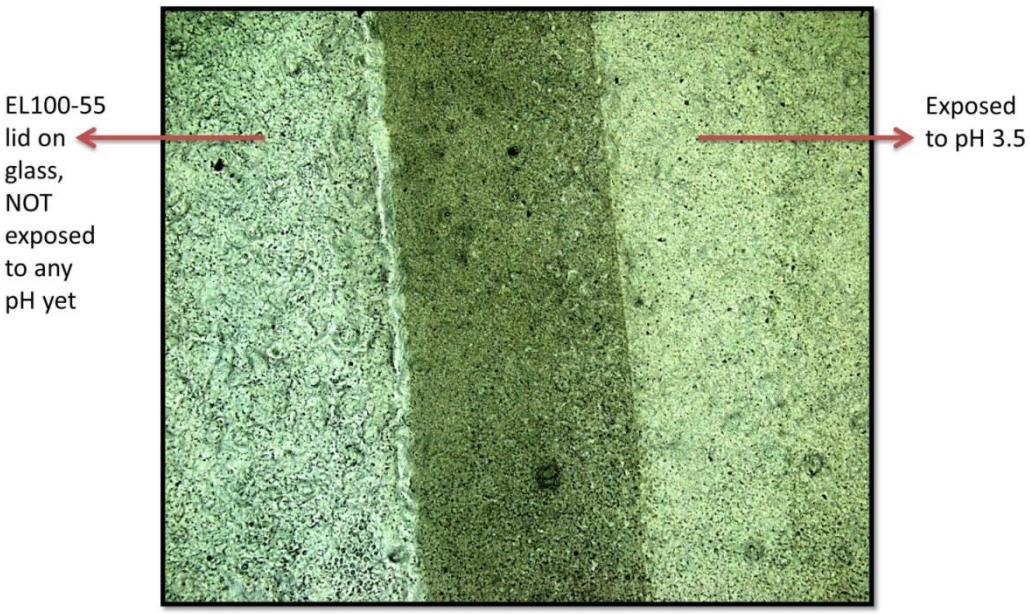

Fig. 5.8: *The EL lid on glass slide exposed to phosphate buffer pH3.5 for 2 hours*

No significant difference was visible after the exposure of the EL lid to pH 3.5 medium which is the gastric pH of mice, and thus the finding meets the hypothesis that the EL lid remains stable in gastric medium.

Then the same part of the glass slide was dipped into 100mM phosphate buffer of pH 5.0 for 5 hours and the optical microscopic view of the lid morphology is presented in Fig. 5.9 below.

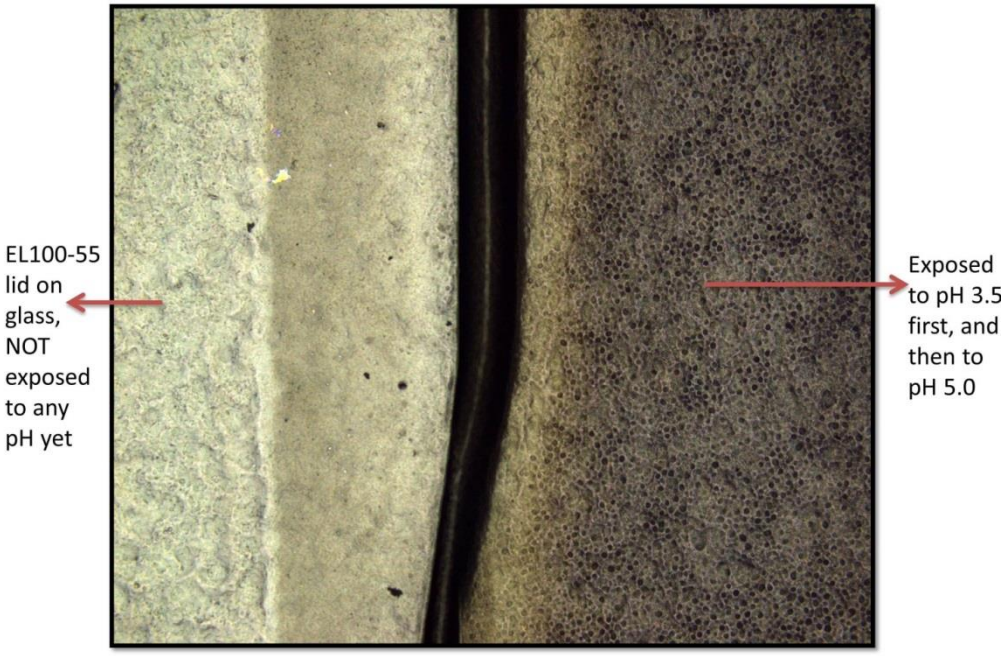

Fig. 5.9: *The EL lid on glass slide, which was exposed to pH 3.5 for 2 hours earlier, is now exposed to phosphate buffer pH 5 for 5 hours*

Unlike Fig. 5.8, the optical microscopic view of the above lid in Fig. 5.9 shows big pores or porous structures on the EL lid. It indicates that the EL has started to decay and it is no longer as stable as before. However, the hypothesis was that the lid would completely be dissolved in pH 5.0 medium, the small intestinal pH of mice, and thus the encapsulated drug from microcontainers would be released in the small intestine.

Nevertheless, as the lid is partially dissolved with many porous structures on it, the next trial experiments focused on the lid thickness as well as the spray coating CNTR or number of passes in order to develop a lid with convenient thickness which would probably meet the hypothesis. The Fig. 5.10 captures the event in a nutshell.

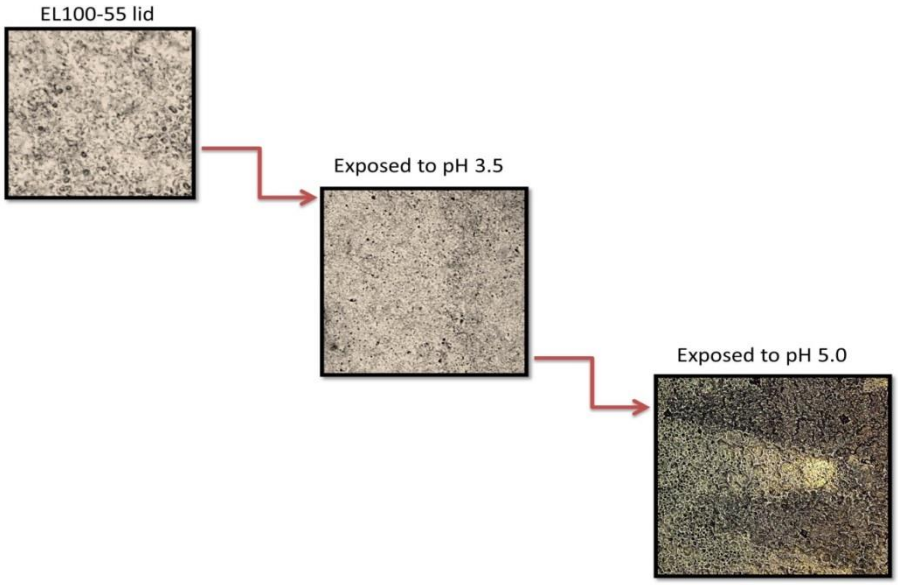

Fig. 5.10: *Eudragit lid stability and pH sensitivity test on a glass slide in phosphate buffer solution of pH 3.5 and pH 5.0*

Similar to the 1st pilot study, the lid morphology analysis of the 2nd pilot study on ASSF-loaded and EL coated samples proves part of the hypothesis that the EL lid remains intact in the gastric pH value. However, it does not dissolve in the small intestinal pH value and thus partially meets the hypothesis. The results are presented in Fig. 5.11 below.

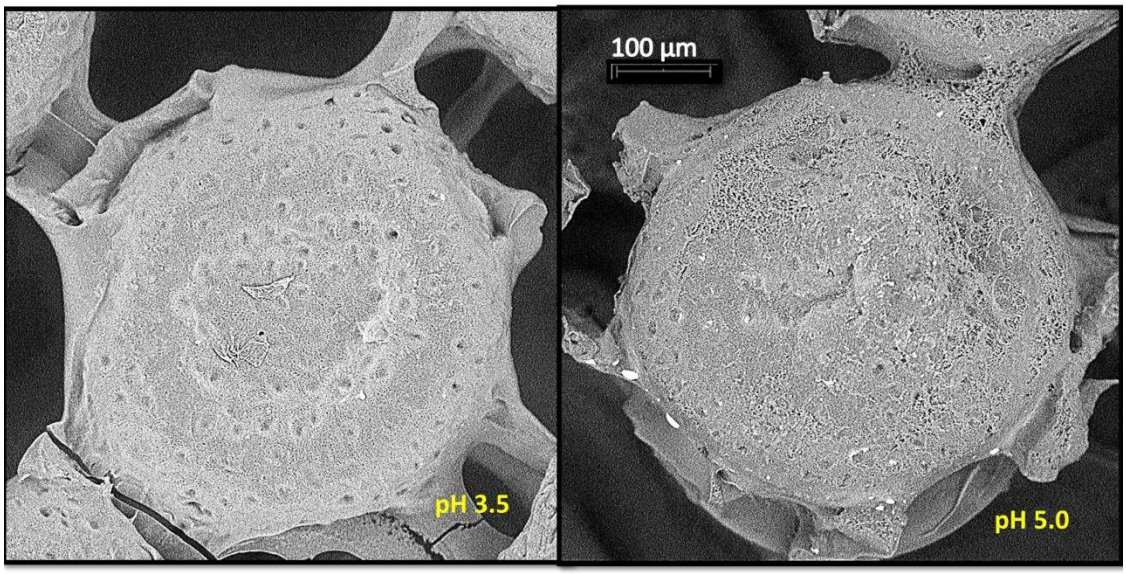

Fig. 5.11: *The stability and pH sensitivity test of ASSF-loaded MC coated with EL100-55 lid on a magnetic stirrer in 100mM phosphate buffer solutions of pH 3.5 for 2 hours and of pH 5.0 for 5 hours, respectively*

The thickness of this EL100-55 lid measured in stylus profiler was found 65.8 +/- 1.8 µm on average of 10 measurements (Fig. 5.12).

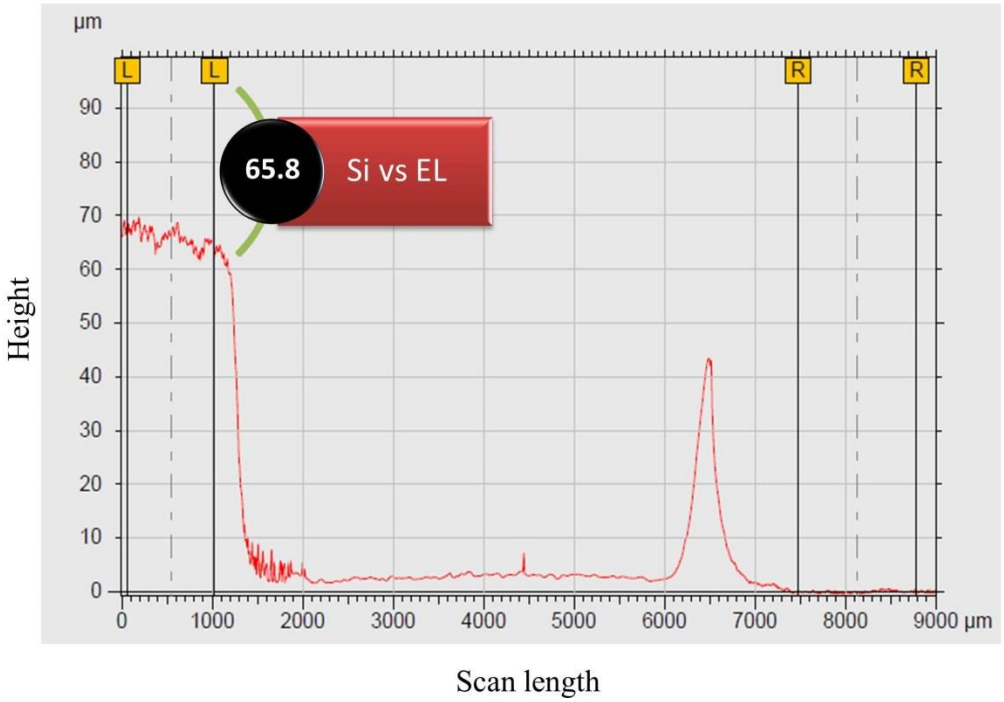

Fig. 5.12: *Thickness measurements of EL100-55 lid using a stylus profiler*

In Fig. 5.12, the x-axis shows the scan leanth of stylus profiler and the y-axis is the height or thickness of the polymer lids. The scan area from 0-1400 µm indicates the area covered by Eudragit lid, whereas 8000-9000 µm is the plane silicon surface.

Following these pilot studies, EL100-55 lid was tested *in vitro* in µDiss profiler to investigate the drug dissolution from MCs coated with the EL lid in different pH media as described in the following subsections.

5.5.2 Analysis of Eudragit L100-55 lid containing TEC Plasticizer

1% w/v EL100-55 solution mixed with 15% w/w TEC was spray coated on top of the ASSF-loaded MCs to form the pH-sensitive EL lid. Fig. 5.13 shows the SEM investigation of the EL lid spray coated with a CNTR of 60.

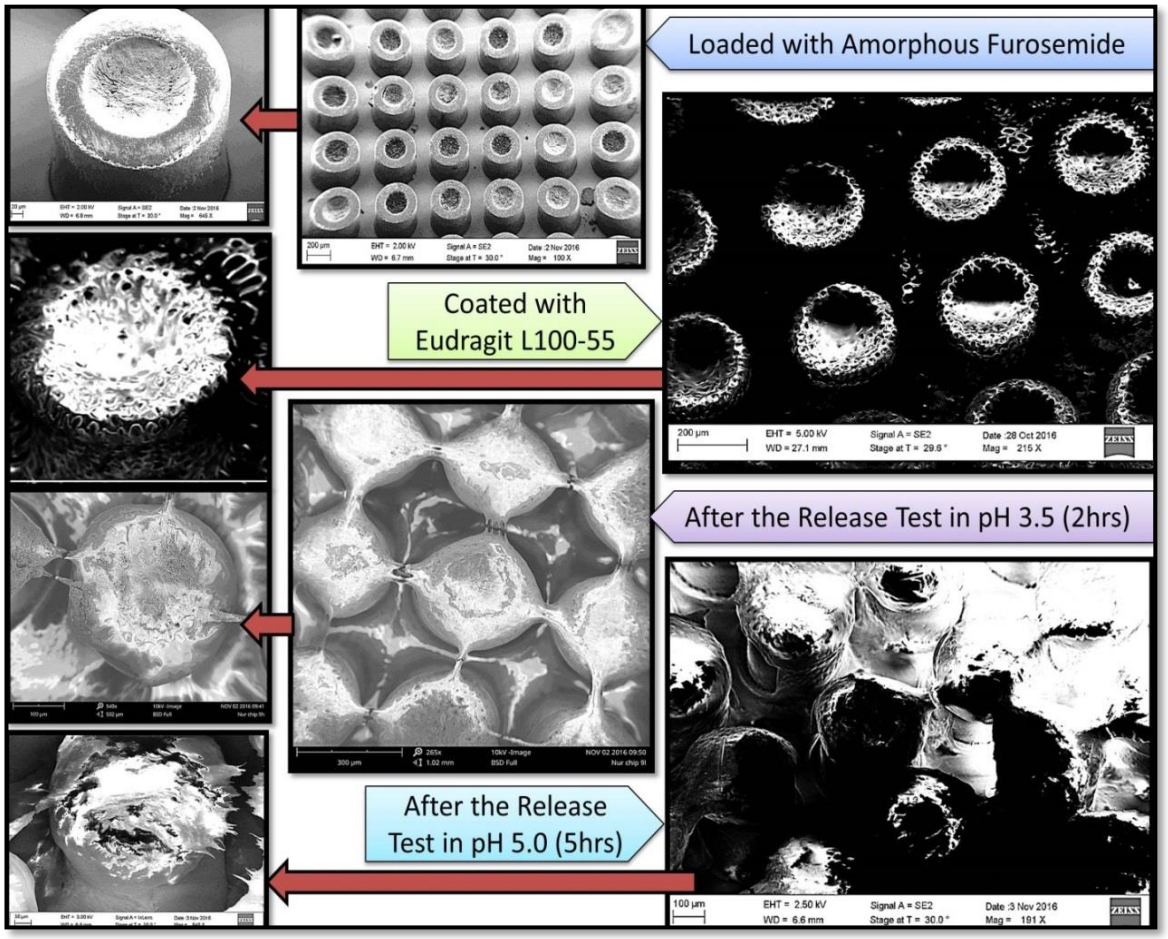

Fig. 5.13: *Lid morphology analysis of 1% EL100-55 lid with 15% TEC plasticizer (Spray CNTR=60)*

After the release test in pH 3.5 buffer medium for 2 hours, the SEM images revealed that the EL lid was completely intact which meets the first part of the hypothesis that the lid would survive in gastric pH of mice. Therefore, the next step was to let the lid to be exposed to small intestinal medium i.e. 100mM phosphate buffer medium of pH 5.0 for 5 hours. After 5 hours exposure, the SEM images show some rifts and holes in the EL lid, but the lid was not completely dissolved (about 5%) and thus it did not meet the second part of the hypothesis.

The thickness of the EL lid measured in a stylus profiler was 63.5 +/- 2.4 µm on an average of 9 measurements. It was anticipated that the thickness of the EL lid might be the reason of not dissolving the lid completely in pH 5.0. Therefore, the next study focused on the lid thickness using the same polymer solution, while only the CNTR of spray coating was decreased to 15, instead of 60 in order to form a much thinner lid. After spray coating the polymer with CNTR=15, the thickness measurement in stylus profiler

is shown in Fig. 5.14. The average thickness of the lid was 9.86 +/- 0.39 µm after 10 measurements, which is more than 6 folds thinner than the previous EL lid.

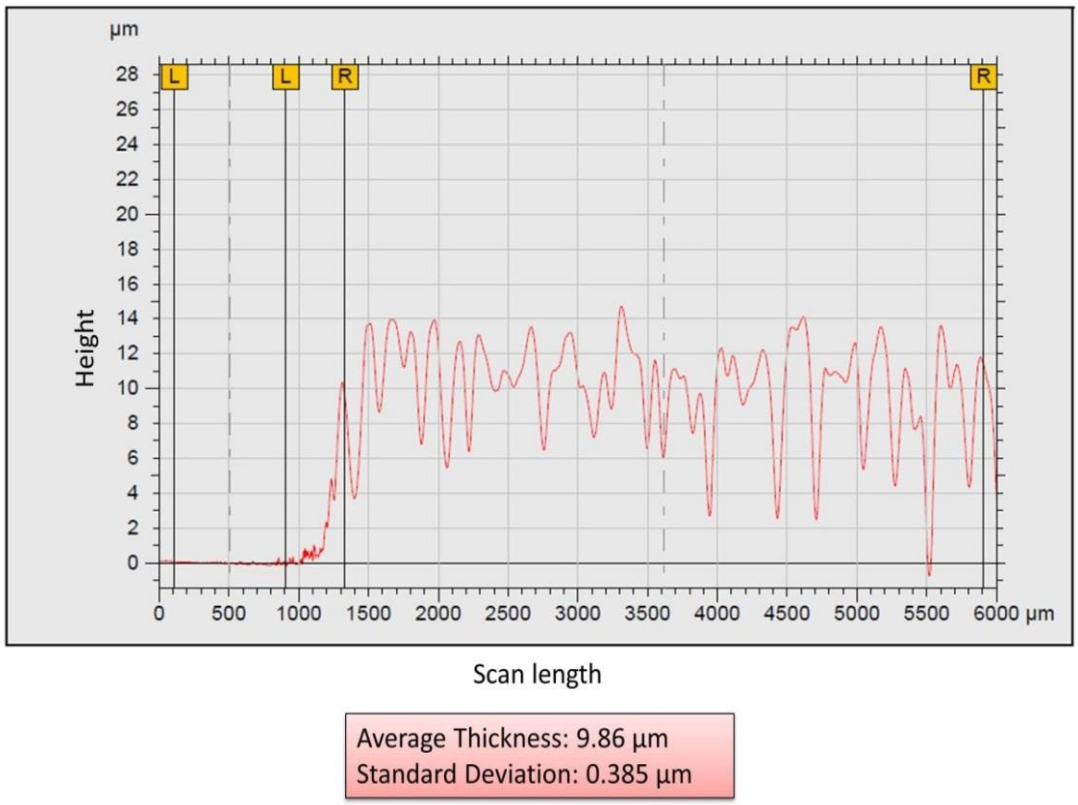

Fig. 5.14: *Thickness measurement of EL100-55 lid (contains 15% TEC) after spray coating with CNTR = 15*

In addition, the surface roughness of the new lid was much higher than the previous EL lid as indicated by the surface noise of the stylus profiler. The SEM images prior to the release test also reveal that the lid morphology was very uneven and patchy with irregular ups and downs (Fig. 5.15). The reason might be a combination of both thinner lid and poor loading of samples.

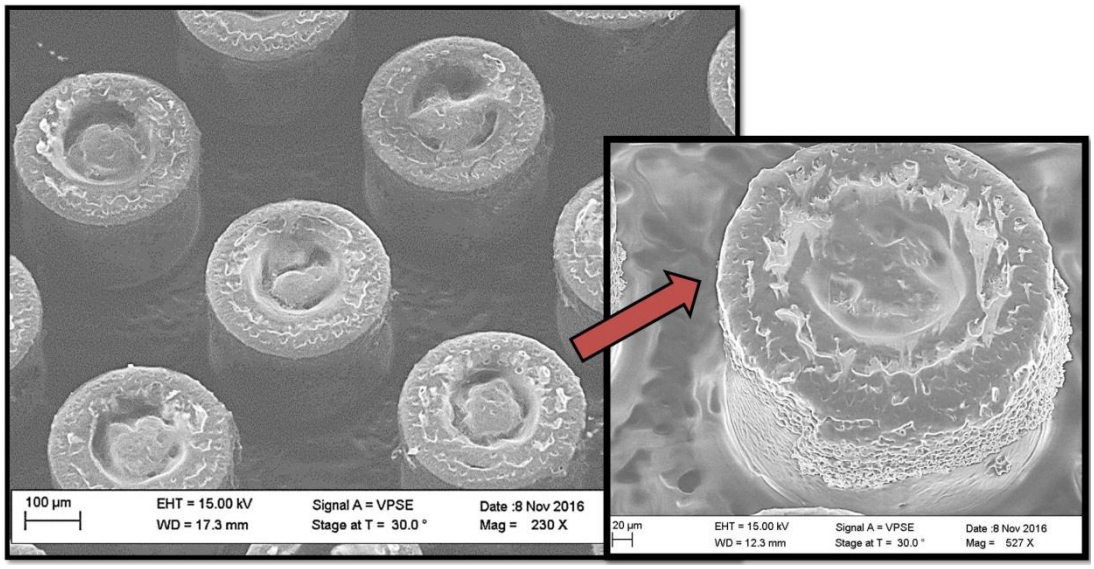

Fig. 5.15: *Lid Morphology of EL100-55 lid with 15% TEC after spray coating with CNTR = 15*

After the thickness measurement and the lid morphology analysis, the drug release test was performed in pH 3.5 release medium (Fig 5.16).

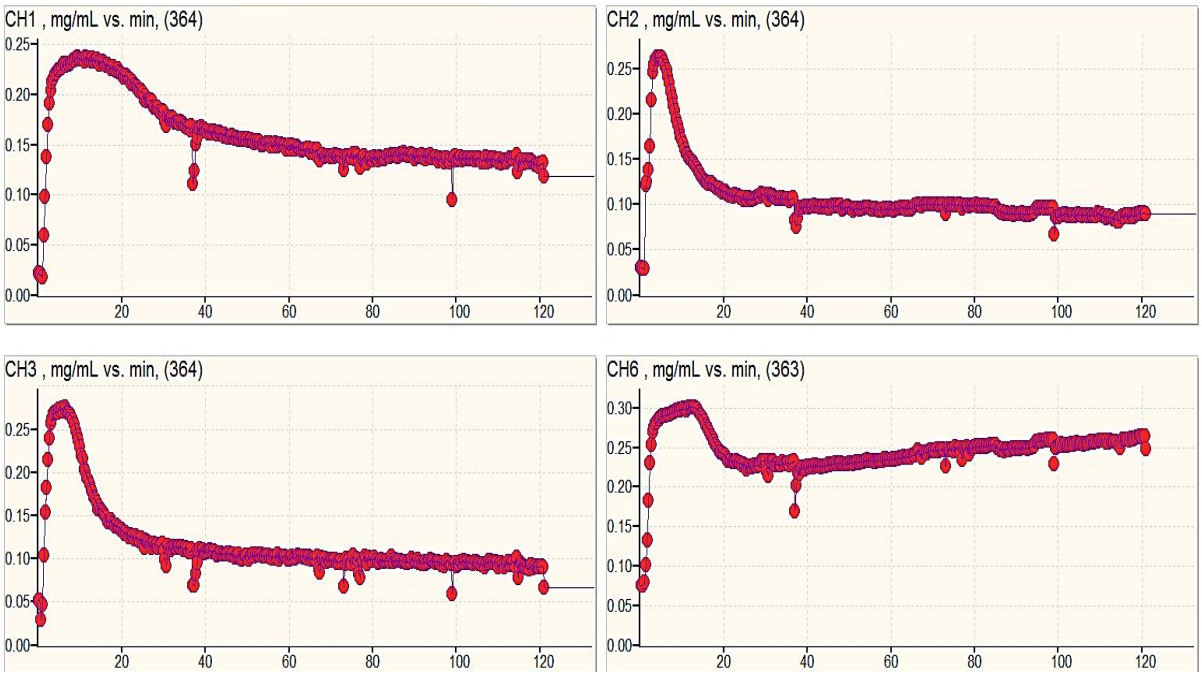

Fig. 5.16: *Release Curves of ASSF from SU-8 MCs coated with EL100-55 polymer (15%TEC) with 15 passages. The data presents mean of 4 measurements ± SD.*

The drug release experiment was run for 2 hours but the release curves in four individual samples (Fig. 5.16) show that the drug release was very fast which occurred between 5-10 minutes and after 20 min of the release test, all the curves reach almost the saturation level indicating the completion of the drug release. From these results, it is assumed that the thickness of the lid was too thin to survive for more than 15-20 min. These results are also supported by the SEM images in Fig. 5.17 where the trace of EL100-55 lid could barely be found after the release test in pH 3.5 buffer medium. Moreover, a lot of white crystalline furosemide is all over the samples outside the SU-8 MCs. This phenomenon proves that the number of passages (CNTR) during spray coating should be increased in order to maintain an optimum thickness which can survive in pH3.5 (gastric medium), but gets dissolved in pH5.0 or higher (small intestinal medium).

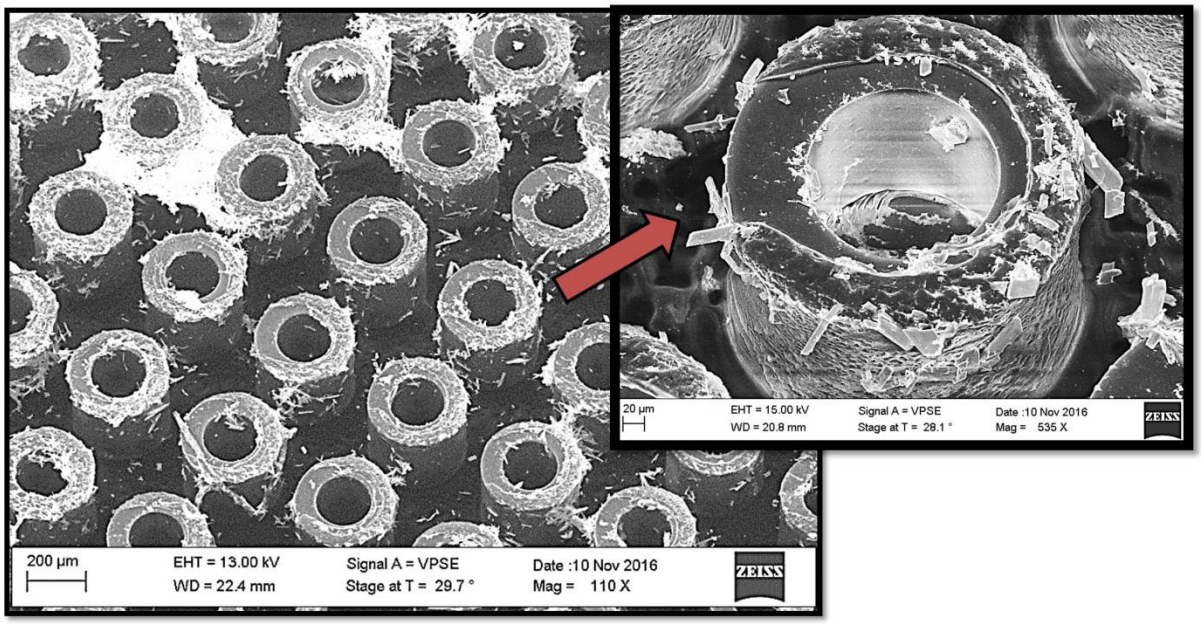

Fig. 5.17: *Morphology analysis of EL100-55 lid with 15% TEC (CNTR = 15) after the release test in pH 3.5 medium for 2 hours*

At this point, it was anticipated that along with the thickness issue (i.e. number of spray coating passes, or CNTR), the plasticizer might play an important role in EL lid stability as discussed in several literatures (61–65, 96). Therefore, the hydrophilic plasticizer TEC used in the preparation of EL solution was replaced by a hydrophobic plasticizer called DBS (di butyl sebacate). The differences between these two plasticizers in terms of their physio-chemical properties are discussed earlier in Subsection 2.8.3.

5.5.3 Analysis of Eudragit L100-55 lid containing DBS Plasticizer

1% w/v EL100-55 solution mixed with 5% w/w DBS was spray coated on top of ASSF-loaded MCs to form the Eudragit lid. The CNTR during spray coating was adjusted at 20 in order to investigate if it can survive in pH 3.5 medium and gets dissolved in pH 5.0 medium, supporting both parts of the hypothesis.

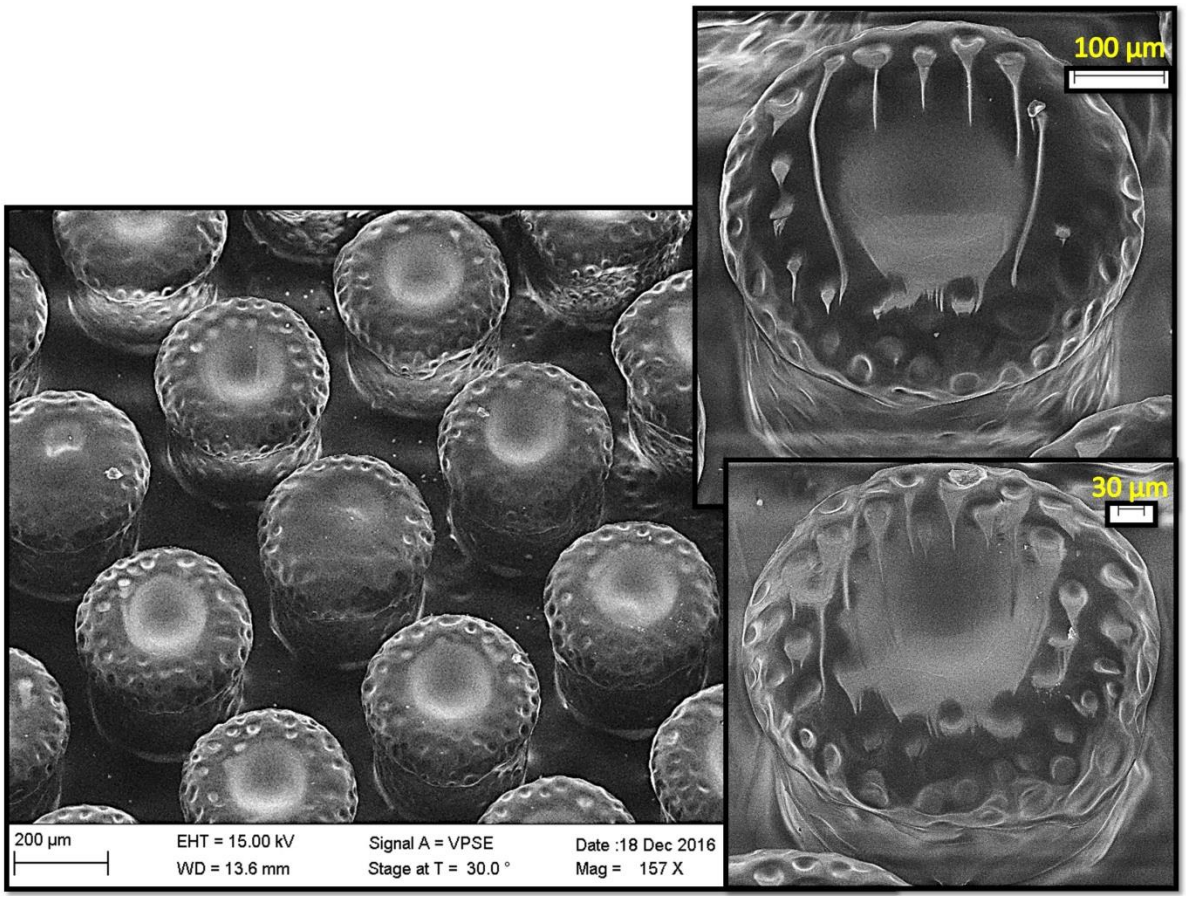

Fig. 5.18: *SEM images of samples spray-coated with 1% Eudragit polymer containing 5% DBS (CNTR = 20)*

The lid morphology analysis following spray coating Eudragit solution with DBS plasticizer looked robust from the SEM images depicted in Fig. 5.18. Compared to Fig. 5.15 (CNTR=15), the lid in Fig. 5.18 (CNTR=20) looks much intact and properly covering the drug-loaded MCs.

The average thickness of this EL lid measured using the stylus profiler (Fig. 5.19) was 42.96 +/- 5.51 µm which is almost 4 times thicker than the previous EL-lid containing TEC. However, the standard deviation of this new lid seems much higher than before despite having less rough surface. The different location of the samples inside the spray

coater hot plate might be the reason of this phenomenon. For instance, if the silicon wafer is placed very near to the spray coater fan, then due to air blow, the lid layer on the silicon wafer becomes thinner and the lid surface looks rougher, compared to the lid on the silicon wafer that is placed far away from the fan.

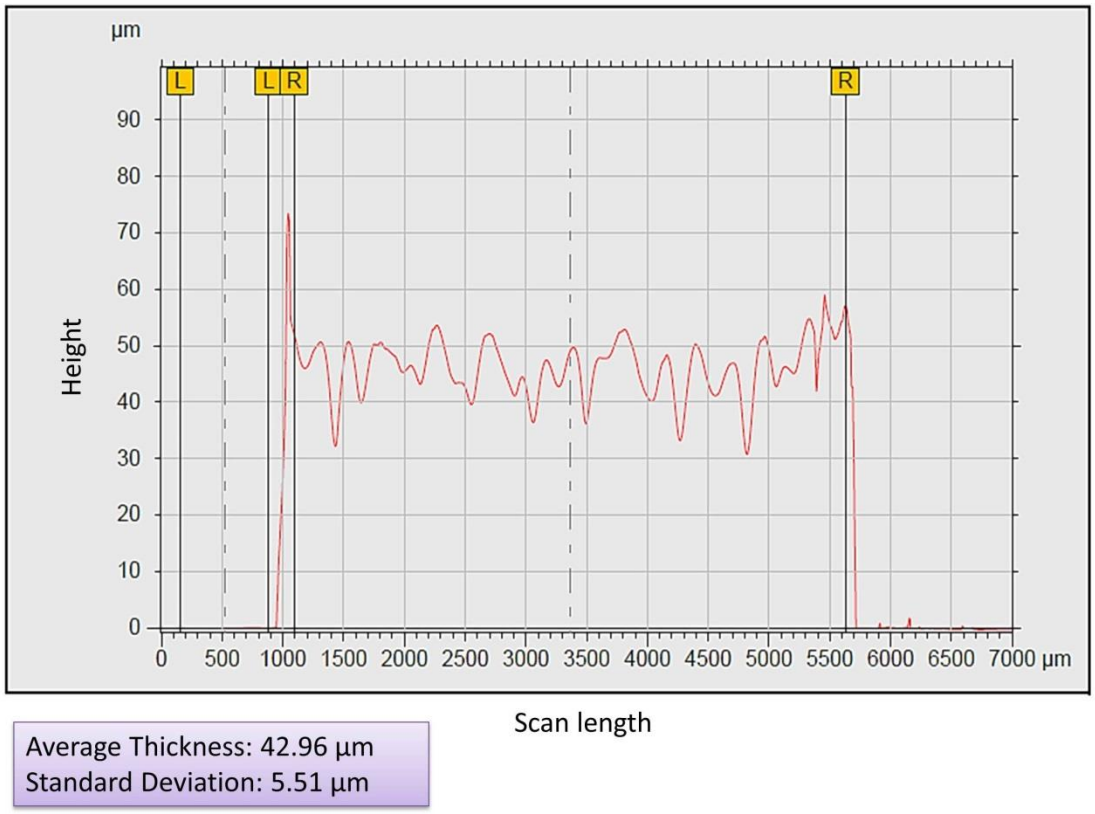

Fig. 5.19: *Thickness measurement and analysis of Eudragit-DBS lid in Stylus profiler*

These samples were then put into the release test using magnetic stirring following the method of the 2nd pilot study. After the release test in pH3.5 (100 mM phosphate buffer) for 2 hours on magnetic stirring at 37 ºC, the SEM images reveal that the Eudragit-DBS lid is completely intact (Fig. 5.20).

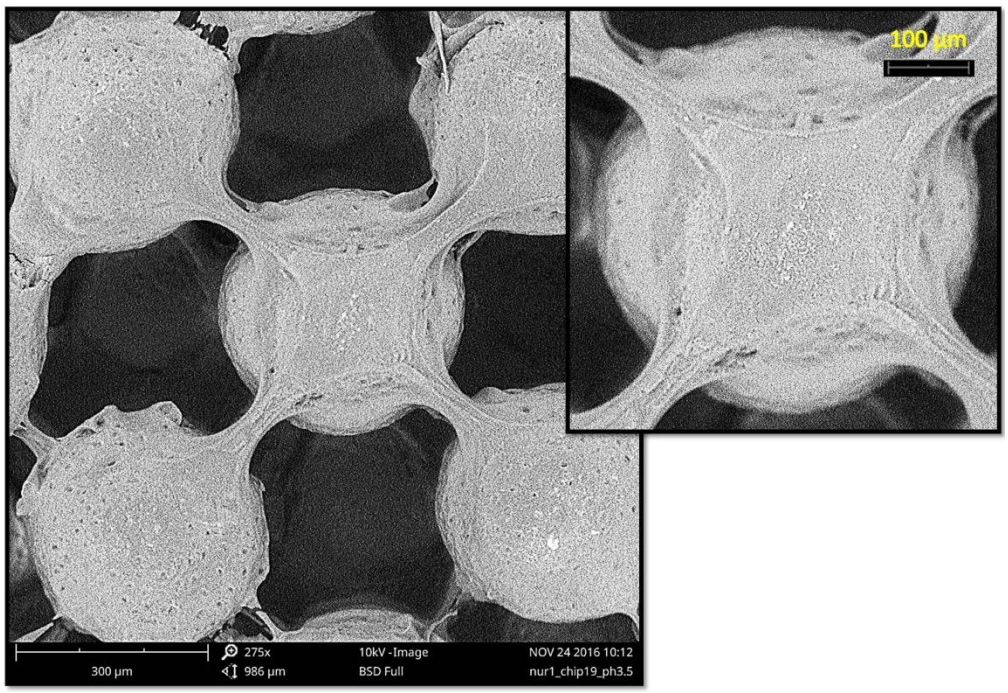

Fig. 5.20: *SEM view of EL lid containing 5% DBS (CNTR=20) after being in buffer medium of pH3.5 for 2 hours on magnetic stirring*

After the lid morphology analysis, the samples were further put in the 100mM phosphate buffer of pH5.0 on magnetic stirring for 5 hours at 37 ºC. After the release test, the lid morphology was analysed using SEM again which shows that the lids were not completely dissolved (Fig. 5.21).

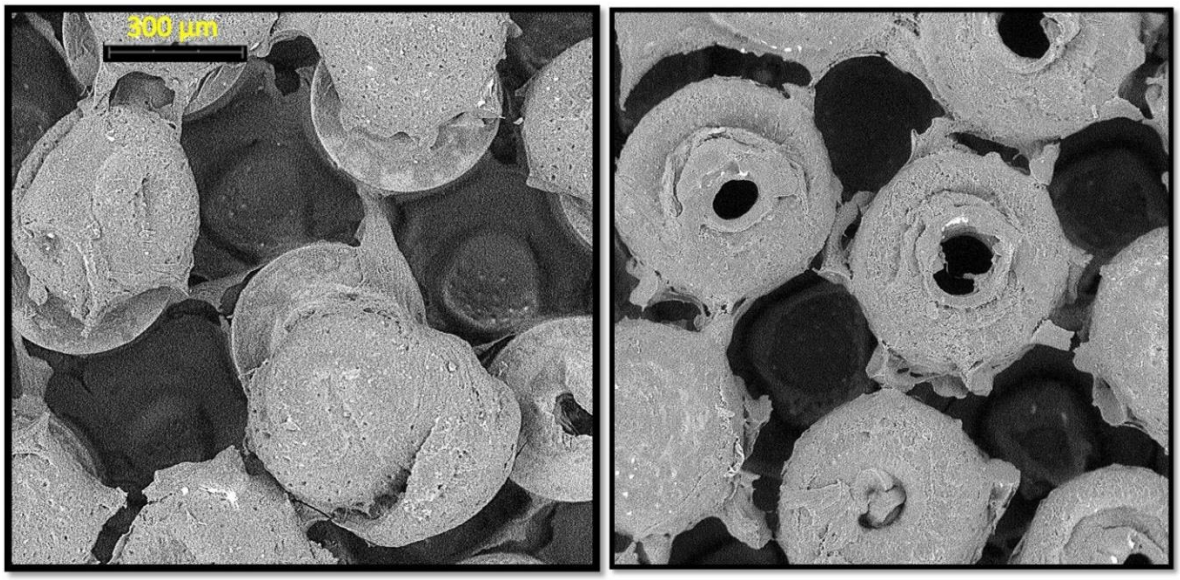

Fig. 5.21: *Morphology of EL lid containing 5% DBS (CNTR=20) after being in buffer solution of pH5.0 for 5 hours on magnetic stirring*

In Fig. 5.21, only about 25% of the EL-DBS lid was dissolved. Likewise almost all the previous experiments with Eudragit lid performed in this study, the lid was meeting the first part of the hypothesis by being intact in pH 3.5 medium, however it was not aligning with the second part of the hypothesis which expects the lid to be completely dissolved in pH 5.0 medium. Therefore, it was decided to let the samples to be in the same pH 5.0 medium for another 5 hours and analyze the lid morphology after a total of 10 hours exposure to the pH 5.0 medium. However, the SEM images of the EL lids even after 10 hours of exposure at pH 5 medium (Fig. 5.22) shows the similar result i.e. the lids are not completely dissolved. About 70% of the lid was still intact.

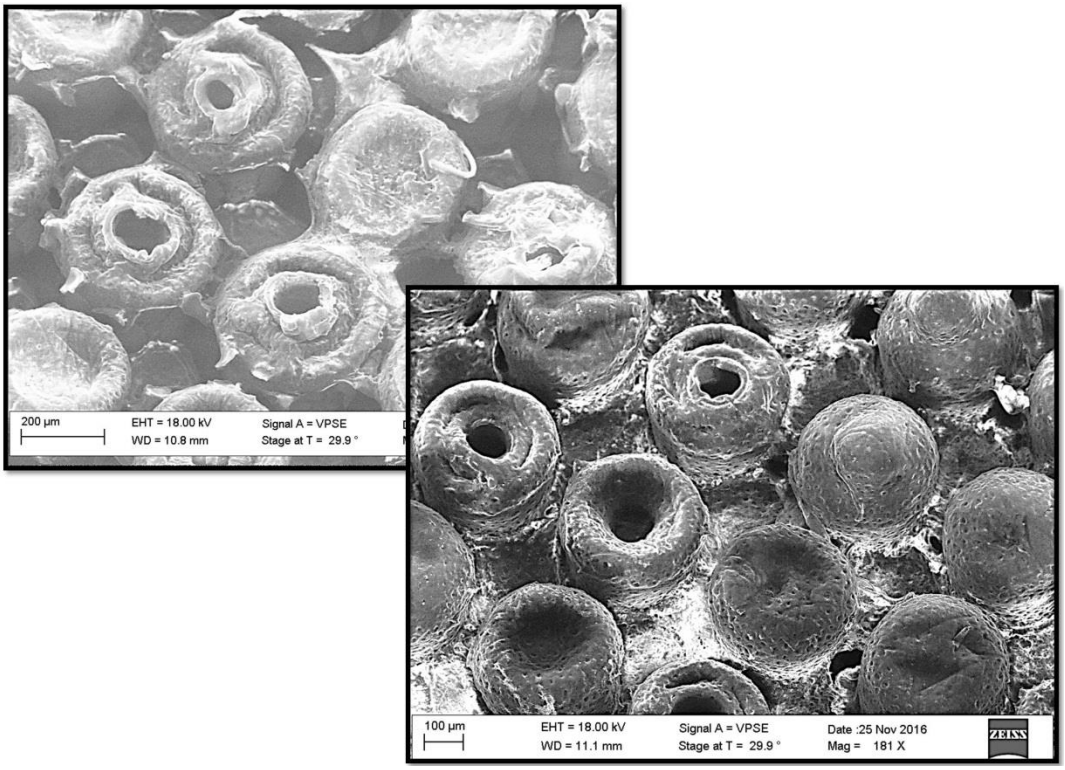

Fig. 5.22: *Morphology of EL lid containing 5% DBS (CNTR=20) after being in buffer solution of pH5.0 for 10 hours on magnetic stirring*

After all these experiments with changes in the CNTR, plasticizers and duration of release test, it was not possible to get the Eudragit L100-55 lid to be dissolved in pH5.0 medium. Hence, release medium of higher pH value was chosen for this part of the study. As rat has the intestinal pH value of 6.0 (95), therefore, the release experiments were performed in 100Mm phosphate buffer of pH 6.0 mimicking the small-intestinal medium of rat instead of domesticated mice.

The next experiment was exactly the same as the previous one; except the pH value was 6.0 instead of 5.0 in the second release test. The release test in pH 3.5 after 2 hours

showed in SEM analysis that the lid was completely intact as the previous experiments and thus meets the 1st part of the hypothesis. Next, the samples were put in the second release test where the release medium had pH 6.0. After running the release test for 7 hours in µDiss profiler, the samples were analyzed using SEM (Fig. 5.23).

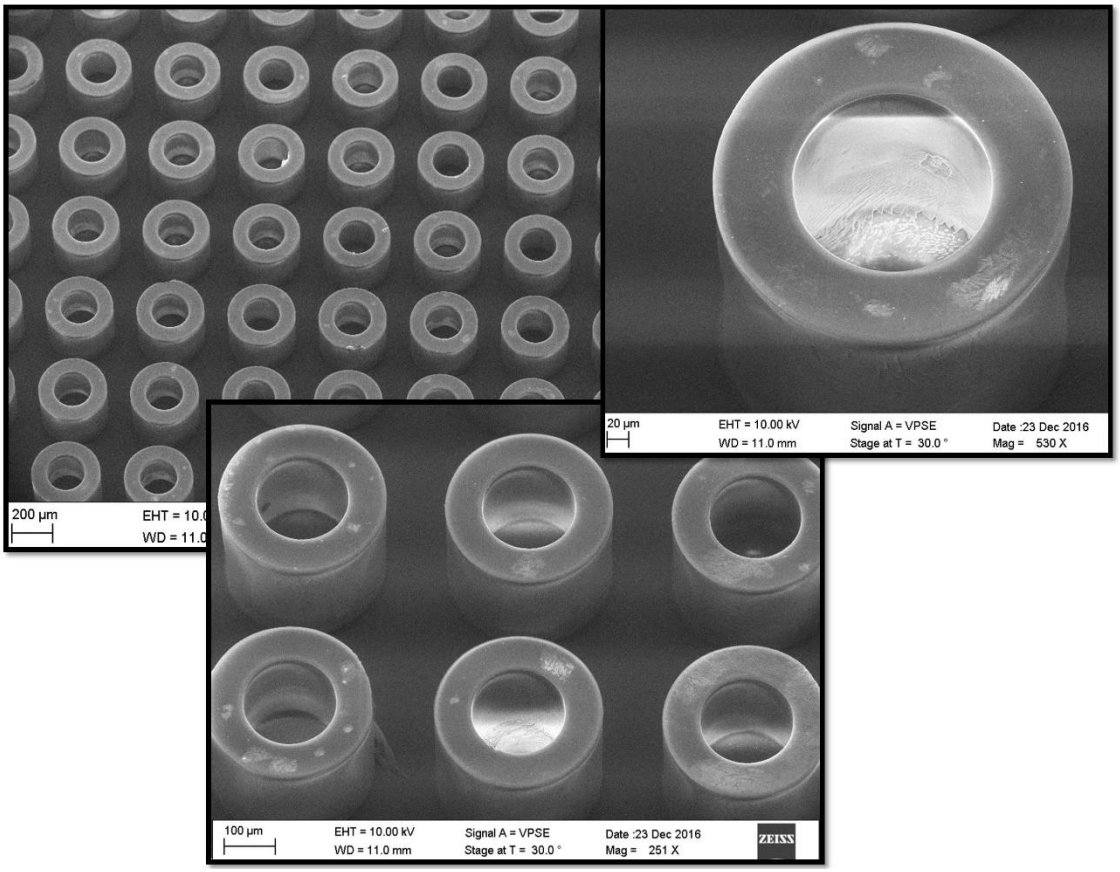

Fig. 5.23: *SEM images of samples with Eudragit -DBS lid after its exposure to pH6.0 medium for 7 hours in µDiss profiler*

The SEM images above show that the Eudragit lid was completely dissolved after being in 100mM phosphate buffer of pH6.0 for 7 hours, finally meeting the 2nd part of hypothesis.

The percentage dissolution curve of both the release tests at pH 3.5 and pH 6.0 are presented in Fig. 5.24 below.

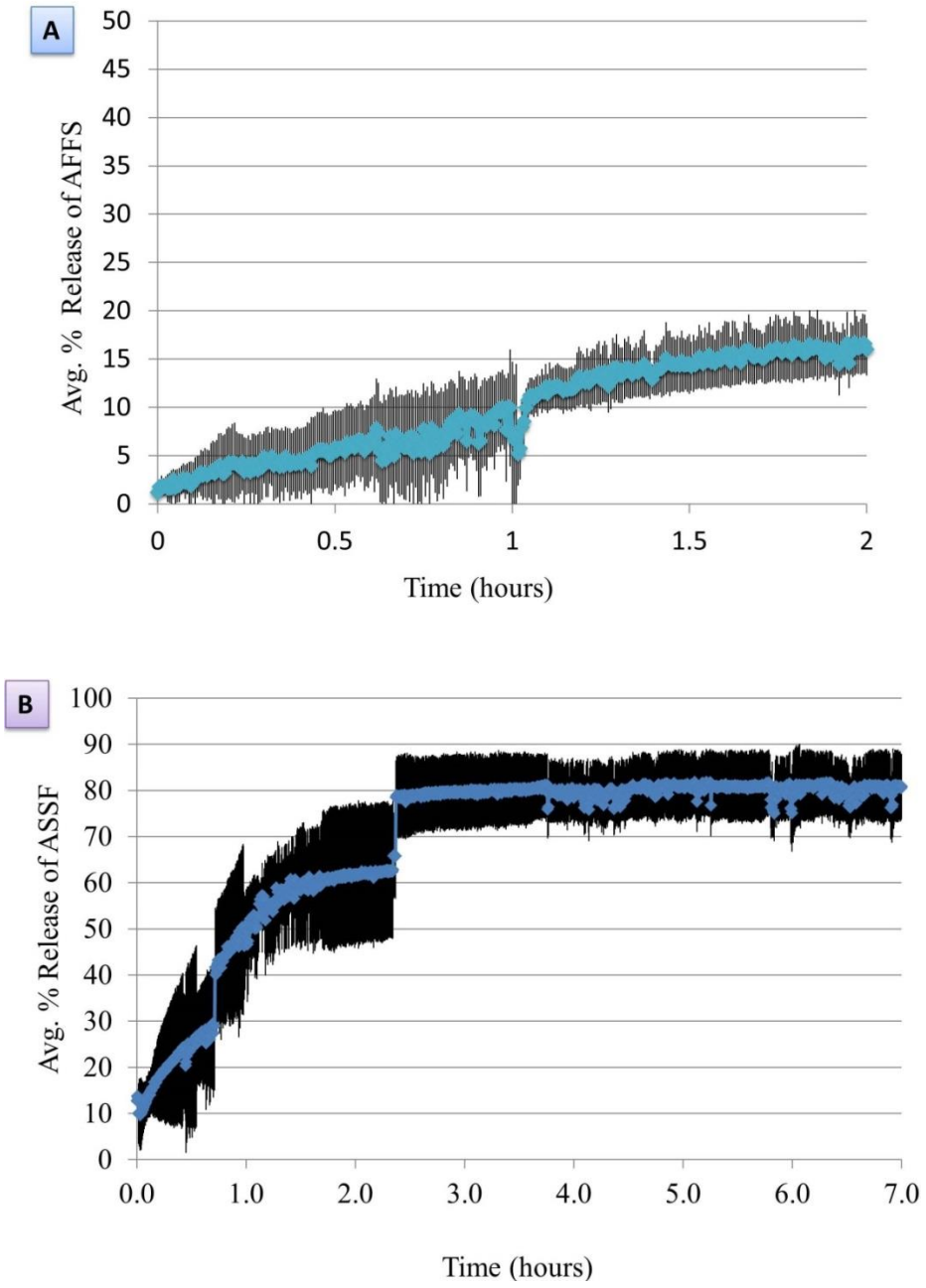

Fig. 5.24: A. *Average % Release of ASSF in buffer pH 3.5 for 2 hour;* ***B.*** *Average % ASSF dissolution during the release test for 7 hours in buffer of pH 6.0. The data represents an average of 4 measurements ± SD.*

The % release study shows how fast the drug started to get released into the medium from the SU-8 MCs which were sealed with EL lid as well as the nature or trend of the release.

After the release test, the percentage dissolution curve was calculated as shown in Fig. 5.24 A. For the first 1 hour, the %dissolution was below 10% on average and then in the last hour, there was very slight increasing trend in the release curve showing up to 16-17% of drug release as maximum. The drug release results in pH 6.0 buffer medium presented in Fig 5.24 (B) shows that the trend of the average dissolution curve swiftly increases till 2.5 hours and reaches highest plateau of the drug release (i.e. 81%). After that, the average release curve reaches its stationary level which indicates that the Eudragit lid was completely dissolved after 2.5 hours during the release test in pH 6.0 medium.

Comparing the average % release of ASSF in pH 3.5 and pH 6.0 for 2 hours and 7 hours, respectively for the same samples (n=4) with the same EL lid (containing 5% DBS), it can be seen that the average % dissolution in pH 3.5 medium is very negligible, whereas it is above 80% in pH 6.0 medium. It suggests that this Eudragit lid satisfies both parts of the hypothesis and its pH sensitivity is stable for the gastric environment as well as for small intestine of rat.

Fig. 5.25 demonstrates comparison between morphology of EL lids (1% w/v EL with 5% w/w DBS) spray coated using different CNTR number. In addition, a comparison table (Table 5.2) is provided below to summarize the differences between the different Eudragit L100-55 lids tested during this study.

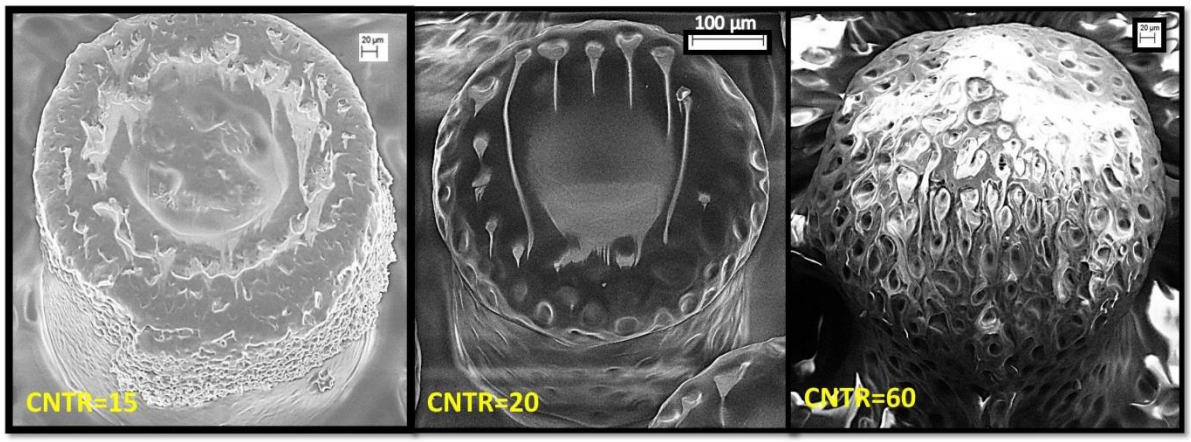

Fig. 5.25: *Lid morphology analysis of EL lid with different spray coating CNTR*

Table 5.2: *Comparing differences in different EL lids in terms of their composition, thickness and pH sensitivity in gastric and intestinal media*

EL Lid composition	Spray coating CNTR	Avg. Thickness (µm)	Stability in pH 3.5 medium after 2 hours	Stability in pH 5.0 medium after 5 hours
Eudragit L100-55 with 15% TEC	60	63.50 +/- 2.40 83.41 +/- 3.57* 125.0 +/- 1.70*	Very stable	Partially dissolved (about 5% gone)
**The placement of samples in relation to the location of the fan inside spray coater was different in each case*				
Eudragit L100-55 with 15%TEC	15	9.86 +/- 0.39	Almost completely dissolved in about 10-15 min	Based on the release test result in pH3.5, it was considered pointless to perform release test in pH5.0
Eudragit L100-55 with 5% DBS	20	42.96 +/- 5.51	Quite stable	Partially dissolved (about 25% gone)
---	---	---	---	After **another 5 hours (total = 10 hours)**, not yet completely dissolved (about 30% gone)
Eudragit L100-55 with 5% DBS	20	31.44 +/- 2.82	Stable	Completely dissolved (**pH 6.0 was used, instead of 5.0**) after 7 hours

Now, the next step was to combine both chitosan and Eudragit-DBS lids together and perform release test using this double lids.

5.6 pH-Sensitivity and Drug Release with Chitosan-Eudragit Double Lids

The Eudragit lid formed on top of the drug-loaded MCs satisfied the hypothesis of drug release. However, in the actual scenario the Eudragit lid would act as an outer lid on top of an inner lid i.e. the chitosan lid, as previously discussed. Thus, following the investigation of both lids separately, double layered lids were prepared on top of the ASSF-loaded MCs. The double-lids-release test experiments were performed **four times** in

order **to validate the results** of both pH sensitivity and targeted drug delivery of the Eudragit and chitosan polymer lids.

First, chitosan lid was formed over the ASSF-loaded MCs by spray coating as shown in Section 5.4, and SEM analysis was done in order to ensure the lid's homogeneity, smoothness and completeness. Then, the EL100-55 lid containing DBS was spray coated on top of the chitosan lid. For, Chi lid the CNTR were 60 and the avg. thickness was 6.45 +/- 0.31 µm, whereas the CNTR for EL lid was 20 and it yield a lid thickness of 34.2 +/- 1.8 µm. Fig. 5.26 shows the lid morphology of the double-lids formed on ASSF-loaded MCs.

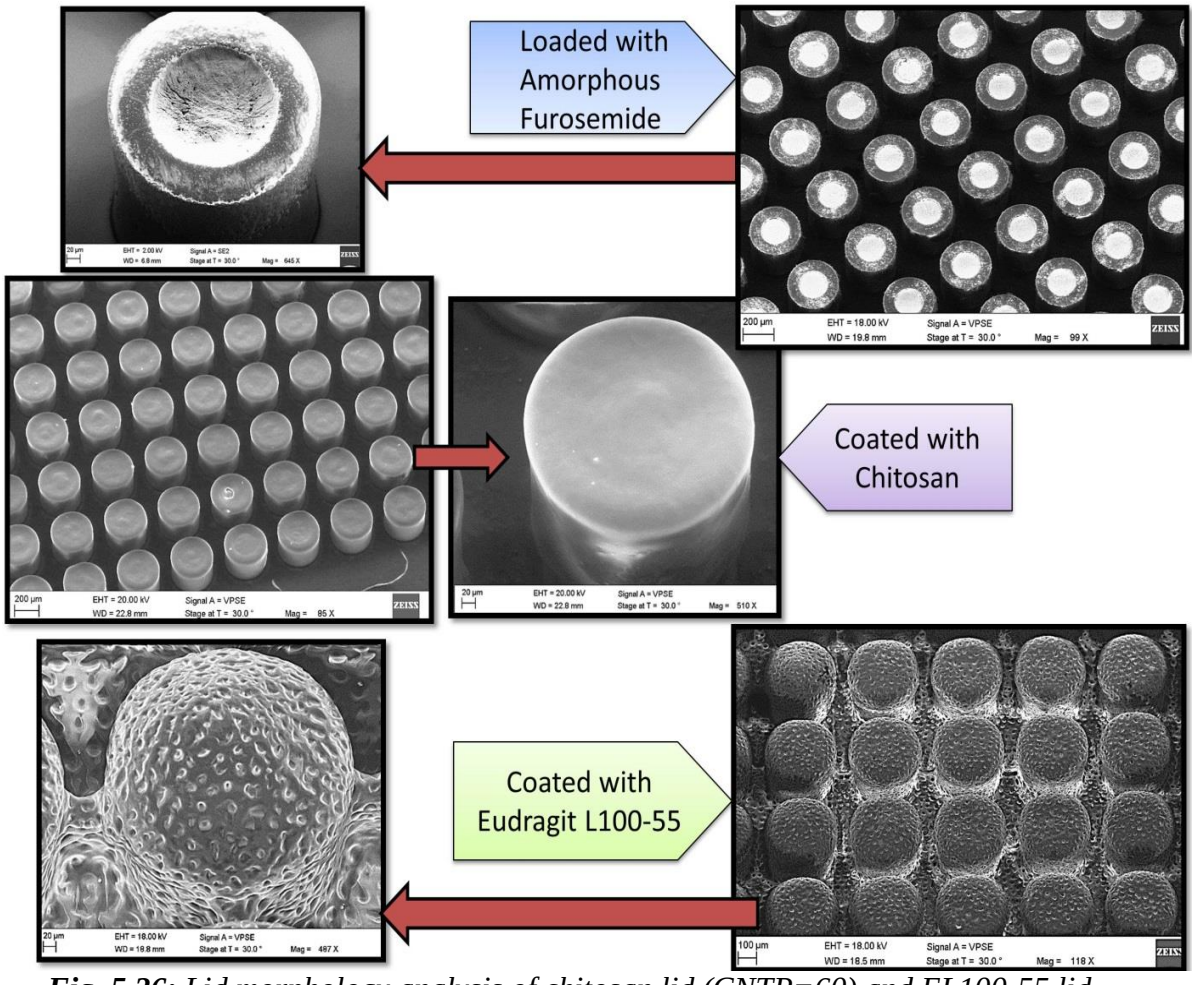

Fig. 5.26: *Lid morphology analysis of chitosan lid (CNTR=60) and EL100-55 lid (CNTR=20)*

Following in the morphology study of the Chi-EL double-lids, the release test was run in 100mM phosphate buffer of pH 3.5 medium for 2 hours and then the lid morphology

analysis of the double-lids were performed, as presented in Fig. 5.27 and in Fig. 5.28, respectively.

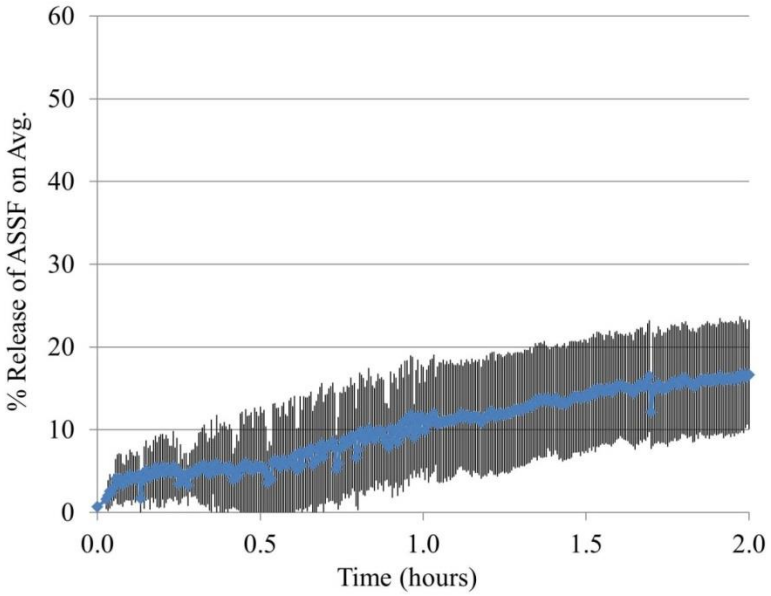

Fig. 5.27: *Average % Release of ASSF in buffer pH 3.5 for 2 hours. The data represents an average of 4 measurements ± SD.*

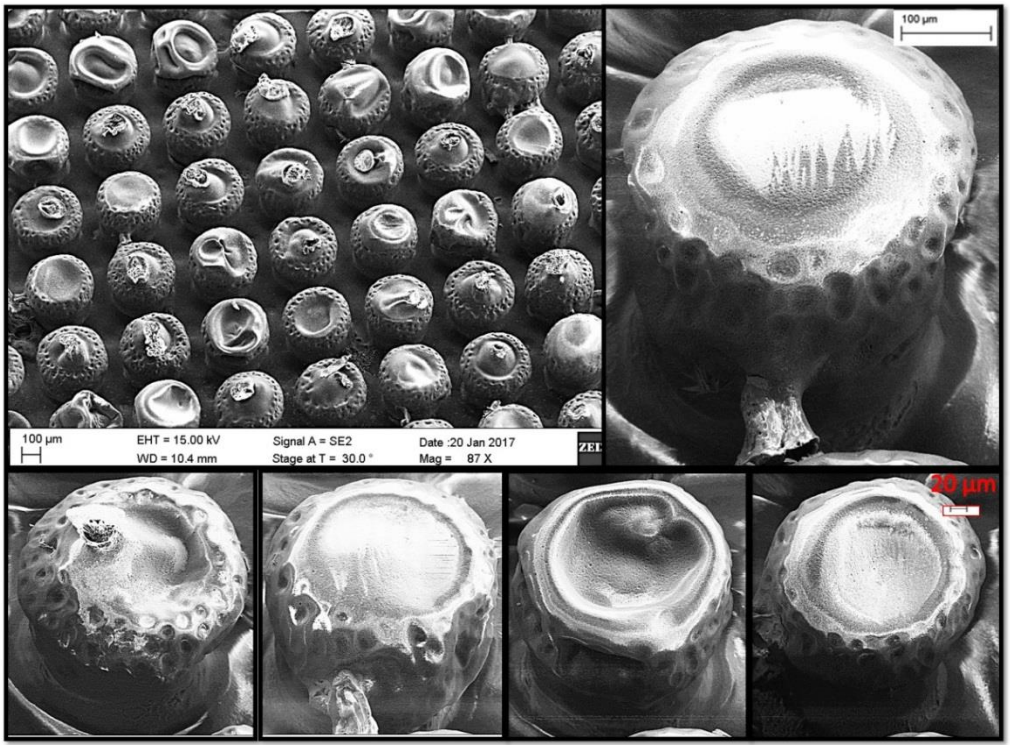

Fig. 5.28: *Lid morphology analysis of chitosan-Eudragit double-lids after the release test in 100mM phosphate buffer of pH 3.5 for 2 hours*

The avg. % dissolution curve in Fig. 5.27 looks very similar to the other avg. % dissolution curves in other previous experiments performed in 100mM phosphate buffer of pH3.5 medium. Here, the highest average % drug release is only about 16%, which is very negligible.

The lid morphology analysis in Fig. 5.28 resembles the results of earlier single lid experiments, where the EL lid does not dissolve in gastric pH value. In these double-lids samples, the EL lid is still intact in pH3.5 medium which allows the samples to proceed for the next release test in pH6.0 medium.

Following the release test in pH 3.5 medium, the Chi-EL double-lids samples were then ran in µDiss profiler in 100mM phosphate buffer of pH 6.0 medium for 7 hours. The average % release of ASSF from 4 samples is presented in Fig. 5.29 and the lid morphology analysis of the double-lids afterward the release test is presented in Fig. 5.30 below.

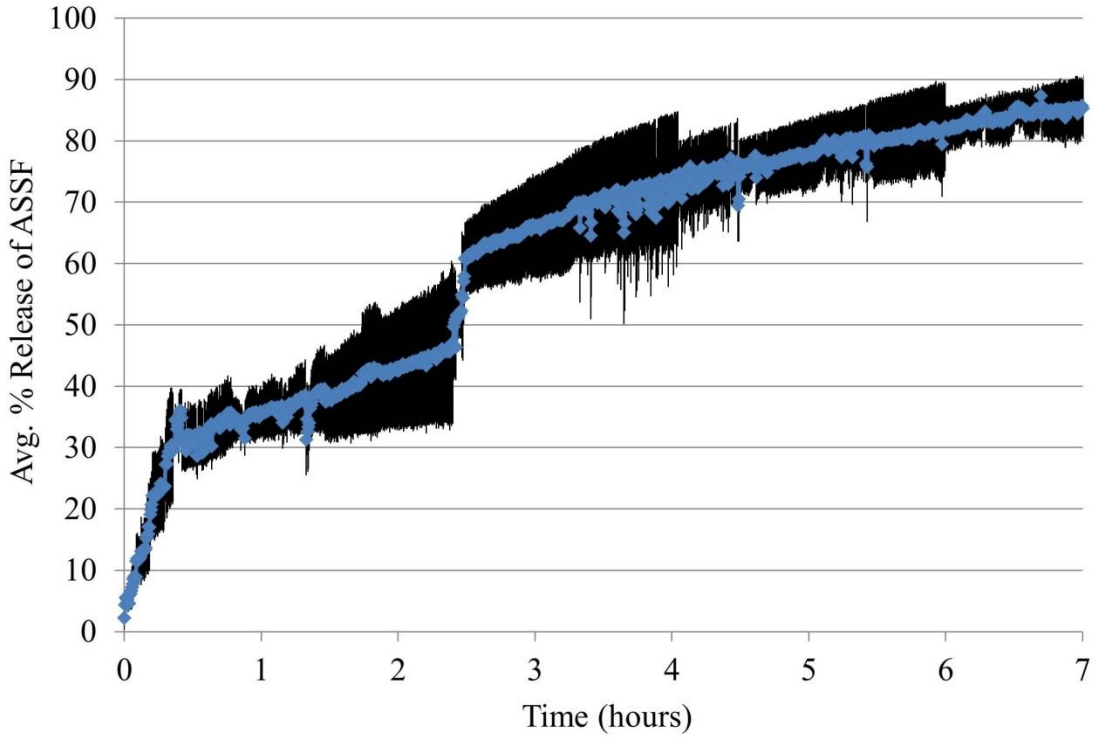

Fig. 5.29: *Average % Release of ASSF in buffer pH 6.0 for 7 hours. The data represents an average of 4 measurements ± SD.*

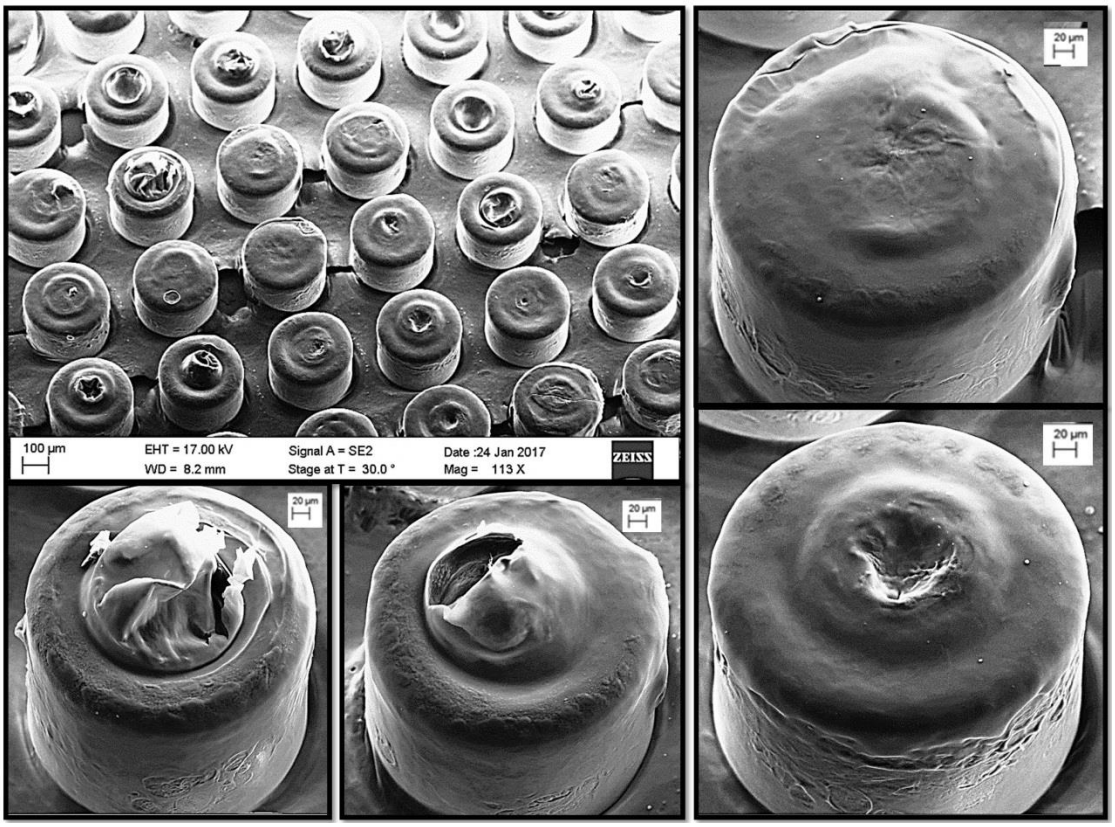

Fig. 5.30: *Lid morphology analysis of chitosan-Eudragit double-lids after the release test in 100mM phosphate buffer of pH 6.0 for 7 hours*

In Fig. 5.29, the highest avg. % of drug release is about 85%, which was only about 60% in Chi single lid release experiment (Fig. 5.6) and 81% in EL single lid release experiment (Fig. 5.24 B) in the same pH medium as shown in the previous sections. In addition, another comparison can be found in the trend of the % release curves among these samples with three different lids (i.e. Chi lid, EL lid and Chi-EL double-lids). The avg. % of ASSF release starts to almost be stationary after 2 hours in Chi single lid samples, and after 2.5 hours in EL single lid samples; whereas the avg. % release curve keeps increasing till 7 hours in samples with Chi-EL double lids. The increasing trend of drug release was though gradual after 2.5 hours of the drug release as shown in Fig. 5.29. These results suggest that the Chi-EL double-lids perform much better in terms of higher but gradual drug release in targeted site, compared to the single lid samples.

Following the above ASSF release test, the SEM investigation on lid morphology was performed as presented in Fig. 5.30. Unlike, Fig. 5.28, the porous texture of the outer lid (i.e. EL lid) cannot be seen in Fig. 5.30; instead a very smooth texture inner lid (i.e. Chi lid) has been found. It means that the EL lid is completely dissolved in pH 6.0 medium and the Chi lid is then exposed to the release medium. It allows the inner Chi lid to be

swollen and thus the ASSF to disperse through the lid into the release medium. The SEM images capture the scratches and some cracks on the Chi lid. These images also resemble the lid morphology of other similar experiments performed during this validation study. The major results of the validation experiments using Chi-EL double-lids are summarized below in Table 5.3. This is to be noted that some of the results were affected by unfavorable circumstances such as clogging in spray coater nozzle during chitosan lid formation, swollen lid due to environmental factors e.g. humidity and air exposure, and biased release curve due to broken samples during the release test. Images of such exceptional scenarios are shown in APPENDIX D-G.

Table 5.3: *Summary of validation experiments involved in Chi-EL double-lids*

Avg. Thickness +/- SD (µm) n=4-5		Highest avg. % release of ASSF in pH 3.5	Highest avg. % release of ASSF in pH 6.0
Chi lid	EL lid		
6.45 +/- 0.31	34.2 +/- 1.8	16%	85%
6.31 +/- 0.40	35.8 +/- 2.1	15%	84%
6.20 +/- 0.30	31.4 +/- 2.8	16%	87%

5.7 pH-Sensitivity and Drug Release Test using Adjuvant-based Chitosan-MPLA Lid and Eudragit Lid

After the promising and reproducible results of the above validation study involving the Chi-EL double-lids samples, the adjuvant, MPLA, was incorporated to the Chi-lid using the polymer solution from **Section 4.4.4** and spray coating method from **Section 4.5**.

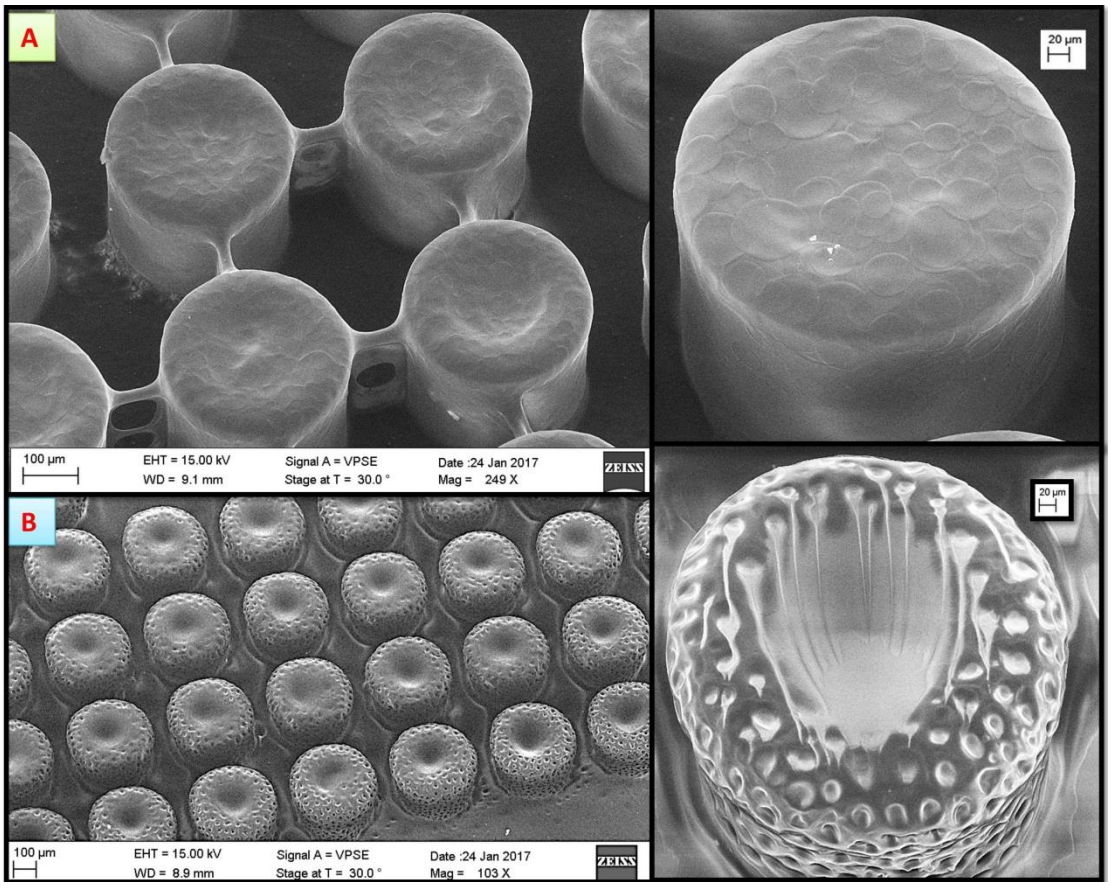

Fig. 5.31: A. *Lid morphology analysis of chitosan-MPLA lid (CNTR=60) and* ***B.*** *1% EL100-55 with 5% DBS lid (CNTR=20) coated on top of Chi-MPLA lid*

Fig. 5.31 A. shows the lid morphology analysis of chi-MPLA lid spray coated on ASSF-loaded samples and Fig. 5.31 B. represents the EL lid spray coated on top of chi-MPLA lid, in order to protect the chitosan-MPLA lid from dissolving in gastric pH (e.g. pH3.5). These newly formed adjuvant-based lid (i.e. Chi-MPLA lid) and pH-sensitive lid (i.e. EL lid) have an avg. thickness of 6.4 +/- 0.5 µm and 33.1 +/- 1.1 µm, respectively.

The release test results in 100mM phosphate buffer of pH 3.5 for 2 hours and of pH 6.0 for 15 hours are presented in Fig. 5.32 A. and 5.32 B. respectively. Fig. 5.32 A. resembles the earlier release test results in pH 3.5 with a negligible drug release in gastric medium. However, in Fig. 5.32 B., the highest % releases is about 80% on average which is similar to the avg. % dissolution results of the previous validation experiments in the pH 6.0 medium. Comparing Fig. 5.29 and Fig. 5.32 B., both of the avg. release curves have sharp increase till 2.5 hours and after that there is gradual increase in the % drug release. In Fig. 5.32 B., after 11 hours of drug release, the % release curve seems to be reaching stationary phase which could not be found in the Fig. 5.29 since that ex-

periment was run for 7 hours only and till the end it had slow increase in the % release curve.

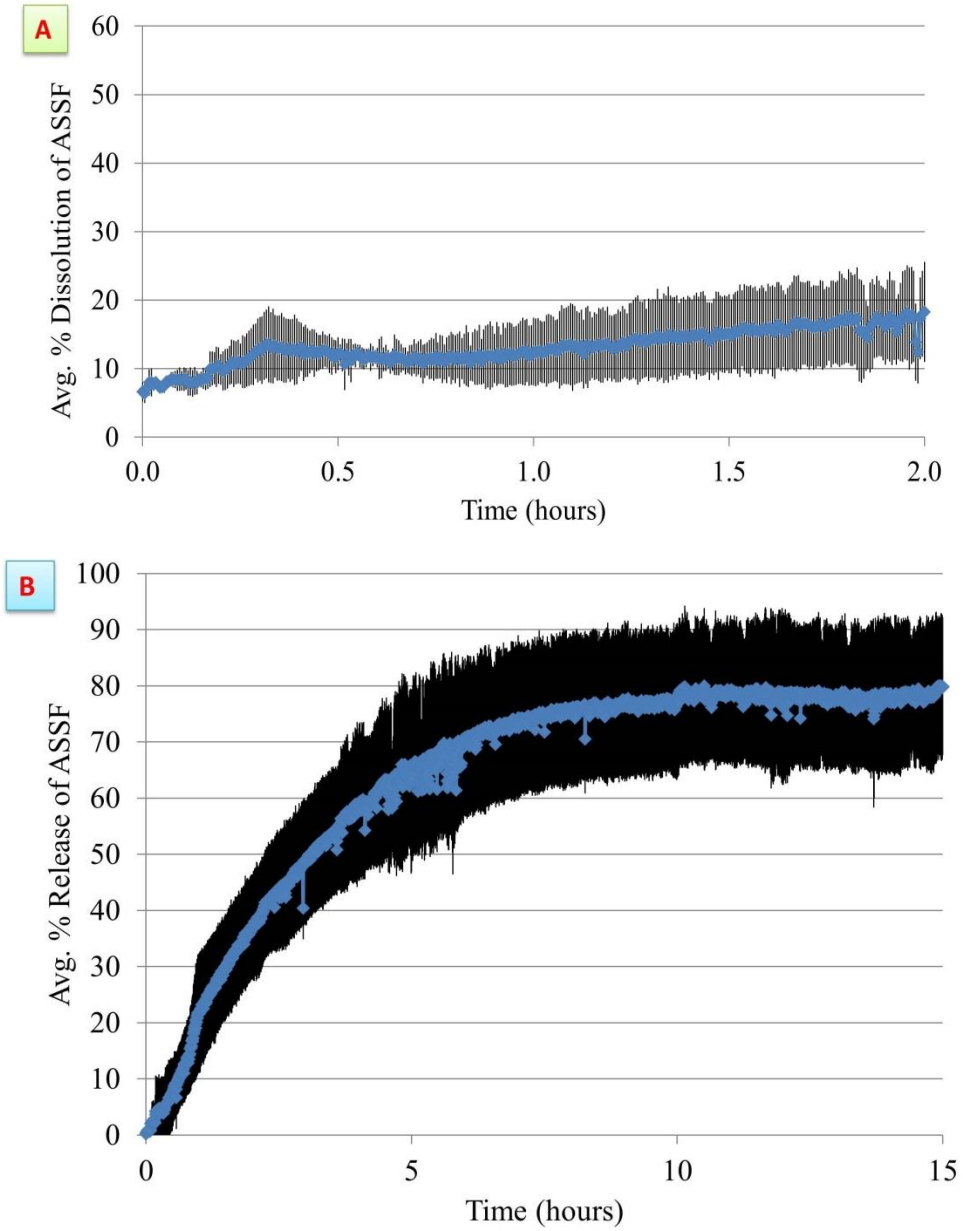

Fig. 5.32: A. *Average % Release of ASSF from Chi-MPLA & EL lids coated MCs in buffer pH 3.5 for 2 hour;* ***B.*** *Average % ASSF dissolution during the release test for 15 hours in buffer of pH 6.0. The data represents an average of 4 measurements ± SD.*

Thus, the % drug release of ASSF from Chi-MPLA and EL (double-lids coating) coated MCs in both gastric and small intestinal media looks reproducible and promising in terms of their pH-sensitivity and targeted drug release capacity.

The lid morphology analysis of this double-lids samples after the release test in pH 3.5 and in pH 6.0 media are presented in Fig. 5.33 A. and B. respectively.

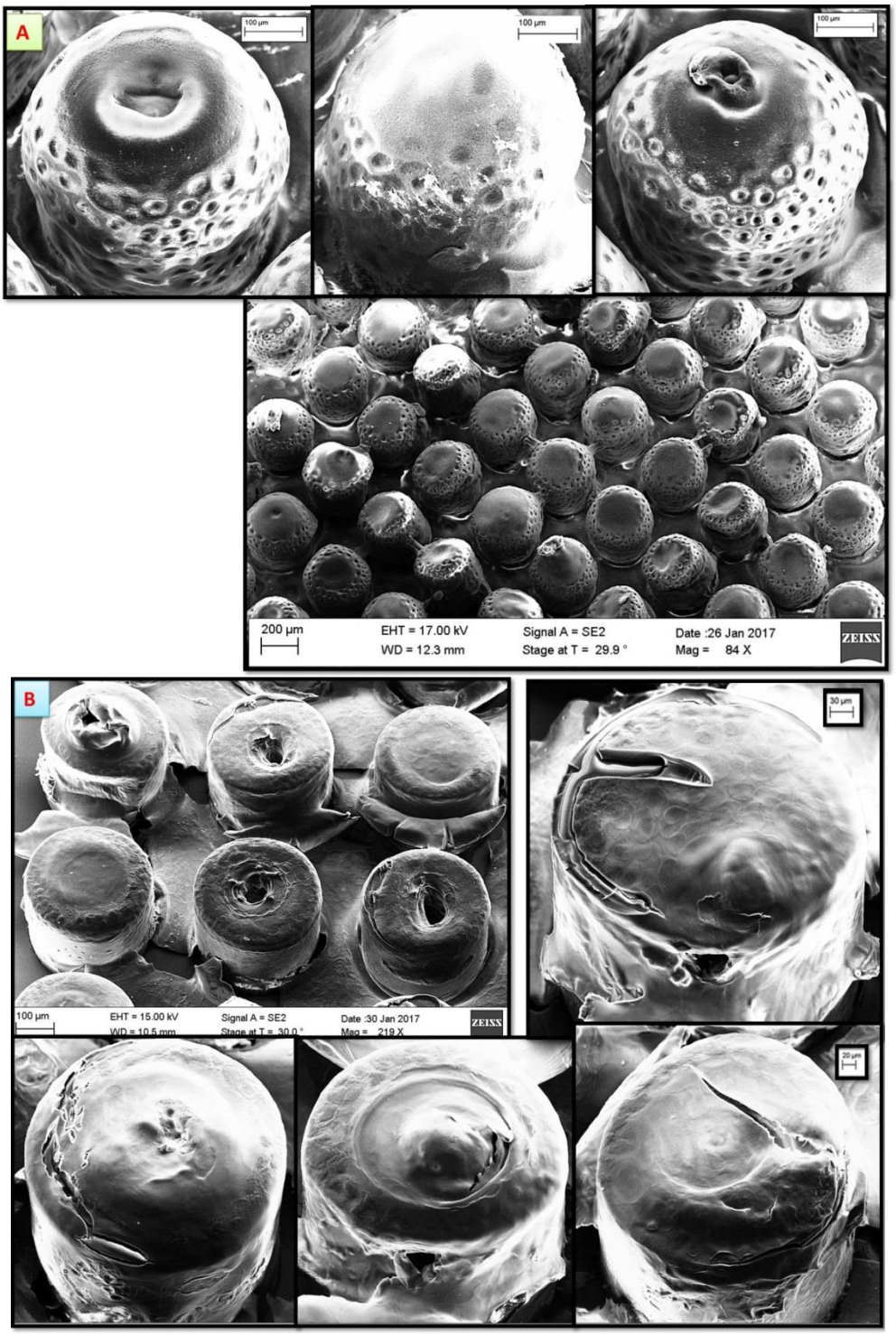

Fig. 5.33: *Lid morphology analysis of chitosan-MPLA-EL double-lids after-* ***A.*** *the release test in pH 3.5 for 2 hours (Fig. 5.31 A.);* ***B.*** *the release test in pH 6.0 for 15 hours (Fig. 5.31 B.)*

The lid morphology analysis in SEM (Fig. 5.33) after both release tests resembles that of the similar previous experiments in terms of lid texture and roughness. However, since the release experiment in pH 6.0 medium was run for 15 hours, therefore, there are more scars found in the lid in Fig. 5.33 B. and also, the lid looks a bit lifted in many places on the samples, compared to the similar double-lids release test experiment in Fig. 5.30 for 7 hours.

Hence, the pH-sensitive and adjuvant-based Chi-MPLA-EL double-lids have been proven to be promising in terms of targeted drug delivery for oral vaccination.

5.8 Statistical Analysis of the Effects of Polymeric Lids on Drug Release

In this section, the effects of different polymeric lids on the ASSF-loaded MCs are investigated in terms of their drug release capacity at the pH value of small intestine (pH 6.0). Five different samples i.e. i) control samples with no polymeric lid, ii) samples with chitosan (Chi) lid, iii) samples with Eudragit (EL) lid, iv) samples with EL + Chi lid and v) samples with EL+MPLA incorporated Chi lid are analyzed in Fig. 5.34.

In this analysis, the two variables considered are the average percentage of drug release and the time of release in hours. The ASSF release investigation was performed at pH 6.0 buffer medium in µDiss profiler for 7 hours.

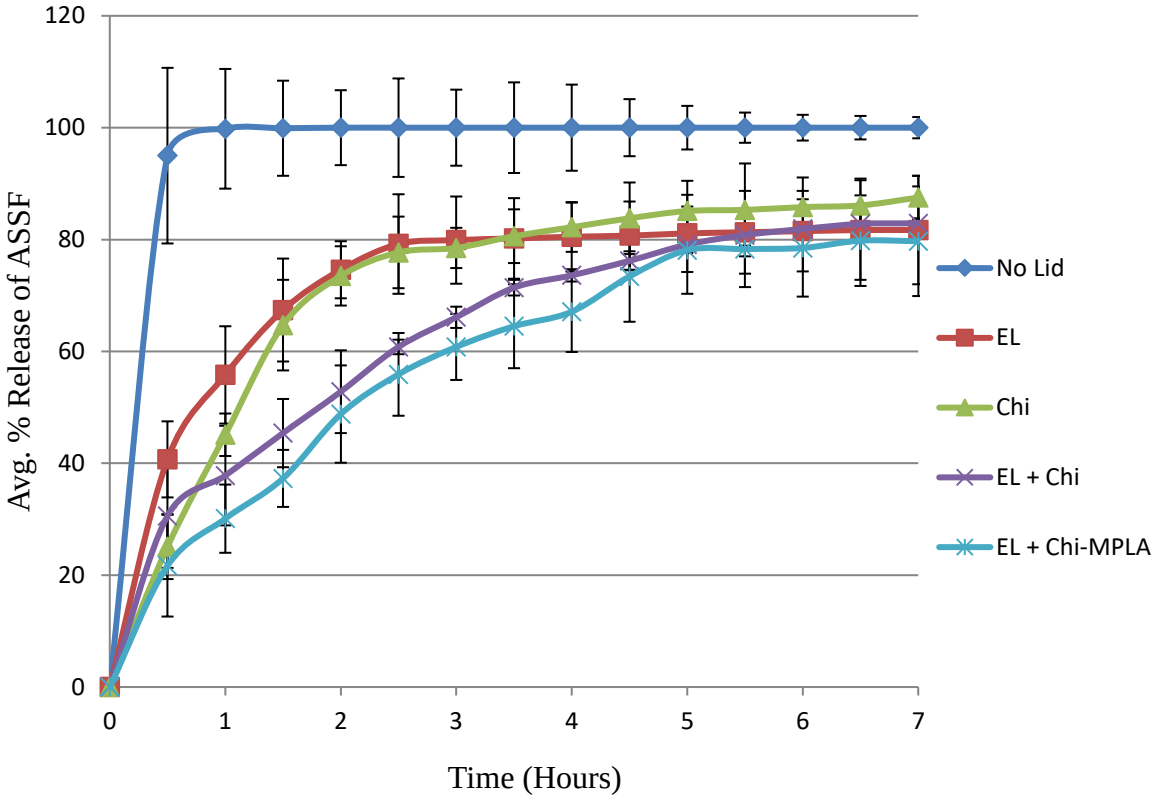

Fig. 5.34: *The average % release of ASSF from MCs coated with no lid, EL lid, Chi lid, both EL & Chi lids, and both EL & Chi-MPLA lids, respectively in pH 6.0 buffer medium over 7 hours. The data represent 5 measurements (n=5) for each sample category +/- SD*

Fig. 5.34 shows clear difference in % release of ASSF between uncoated (without lid) samples and coated samples. One-way ANOVA test with 95% confidence interval was performed between the samples of these 5 different categories including the control sample. The test result ($p = 0.0015$) proves that there is statistically significant difference in % release of ASSF over time among the samples with different polymeric coatings.

In addition, comparing the single-coated samples (EL lid and Chi lid) and double-coated samples (EL lid + Chi/Chi-MPLA lid) from the above figure, the single-coated samples release the drug much faster than the double-coated ones. The single-coated samples release the drug completely by 2.5 hours and reach equilibrium, whereas the double-coated ones need about 5-6 hours to release the drug completely. This shows that double-coated MCs behave in line with the hypothesis that it possesses slower and more controlled drug dissolution capacity.

Furthermore, comparing the two single-coated samples, the EL-coated sample releases almost 60% of drug during the 1st hour of the experiment whereas the Chi-coated sample releases about 40% of the drug in the same duration. This shows that the EL lid dissolves much quicker than the chitosan lid because chitosan, as a coating has the property of controlled drug release (97,98).

One-way ANOVA test with 95% confidence level was also executed only between the two different double-coatings – i) EL lid + Chi lid and ii) EL lid + Chi-MPLA lid. The test result ($p = 0.6135$) asserts that there is no statistically significant difference between these double-coatings in terms of % release of ASSF. This shows that the incorporation of MPLA into chitosan lid does not affect the drug release properties of chitosan lid.

Thus, it can be concluded that the drug release is affected by different polymeric lids while being released in the same medium under the same conditions.

5.9 MPLA Detection using X-ray Photoelectron Spectroscopy

This section discusses the results of MPLA detection by XPS where three samples were used. These samples were- 1) plane silicon chip 2) Chitosan lid spray coated on plane silicon chip and 3) Chitosan-MPLA lid spray coated on plane silicon chip. The resulted scanning curves and their peaks were analysed using XPS handbook. For detecting the chemical composition, the XPS results are presented in count/second on y-axis, over the binding energy (eV) on x-axis. The experimental results show that the peak for silicon is present only in the sample 1 where no lid was coated (Fig. 5.35). However, the XPS results for both chitosan and chitosan-MPLA lids look almost similar in terms of their chemical compositions as shown in Fig. 5.35.

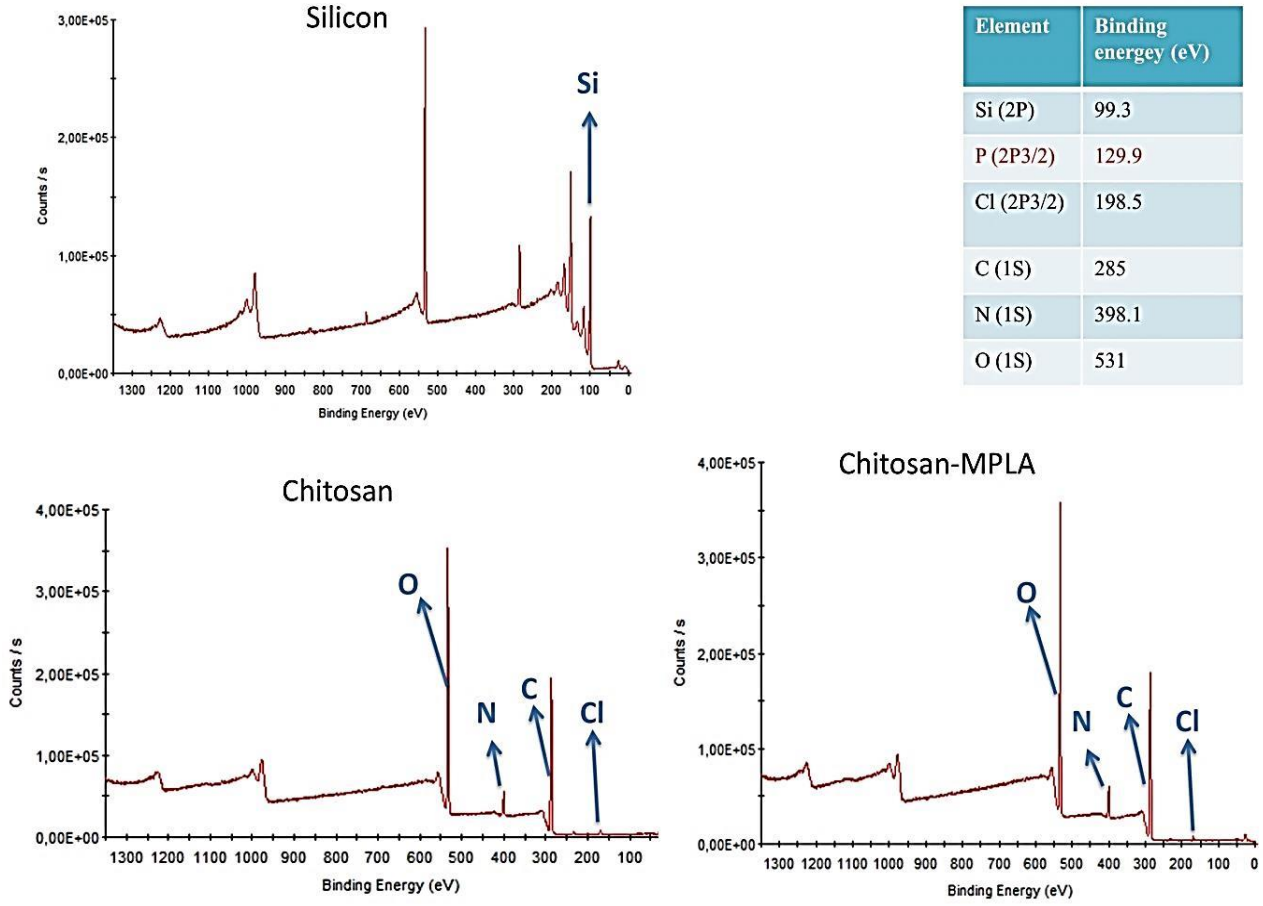

Element	Binding energy (eV)
Si (2P)	99.3
P (2P3/2)	129.9
Cl (2P3/2)	198.5
C (1S)	285
N (1S)	398.1
O (1S)	531

Fig. 5.35: *The chemical compositions of lid samples analysed in XPS*

The distinguishing component between chitosan and chitosan-MPLA lids was the phosphorous. However, likewise all techniques, the XPS has its own limit of detection which might be the reason why the phosphorous molecule was not found in XPS while detecting chitosan-MPLA lid compositions. According to studies, depending on the element of detection, the required minimal concentration of the element has to be above 0.05-1.0 atom% in order to be detected by XPS (99).

In Fig. 5.36, it can be seen that a large molecule of MPLA contains only one phosphorous molecule. The chemical formula of MPLA is $C_{96}H_{184}N_3O_{22}P$ and the percentage composition of phosphorous in MPLA is only 1.76%. (100).

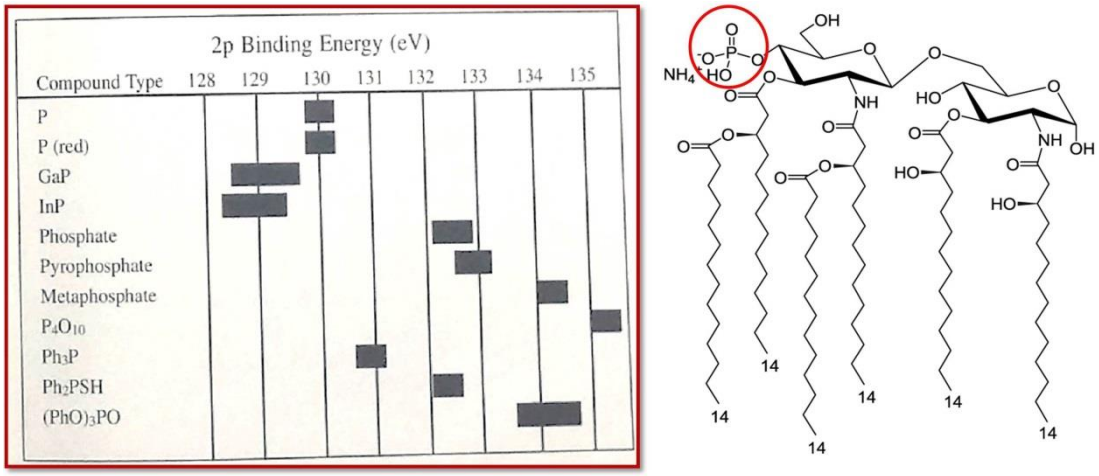

Fig. 5.36: *The binding energy chart for phosphorous detection in XPS (left; Ref. XPS Handbook from Danchip); and the chemical structure of MPLA* (right; (100))

In addition, in this experiment, only about 0.10 mg of MPLA incorporated into chitosan solution was spray coated on one sample. 0.10 mg of MPLA contains only 0.00176 mg of phosphorous molecule, which is equivalent to $5.68*10^{-8}$ mol of phosphorous. This tiny amount of phosphorous would be less than the required concentration needed for XPS detection technique. Therefore, the due to limit of detection the phosphorous and thus the MPLA adjuvant could not be detected in XPS.

6. CONCLUSION AND FUTURE IMPLICATIONS

This chapter concludes the thesis with some conclusive remarks. Moreover, some future perspectives of this study are discussed.

6.1 Conclusion

The thesis project exclusively focuses on the development of pH sensitive and adjuvant based polymeric lids of MCs for targeted delivery of oral vaccines via a mucosal route. The objectives of the study have been successfully achieved by establishing polymeric pH-sensitive and adjuvant-based double-lids that can remain intact in the gastric environment and then release vaccine formulation at targeted site in the small intestine.

In this study, the adjuvant MPLA has been incorporated with chitosan for forming the double-layered lids which is a novel achievement of this thesis project. Furthermore, all the necessary steps to form these double-lids have been optimized in the study. The production of the model drug ASSF was optimized to obtain a yield of 73.4% with increased repeatability. By incorporating different plasticizers and optimizing the spray coating parameters, the formation of both the inner and outer lid has been optimized. The average thickness of the inner lid (chitosan-MPLA) and outer lid (Eudragit-DBS) was 6.2 +/- 0.3 µm and 31.4 +/- 2.8 µm, respectively. The lid morphology study in SEM proves effective formation of the lids over the drug-loaded MCs. Finally, the repetitive drug release experiments in different pH media validate the effectiveness of the lids to remain intact at gastric medium and then to dissolve followed by releasing the drug at intestinal medium.

The study thus, provides a detailed analysis of the necessary variables and parameters along with the methods to effectively form a double-layered lid on the drug-loaded MCs. The comparison between the drug release percentage from the MCs with MPLA incorporated double lids and the double lids free of MPLA shows no statistically significant difference. This shows that the presence of MPLA does not affect the lid development as well as the drug release. This means that the MPLA can be used in the inner lid to trigger the immune response in living cells without compromising the pH-sensitivity of the double-lids. Moreover, the statistical analysis comparing the drug re-

lease from single-coated MCs and double-coated MCs demonstrate much slower and more controlled release while using the double-layered lids. This further proves the effectiveness of the double-layered lids for a controlled drug release.

6.2 Future Perspectives

In this study, MPLA has been incorporated with chitosan for triggering the immune response at the drug release site. However, as this is an *in vitro* study, the triggering of immune response could not be verified. Thus, this needs to be verified in future by *in vivo* and animal studies.

XPS analysis was performed to verify different components in the lids. Nevertheless, the presence of MPLA could not be detected using this technique because of the limit of detection of the XPS instrument. Therefore, alternative detection methods such as liquid chromatography-mass spectrometry (LC-MS) could be used instead to detect MPLA.

In this study, a silicon chip accommodating 625 MCs has been used as a single sample while performing the drug release tests. As in the animal studies, instead of a silicon chip full of MCs, individual MC extracted from the chip is needed to feed the animals, it would be interesting to study the drug release from a single MC with the double-lids for replicating the actual scenario.

In addition, the thickness of the double-lids could be optimized in future studies, so that for the animal studies, the extraction of each MC from the silicon chip becomes easier and convenient ensuring the lids remain intact. The thickness optimization study, therefore, should focus on two aspects- 1) the ease of microcontainer extraction and 2) the stability of the lids in release media. This study has further potentials to investigate the double-lids' sealing using other clinically significant biocompatible polymers, along with incorporating antigens, such as ovalbumin, in a particulate system as for example the cubosomes. Therefore, the next step of this study could be the cell studies (e.g. m-cells) and then the animal studies using the double-lids for different vaccine formulations.

REFERENCES

1. Aguila A, Donachie AM, Peyre M, McSharry CP, Sesardic D, Mowat AM. Induction of protective and mucosal immunity against diphtheria by a immune stimulating complex (ISCOMS) based vaccine. Vaccine. 2006; 24(24): 5201–5210.

2. NPS: Medecinewise. What is vaccination? [Internet]; [cited 2017 Mar 1]. Available from: http://www.nps.org.au/medicines/immune-system/vaccines-and-immunisation/for-individuals/what-is-vaccination

3. CDC. A CDC Framework For Preventing Infectious Diseases. 2011; [cited 2017 Mar 1]. Available from: https://www.cdc.gov/oid/docs/ID-Framework.pdf

4. MODULE 2 – Components of a vaccine - WHO Vaccine Safety Basics [Internet]; [cited 2017 Mar 1]. Available from: http://vaccine-safety-training.org/vaccine-components.html

5. Plotkin SA, editor. Mass Vaccination: Global Aspects — Progress and Obstacles [Internet]. In: Current Topics in Microbiology and Immunology; vol. 304. Berlin, Heidelberg: Springer; 2006 [cited 2017 Mar 1]. Available from: http://link.springer.com/10.1007/3-540-36583-4

6. Foged C, Rades T, Perrie Y, Hook S, editors. Subunit Vaccine Delivery [Internet]. In: Advances in Delivery Science and Technology. New York: Springer; 2015 [cited 2017 Mar 1]. Available from: http://link.springer.com/10.1007/978-1-4939-1417-3

7. Ensign LM, Cone R, Hanes J. Oral drug delivery with polymeric nanoparticles: The gastrointestinal mucus barriers. Adv Drug Deliv Rev. 2012; 64(6):557–70.

8. Giersing BK, Modjarrad K, Kaslow DC, Okwo-Bele J-M, Moorthy VS. The 2016 Vaccine Development Pipeline: A special issue from the World Health Organization Product Development for Vaccine Advisory Committee (PDVAC). Vaccine. 2016; 34(26):2863–4.

9. Nielsen L, Singh R, Sylvest S. Microcontainers -an oral drug delivery system for poorly soluble drugs. 2015 [cited 2017 Mar 1]. Available from: https://worldwidescience.org/topicpages/p/poorly+soluble+drug.html

10. Sant S, Tao SL, Fisher OZ, Xu Q, Peppas NA, Khademhosseini A. Microfabrication technologies for oral drug delivery. Adv Drug Deliv Rev. 2012; 64(6):496–507.

11. Chirra HD, Desai TA. Emerging microtechnologies for the development of oral drug delivery devices. Adv Drug Deliv Rev. 2012; 64(14):1569–78.

12. Ahmed A, Bonner C, Desai TA. Bioadhesive microdevices with multiple reservoirs: a new platform for oral drug delivery. J Control Release. 2002; 81(3):291–306.

13. IDUN Drug - IDUN [Internet]; 2016 [cited 2017 Mar 2]. Available from: http://www.idun.dtu.dk/Research/Drug

14. Gebril A, Alsaadi M, Acevedo R, Mullen AB, Ferro VA. Optimizing efficacy of mucosal vaccines. Expert Rev Vaccines. 2012; 11(9):1139–55.

15. Marasini N, Skwarczynski M, Toth I. Oral delivery of nanoparticle-based vaccines. Expert Rev Vaccines. 2014; 13(11):1361–76.

16. Baldridge JR, Yorgensen Y, Ward JR, Ulrich JT. Monophosphoryl lipid A enhances mucosal and systemic immunity to vaccine antigens following intranasal administration. Vaccine. 2000; 18(22):2416–25.

17. Alberts B, Johnson A, Lewis J, Raff M, Roberts K, Walter P. The Adaptive Immune System. In: Molecular Biology of the Cell [Internet]. 4th ed. New York: Garland Science; 2002 [cited 2017 Mar 1]. Available from: https://www.ncbi.nlm.nih.gov/books/NBK21070/

18. Azizi A, Kumar A, Diaz-Mitoma F, and Mestecky J. Enhancing Oral Vaccine Potency by Targeting Intestinal M Cells. PLoS Pathogens. 2010; 6(11), e1001147.

19. Abbas AK, Lichtman AH, Pillai S. Cellular and molecular immunology. 7th ed. United States: Saunders; 2012 [cited 2017 Mar 1]. Available from: https://evolve.elsevier.com/cs/product/9781437715286?role

20. Wang S, Liu H, Zhang X, Qian F. Intranasal and oral vaccination with protein-based antigens: advantages, challenges and formulation strategies. Protein Cell. 2015; 6(7):480–503.

21. Petrovsky N, Aguilar JC. Vaccine adjuvants: Current state and future trends. J Immunol Cell Biol. 2004; 82(5):488–96.

22. Rajput ZI, Hu S, Xiao C, Arijo AG. Adjuvant effects of saponins on animal immune responses. J Zhejiang Univ Sci B. 2007; 8(3):153–61.

23. Sarti F, Perera G, Hintzen F, Kotti K, Karageorgiou V, Kammona O, et al. In vivo evidence of oral vaccination with PLGA nanoparticles containing the immunostimulant monophosphoryl lipid A. Biomaterials. 2011; 32(16):4052–7.

24. Lipid Products | MPLA (PHAD®) | 699800 [Internet]; 2017 [cited 2017 Mar 2]. Available from: https://avantilipids.com/product/699800/

25. MPLA | Sterile Monophosphoryl lipid A for Vaccine Research [Internet]; 2016 [cited 2017 Mar 2]. Available from: http://www.invivogen.com/mpla-vaccigrade

26. Kundi M. New hepatitis B vaccine formulated with an improved adjuvant system. Expert Rev Vaccines. 2007; 6(2):133–40.

27. Elamanchili P, Diwan M, Cao M, Samuel J. Characterization of poly(d,l-lactic-co-glycolic acid) based nanoparticulate system for enhanced delivery of antigens to dendritic cells. Vaccine. 2004; 22(19):2406–12.

28. Cluff CW. Monophosphoryl Lipid A (MPL) as an Adjuvant for Anti-Cancer Vaccines: Clinical Results. In: Advances in experimental medicine and biology [Internet]. 2009 [cited 2017 Mar 2]; p. 111–23. Available from: http://www.ncbi.nlm.nih.gov/pubmed/20665204

29. Ainslie KM, Lowe RD, Beaudette TT, Petty L, Bachelder EM, Desai TA. Microfabricated Devices for Enhanced Bioadhesive Drug Delivery: Attachment to and Small-Molecule Release Through a Cell Monolayer Under Flow. Small. 2009; 5(24):2857–63.

30. Nagstrup J, Keller SS, Müllertz A, Boisen A. Micro Containers With Solid Polymer Drug Matrix For Oral Drug Delivery. In: 16th International Conference on Miniaturized Systems for Chemistry and Life Sciences; 2012 [cited 2017 Mar 2]; Okinawa, Japan. Available from: http://www.rsc.org/images/loc/2012/pdf/M.2.34.pdf

31. Margaroni M, Agallou M, Kontonikola K, Karidi K, Kammona O, Kiparissides C, et al. PLGA nanoparticles modified with a TNFα mimicking peptide, soluble Leishmania antigens and MPLA induce T cell priming in vitro via dendritic cell functional differentiation. Eur J Pharm Biopharm. 2016; 105:18–31.

32. Fichter M, Dedters M, Pietrzak-Nguyen A, Pretsch L, Meyer CU, Strand S, et al. Monophosphoryl lipid A coating of hydroxyethyl starch nanocapsules drastically

increases uptake and maturation by dendritic cells while minimizing the adjuvant dosage. Vaccine. 2015; 33(7):838–46.

33. Pietrzak-Nguyen A, Fichter M, Dedters M, Pretsch L, Gregory SH, Meyer C, et al. Enhanced in Vivo Targeting of Murine Nonparenchymal Liver Cells with Monophosphoryl Lipid A Functionalized Microcapsules. Biomacromolecules. 2014; 15(7):2378–88.

34. Martin FJ, Grove C. Microfabricated Drug Delivery Systems: Concepts to Improve Clinical Benefit. Biomed Microdevices. 2001; 3(2):97–108.

35. Nielsen LH, Melero A, Keller SS, Jacobsen J, Garrigues T, Rades T, et al. Polymeric microcontainers improve oral bioavailability of furosemide. Int J Pharm. 2016; 504(1–2):98–109.

36. Ainslie KM, Lowe RD, Beaudette TT, Petty L, Bachelder EM, Desai TA. Microfabricated devices for enhanced bioadhesive drug delivery: Attachment to and small-molecule release through a cell monolayer under flow. University of North Carolina at Chapel Hill. Small. 2009; 5 (24): 2857-63.

37. Furosemide. United States: Drugs.com; 2017 [cited 2017 Feb 26]. Available from: https://www.drugs.com/furosemide.html

38. Gordon S, Naelapää K, Rantanen J, Selen A, Müllertz A, Østergaard J. Real-time dissolution behavior of furosemide in biorelevant media as determined by UV imaging. Pharm Dev Technol. 2013; 18(6):1407–16.

39. Granero G., Longhi MR, Mora MJ, Junginger HE, Midha KK, Shah VP, et al. Biowaiver Monographs for Immediate Release Solid Oral Dosage Forms: Furosemide. J Pharm Sci. 2010; 99(6):2544–56.

40. Compounds Summary: Furosemide. United States: PubChem; 2017 [cited 2017 Feb 26]. Available from: https://pubchem.ncbi.nlm.nih.gov/compound/furosemide

41. Nielsen LH, Gordon S, Holm R, Selen A, Rades T, Müllertz A. Preparation of an amorphous sodium furosemide salt improves solubility and dissolution rate and leads to a faster Tmax after oral dosing to rats. Eur J Pharm Biopharm. 2013; 85(3):942–51.

42. Nielsen LH, Gordon S, Pajander JP, Østergaard J, Rades T, Müllertz A. Biorelevant characterisation of amorphous furosemide salt exhibits conversion to a furosemide hydrate during dissolution. Int J Pharm. 2013; 457(1):14–24.

43. Nielsen LH, Rades T, Müllertz A. Stabilisation of amorphous furosemide increases the oral drug bioavailability in rats. Int J Pharm. 2015; 490(1–2):334–40.

44. Nielsen LH, Nagstrup J, Gordon S, Keller SS, Østergaard J, Rades T, et al. pH-triggered drug release from biodegradable microwells for oral drug delivery. Biomed Microdevices. 2015; 17(3):55.

45. Why EUDRAGIT ® for oral solid dosage forms? Germany: Evonik; 2017 [cited 2017 Feb 26]; 1–2. Available from: http://healthcare.evonik.com/product/healthcare/en/products/pharmaceuticalexcipients/EUDRAGIT/Pages/default.aspx

46. Eudragit: Setting benchmarks in oral solid dosage forms since 1954. Germany: Evonik; 2017 [cited 2017 Feb 26]. Available from: http://healthcare.evonik.com/sites/lists/NC/DocumentsHC/Evonik-Eudragit_brochure.pdf

47. Kadian SS, Harikumar SL. Eudragit and its Pharmaceutical Significance. India: Researchgate.net; 2009 [cited 2017 Feb 26]. Available from: https://www.researchgate.net/publication/228097715_Eudragit_and_its_Pharmaceutical_Significance

48. Nikam VK, Kotade KB, Gaware VM, Dolas RT. Newsletter Eudragit A Versatile Polymer : A Review. Pharmacol online. 2011; 164:152–64.

49. Eudragit ® l 100-55. Germany: Evonik; 2015 [cited 2017 Feb 26]; 1–6. Available from: https://www.higuchi-inc.co.jp/pharma/excipient/eudragit/pdf/detail_eudragitL100-55.pdf

50. Arakh A. Plasticizer. United States: Slideshare.net; 2013[cited 2017 Feb 26]. Available from: https://www.slideshare.net/AMARARAKH?utm_campaign=profiletracking&utm_medium=sssite&utm_source=ssslideview

51. Definition of plasticizer First Known Use of plasticizer. Massachusetts, United States: Merriam-Webster Inc; 2017 [cited 2017 Feb 26]; 1–11. Available from: https://www.merriam-webster.com/dictionary/plasticizer

52. Laboulfie F, Hémati M, Lamure A, Diguet S. Effect of the plasticizer on permeability, mechanical resistance and thermal behaviour of composite coating films. Powder Technol, 2013. 238: 14-19.

53. Tullo AH. Plasticizer Makers Want A Piece Of The Phthalates Pie. Chem Eng News. 2015; 93(25):16–8.

54. Shomo RE, Baker C, Manura JJ. Note 101 : Identification of Contaminants in Powdered Foods by Direct Extraction Thermal Desorption GC/MS. New Jersey: United States: Scientific Instrument Services Inc; 2016 [cited 2017 Feb 26]; 8–11. Available from: http://www.sisweb.com/referenc/applnote/app-101.htm

55. Emmett SE. The European food intolerance databanks project. In: Trends in Food Science & Technology. 1996; 7(10):313-15.

56. Triethyl 2-acetylcitrate. Germany: Sigma Aldrich; 2016 [cited 2017 Feb 26]; 1–3. Available from: http://www.sigmaaldrich.com/catalog/product/aldrich/388351?lang=en&region=DK 2/

57. Lawson WD. A method of growing single crystals of lead telluride and lead selenide. J Appl Phys. 1951; 22(12):1444–7.

58. Dibutyl Sebacate: Oleris ® Products R. Major applications [Internet]. Arkema; 2017 [cited 2017 Feb 26]; 2–4. Available from: http://www.arkema.com/en/products/productfinder/productviewer/OlerisDibutylSebacate/

59. Chemistry RS of Dibutyl sebacate [Internet]. Germany: Sigma Aldrich; 2015 [cited 2017 Feb 26]; 98–101. Available from: http://www.sigmaaldrich.com/catalog/product/aldrich/d49504?lang=en&region=DK

60. Dibutyl Sebacate [Internet]. Latvia: Biolar; 2012 [cited 2017 Feb 26]; 158-59. Available from: http://www.biolar.lv/en/products/plasticizers/dibutyl-sebacate-dbs.html

61. Zhang G, Feng C, Jiang W, Hu P, Deng P, Zhang Y, et al. [The mechanical properties and moisture permeability of eudragit L100/S100 free films affected by plasticizers and membrane materials ratio] [Internet]. Yao Xue Xue Bao (Acta pharmaceutica sinica J). 2011; 46(9):1144–9.

62. Lin SY, Chen KS, Run-Chu L. Organic esters of plasticizers affecting the water absorption, adhesive property, glass transition temperature and plasticizer permanence of eudragit acrylic films. J Control Release. 2000; 68(3):343–50.

63. Lecomte F, Siepmann J, Walther M, MacRae RJ, Bodmeier R. Polymer blends

used for the aqueous coating of solid dosage forms: importance of the type of plasticizer. J Control Release. 2004; 99(1):1–13.

64. Frohoff-Hülsmann MA, Schmitz A, Lippold BC. Aqueous ethyl cellulose dispersions containing plasticizers of different water solubility and hydroxypropyl methylcellulose as coating material for diffusion pellets. I. Drug release rates from coated pellets. Int J Pharm. 1999; 177(1):69–82.

65. Fang Y, Wang G, Zhang R, Liu Z, Liu Z, Wu X, et al. Eudragit L/HPMCAS blend enteric-coated lansoprazole pellets: enhanced drug stability and oral bioavailability [Internet]. AAPS PharmSciTech. 2014 [cited 2017 Mar 1]; 15(3):513–21. Available from: http://www.ncbi.nlm.nih.gov/pubmed/24590548

66. Ryan EJ, Daly LM, Mills KH. Immunomodulators and delivery systems for vaccinations by mucosal routes. Trends Biotechnol. 2001; 19:293e304.

67. Rajabalaya R, David SRN, Khanam J, Arunabha N. Studies on effect of plasticizer on invitro release and exvivo permeation from eudragit e100 based chlorpheniramine maleate matrix type transdermal delivery system. J Excipients Food Chem. 2010; 1(2).

68. Kumar MNVR. A review of chitin and chitosan applications. Reactive and Functional Polymers. 2000; 46(1):1-27.

69. Chitosan: Find a Vitamin or Supplement [Internet]. 2016 [cited 2017 Mar 1]; 1–2. Available from: http://www.webmd.com/vitamins-supplements/ingredientmono-625-chitosan.aspx?activeingredientid=625

70. Chitosan – A Technologically Important Biomaterial [Internet]. 1999 [cited 2017 Mar 1]; (4):53201. Available from: https://www.sigmaaldrich.com/content/dam/sigma-aldrich/docs/Aldrich/Technical_Ads/al_ms_ad8_chitosan.pdf

71. Cheung RCF, Ng TB, Wong JH, Chan WY. Chitosan: An Update on Potential Biomedical and Pharmaceutical Applications. Mar Drugs. 2015; 13(8):5156–86.

72. Ray SD. Potential aspects of chitosan as pharmaceutical excipient. Acta Pol Pharm. 2011; 68(5):619–22.

73. Carmona-Ribeiro AM. Cationic Nanostructures for Vaccines. In Duc GHT, editor. Immune Response Activation. Croatia: In Tech; 2014 [cited 2017 Mar 1]. Available from: http://www.intechopen.com/books/immune-response-activation/cationic-nanostructures-for-vaccines

74. Ibrahim F, Abu ONA, Usman J and Kadri NA (Eds.). Cell adhesion and degradation behaviors of acetylated chitosan films. In Int Conf on Biomed Eng, 2006. IFMBE Proceedings 2007; 15: 94-97.

75. Chen P-H, Hwang Y-H, Kuo T-Y, Liu F-H, Lai J-Y, Hsieh H-J. Improvement in the Properties of Chitosan Membranes Using Natural Organic Acid Solutions as Solvents for Chitosan Dissolution. J Med Biol Eng, 2007; 27(1): 23-28.

76. Patel RP, Patel MP, Suthar AM. Spray drying technology: an overview. Indian J Sci Technol, 2009; 2(10): 44-47.

77. Sosnik A, Seremeta KP. Advantages and challenges of the spray-drying technology for the production of pure drug particles and drug-loaded polymeric carriers. Adv Colloid Interface Sci. 2015; 223:40–54.

78. Chavarri M, Maranon I, Carmen M. Encapsulation Technology to Protect Probiotic Bacteria. In: Probiotics [Internet]. InTech; 2012 [cited 2017 Mar 1]. Available from: http://www.intechopen.com/books/probiotics/encapsulation-technology-to-protect-probiotic-bacteria

79. In Vitro Technologies: Products [Internet]; 2017 [cited 2017 Mar 1]. Available from: https://industrialscience.invitro.com.au/products/s/BU44699/Buchi-B290-Mini-spray-dryer/

80. Abid Z, Gundlach C, Durucan O, Laier CVH, Nielsen LH, Boisen A, et al. Powder embossing method for selective loading of polymeric microcontainers with drug formulation. Microelectron Eng. 2017; 171:20–4.

81. McGrath MG, Vrdoljak A, O'Mahony C, Oliveira JC, Moore AC, Crean AM. Determination of parameters for successful spray coating of silicon microneedle arrays. Int J Pharm. 2011; 415(1):140–9.

82. Haj-Ahmad R, Khan H, Arshad M, Rasekh M, Hussain A, Walsh S, et al. Microneedle Coating Techniques for Transdermal Drug Delivery. J Pharmaceutics. 2015; 7(4):486–502.

83. Eslamian M. A Mathematical Model for the Design and Fabrication of Polymer Solar Cells by Spray Coating. Int J Dry Technol. 2013; 31(4):405–13.

84. Fagerberg JH, Tsinman O, Sun N, Tsinman K, Avdeef A, Bergström CAS. Dissolution Rate and Apparent Solubility of Poorly Soluble Drugs in Biorelevant Dissolution Media. J Mol Pharm. 2010; 7(5):1419–30.

85. Tsinman K, Avdeef A, Tsinman O, Voloboy D. Powder Dissolution Method for Estimating Rotating Disk Intrinsic Dissolution Rates of Low Solubility Drugs. J Pharm Res. 2009; 26(9):2093–100.

86. Ahnfelt E, Sjögren E, Axén N, Lennernäs H. A miniaturized in vitro release method for investigating drug-release mechanisms. Int J Pharm. 2015; 486(1):339–49.

87. Avdeef A. Solubility of sparingly-soluble ionizable drugs. Adv Drug Deliv Rev. 2007; 59(7):568–90.

88. Paolo M, Boisen A, Keller SS, Müllertz A. Loading of microcontainers for oral drug delivery. Denmark: Technical University of Denmark; 2014. Available from: http://orbit.dtu.dk/files/102863090/PhD_THESIS_28WITH_COVER_29..PDF

89. Hafner B. Scanning Electron Microscopy (SEM) [Online] [Internet]. 2013 [cited 2017 Mar 1]. Available from: http://www.microscopy.ethz.ch/sem.htm

90. Basic Operating Principles - Scanning Electron Microscope User Training. Sci Tech Serv [Internet]. Western Washington University. 2013 [cited 2017 Mar 1]; 106. Available from: http://www.wwu.edu/scitech/sem-competition/SEM_Basic Operating Principles.pdf

91. Wittke J. Signals - Electron microanalysis core facility [Internet]. Northern Arizona University. 2016 [cited 2017 Mar 1]; p. 18–22. Available from: http://nau.edu/cefns/labs/electron-microprobe/glg-510-class-notes/signals/

92. Thermo Scientific XPS: What is XPS [Internet]. 2016 [cited 2017 Mar 1]. Available from: http://xpssimplified.com/whatisxps.php

93. X-Ray Photoelectron Spectroscopy (XPS) Surface Analysis Technique [Internet]. [cited 2017 Mar 1]. Available from: https://www.phi.com/surface-analysis-techniques/xps-esca.html

94. Ultrasonic Spray Systems - Spray Shaping Technology [Internet]. 2017 [cited 2017 Mar 1]. Available from: http://www.sono-tek.com/spray-shaping/

95. Kohl KD, Stengel A, Samuni-Blank M, Dearing MD. Effects of Anatomy and Diet on Gastrointestinal pH in Rodents. J Exp Zool Part A Ecol Genet Physiol. 2013; 319(4):225–9.

96. Snejdrova E, Dittrich M. Pharmaceutical Applications of Plasticized Polymers.

Recent Advances in Plasticizers [Internet]. Czech Republic: InTech; 2012 [cited 2017 Mar 1]. Available from: http://www.intechopen.com/books/recent-advances-in-plasticizers/pharmaceutical-applications-of-plasticized-polymers

97. Vural I, Sarisozen C, Olmez SS. Chitosan coated furosemide liposomes for improved bioavailability. J Biomed Nanotechnol. 2011; 7(3):426–30.

98. Jennings JA, Wells CM, McGraw GS, Velasquez Pulgarin DA, Whitaker MD, Pruitt RL, et al. Chitosan coatings to control release and target tissues for therapeutic delivery. J Ther Deliv. 2015; 6(7):855–71.

99. Smart R, McIntyre S, Bancroft M, Bello I. X-ray Photoelectron Spectroscopy (XPS). City University of Hong Kong. 2009 [cited 2017 Mar 1]; 493–6.

100. Qureshi N, Kaltashov I, Walker K, Doroshenko V, Cotter RJ, Takayama K, et al. Structure of the Monophosphoryl Lipid A Moiety Obtained from the Lipopolysaccharide of *Chlamydia tarchomatis*. J Biol Chem. 1996; 272 (16): 10594-600.

APPENDIX A: Range of furosemide standard solution's concentration chosen to prepare standard curves for the release test in µDiss profiler.

Table A-1: *Standard solutions for phosphate buffer pH 3.5*

STD. NO	Volume of Standard Sol. (µl)	Add Furosemide (µl)	Concentration (mg/ml)
0	0		0
1	10	10	0.01
2	20	10	0.02
3	30	10	0.03
4	40	10	0.04
5	60	20	0.06
6	80	20	0.08
7	100	20	0.1
8	150	50	0.15
9	200	50	0.2

Table A-2: *Standard solutions for phosphate buffer pH 5.0, and pH 6.0*

STD. NO	Volume of Standard Sol. (µl)	Add Furosemide (µl)	Concentration (mg/ml)
0	0		0
1	50	50	0.04975
2	100	50	0.09901
3	200	100	0.1961
4	400	200	0.3846
5	600	200	0.5660
6	800	200	0.7407
7	1000	200	0.9091
8	1500	500	1.3043
9	2000	500	1.6667

APPENDIX B: Some challenges with Powder Embossing method

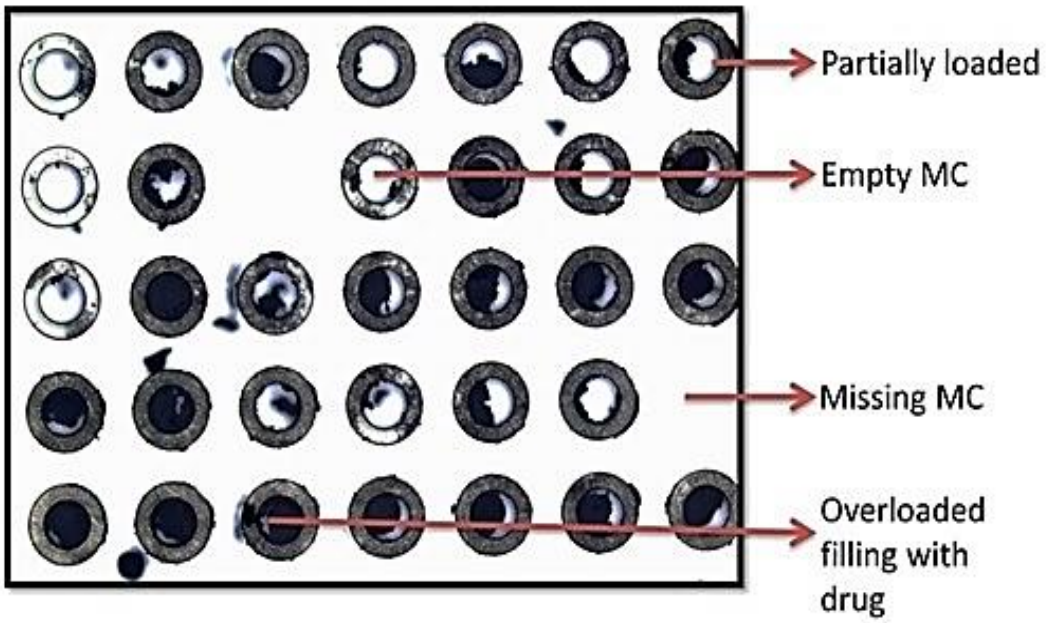

Fig. B 1: *Poorly loaded MCs with ASSF using Powder Embossing method*

Fig. B 2: A. *Wastage of drug (compressed) in powder embossing method and* ***B.*** *Broken sample due to misalignment of shadow mask.*

APPENDIX C: Rugged shadow masks (red circles) due to overuse

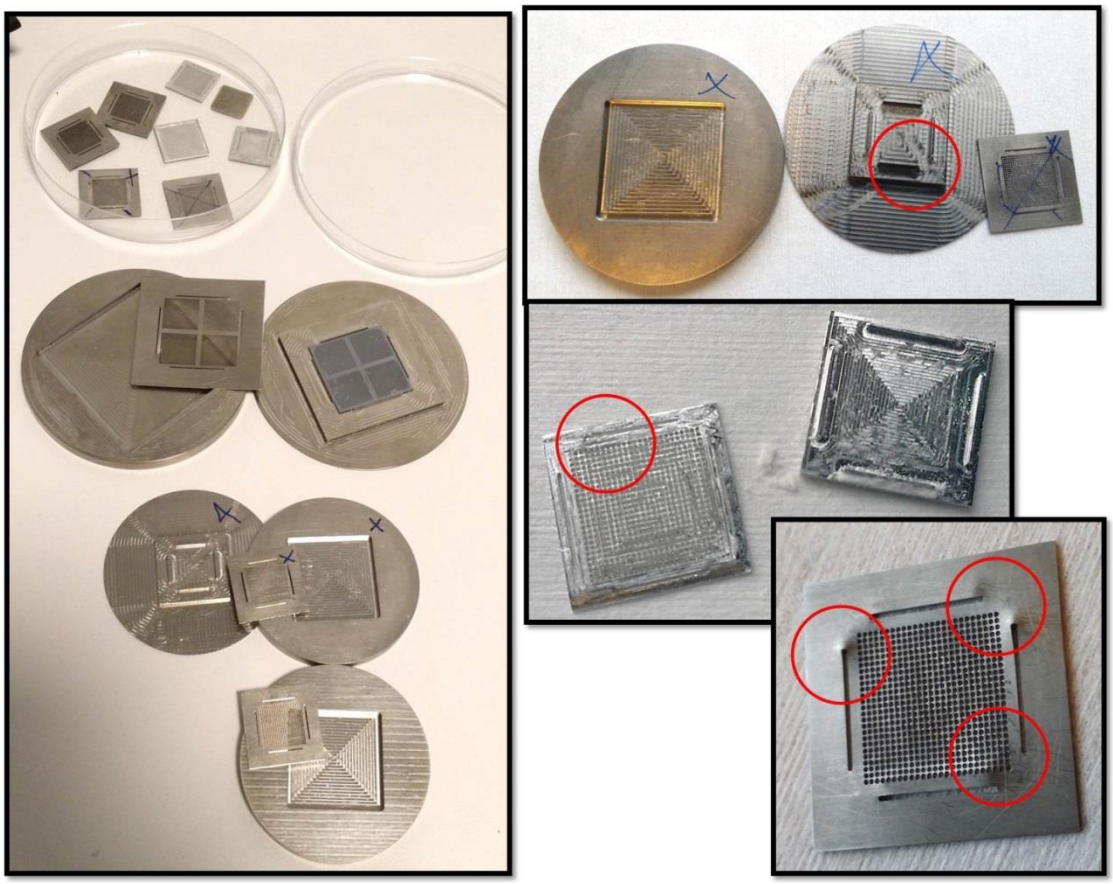

Fig. C: *Different shadow masks (left) and Rugged shadow masks due to being used for a long time in embossing method (right)*

APPENDIX D: Humidity, wet weather and rainy day seem to affect the ASSF, lids and thus the drug release %.

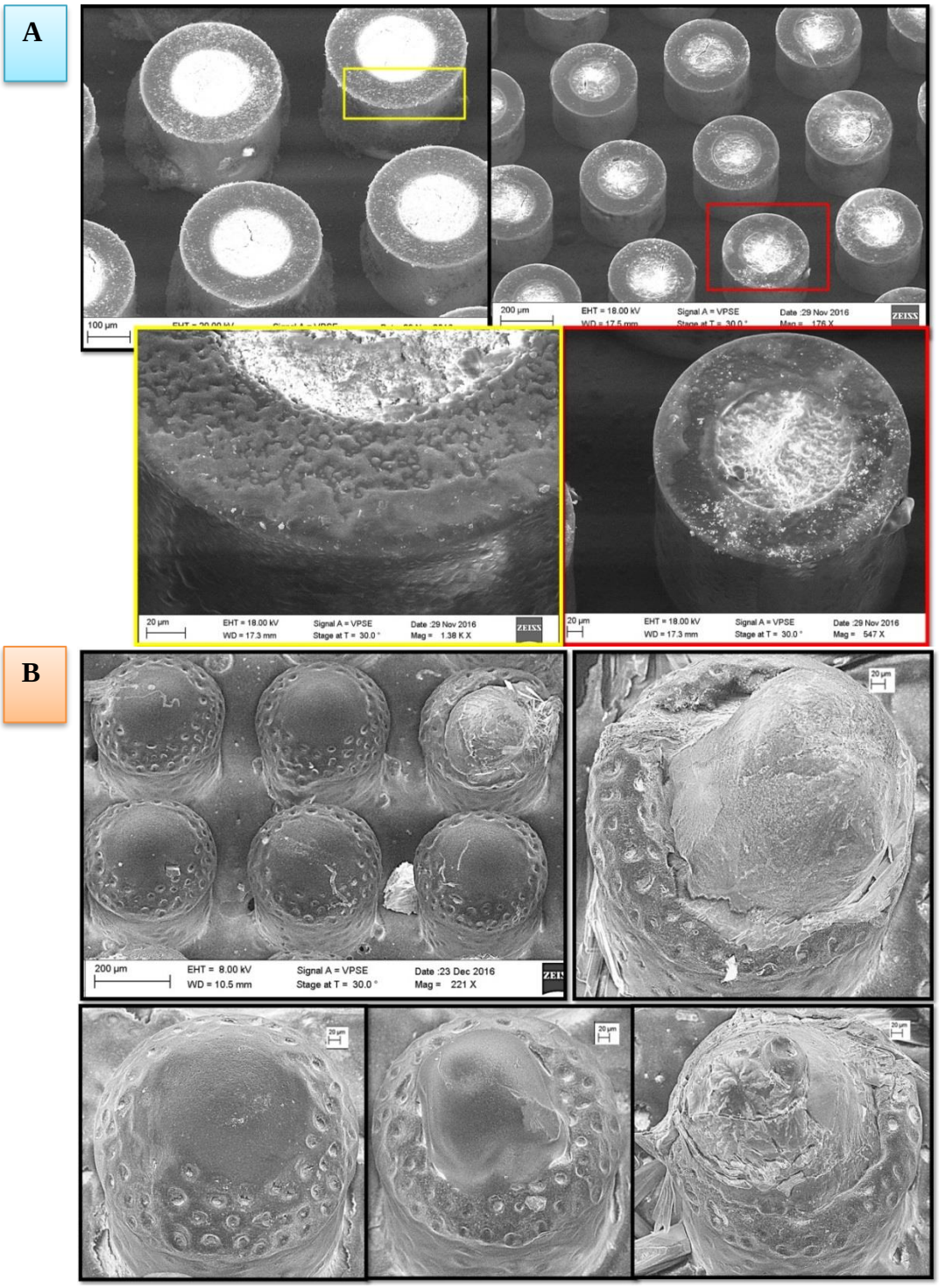

Fig. D: A*. ASSF drug is being hydrated due to humidity and exposure to air* ***B.*** *Swollen of Eudragit L100-55 (with 5% DBS) lid found after 2 hours release test in 100mM phosphate buffer of pH3.5 due to external humid environment*

APPENDIX E: Chitosan lid formation (CNTR=60) affected by technical problem and environmental factors

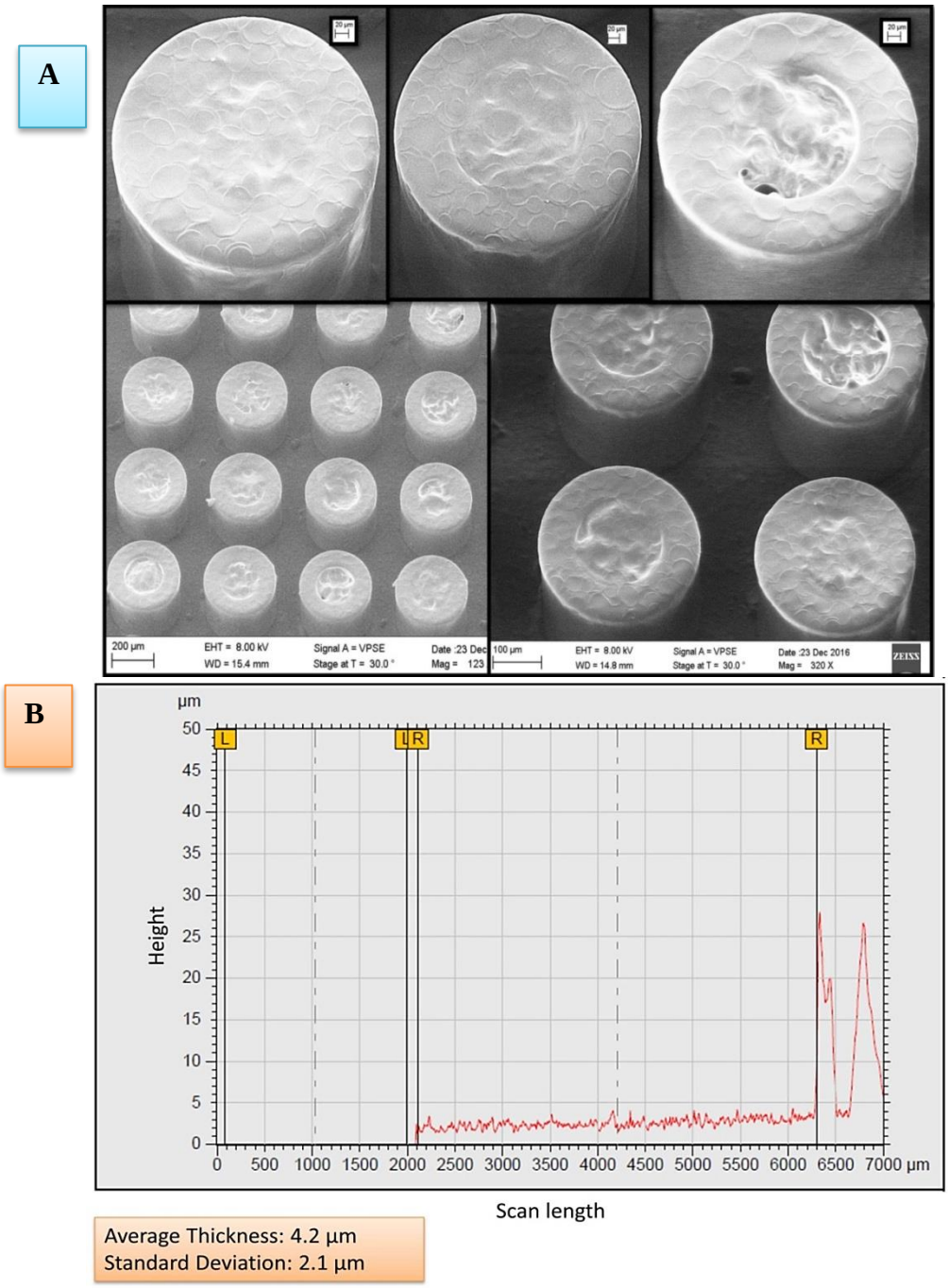

Fig. E 1: A*. Partial clogging of spray coater's nozzle resulted into uneven chitosan lid surface* ***B.*** *It also yields a much thinner Chi lid than usual. This chitosan lid (CNTR=60) is only about 4.2 +/- 2.1 µm thick, as measured by stylus profiler*

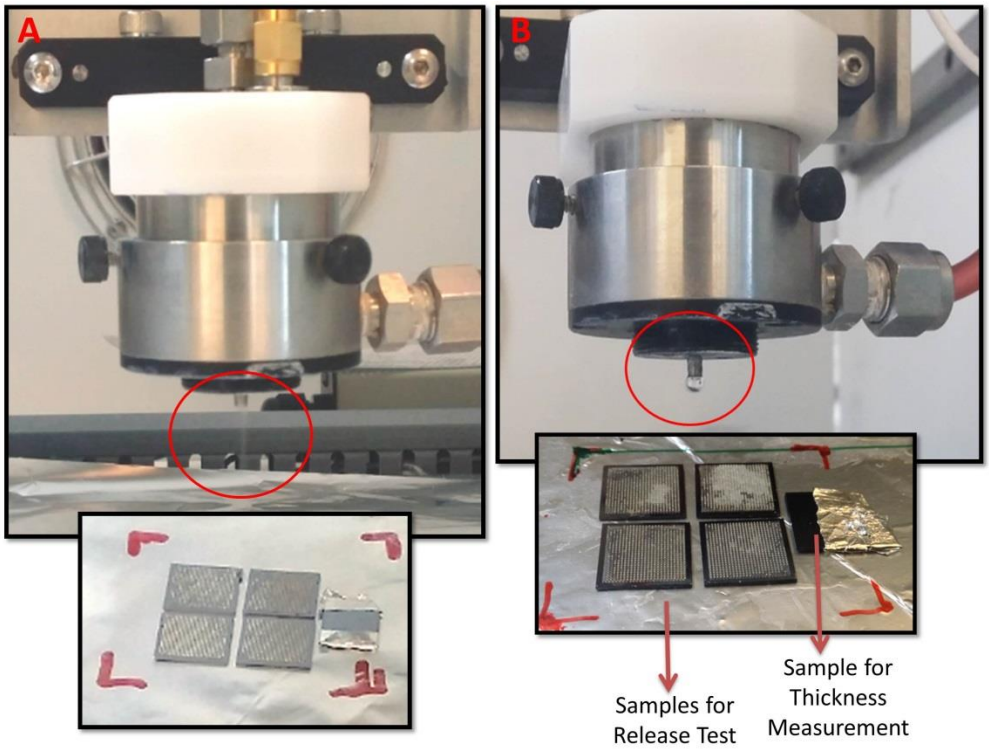

Fig. E 2: A. *The nozzle is properly spraying chitosan solution;* ***B.*** *The nozzle is partially blocked and has stopped spraying, instead drops of solution are pouring off*

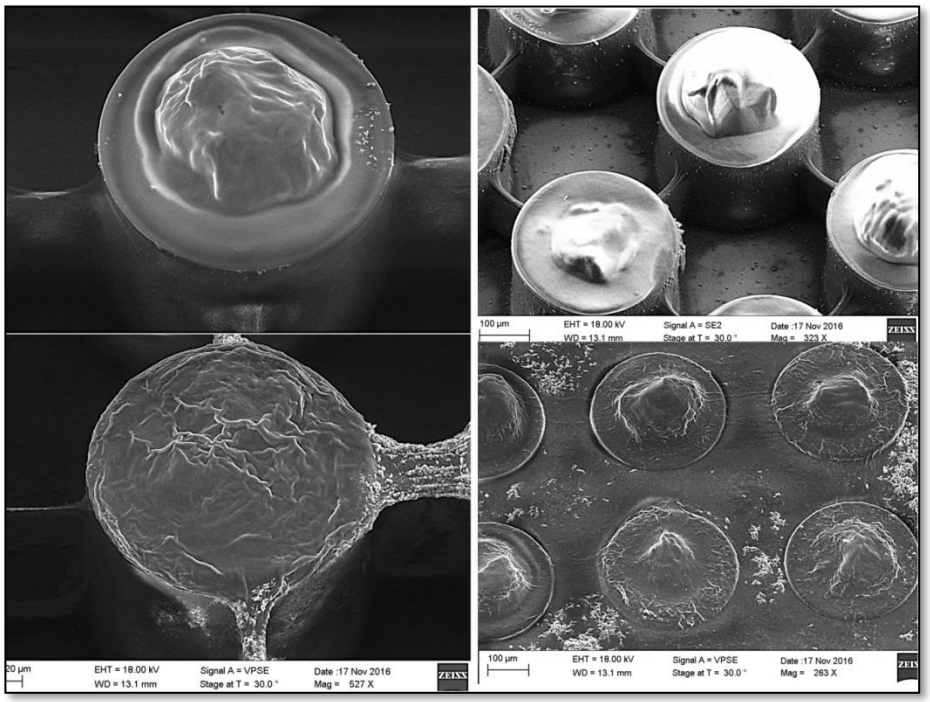

Fig. E 3: *The above Chi-lid was also affected by both humidity (top) and clogging of spray coating nozzle (bottom). The thickness of this lid was only 2.8 +/- 1.2 µm.*

APPENDIX F: SEM images of Chi-EL coated double-lids reveal that the environmental factors such as humidity and air exposure negatively affected the double-lids morphology.

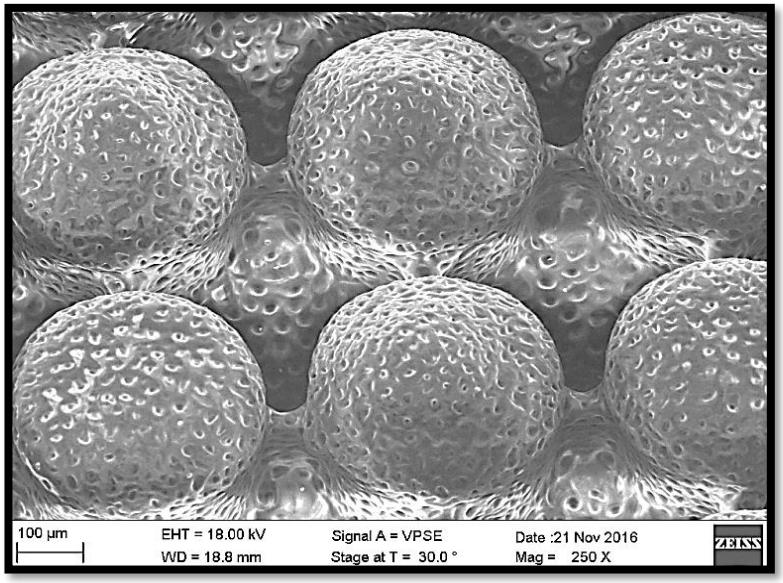

Fig. F 1: *Properly coated Chi-EL double lids on top of ASSF-loaded MCs*

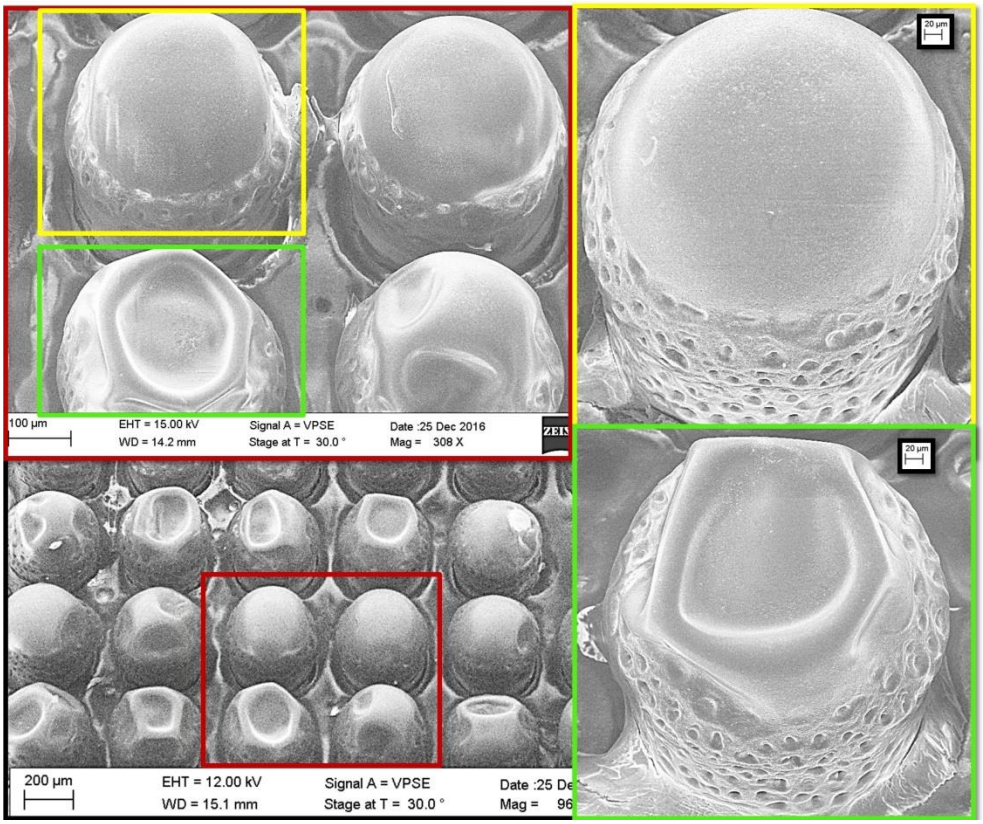

Fig. F 2: *Lid morphology of Chi-EL coated double-lids following the release tests in gastric medium (pH 3.5)*

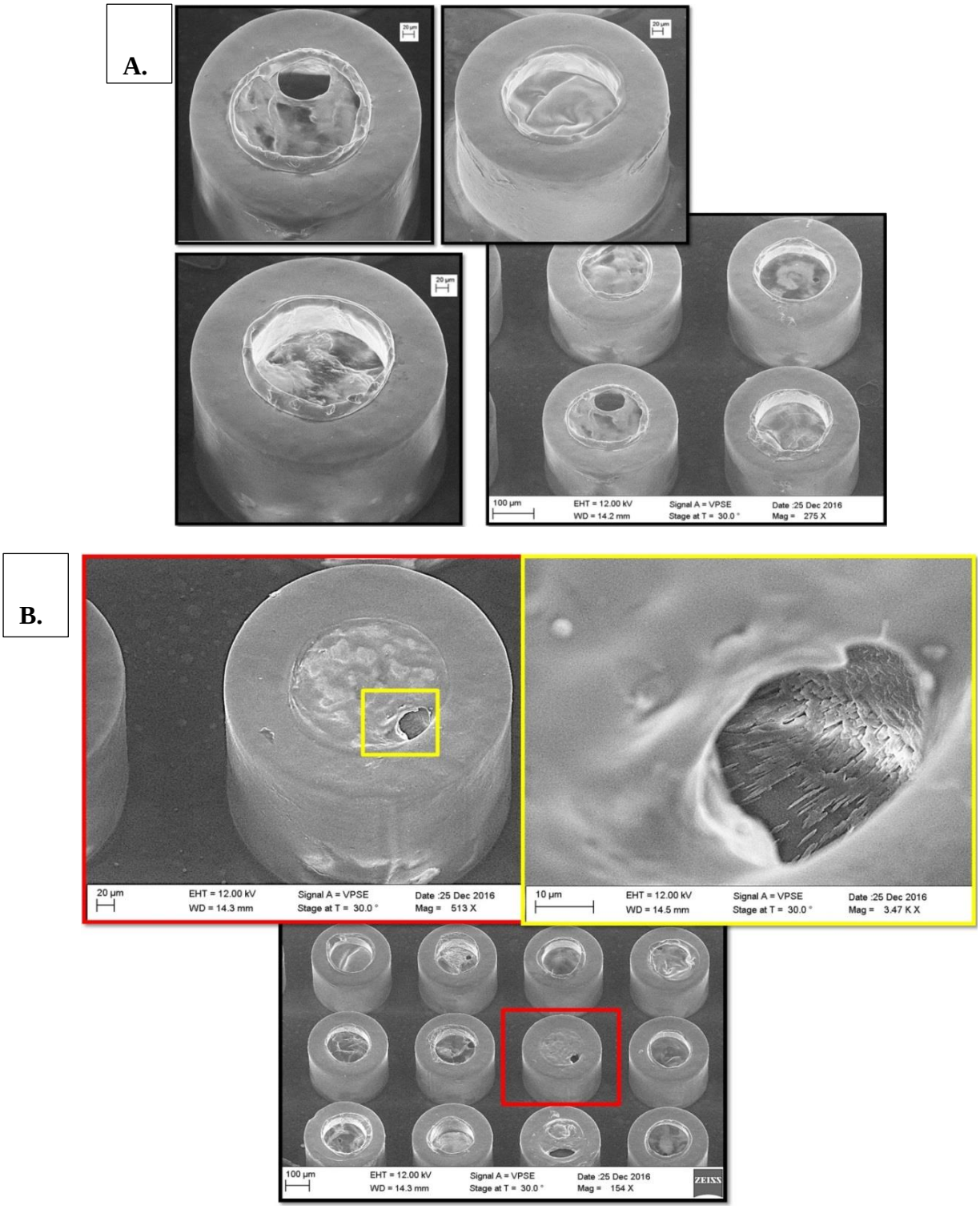

Fig. F 3: A. *Lid morphology of double-coated samples after the release test in pH6.0;* ***B.*** *Crystalline ASSF is found inside the SU8 MCs through the holes on the chitosan lid after the release test in pH6.0. In this experiment, the thickness of the inner lid (Chi-lid) was unexpectedly low due to external factors and therefore, unlike other experiments with double-lids samples, more holes in chitosan lid are seen in the above image.*

APPENDIX G: Biased release curve during a release test study due to broken sample during the ongoing release experiment

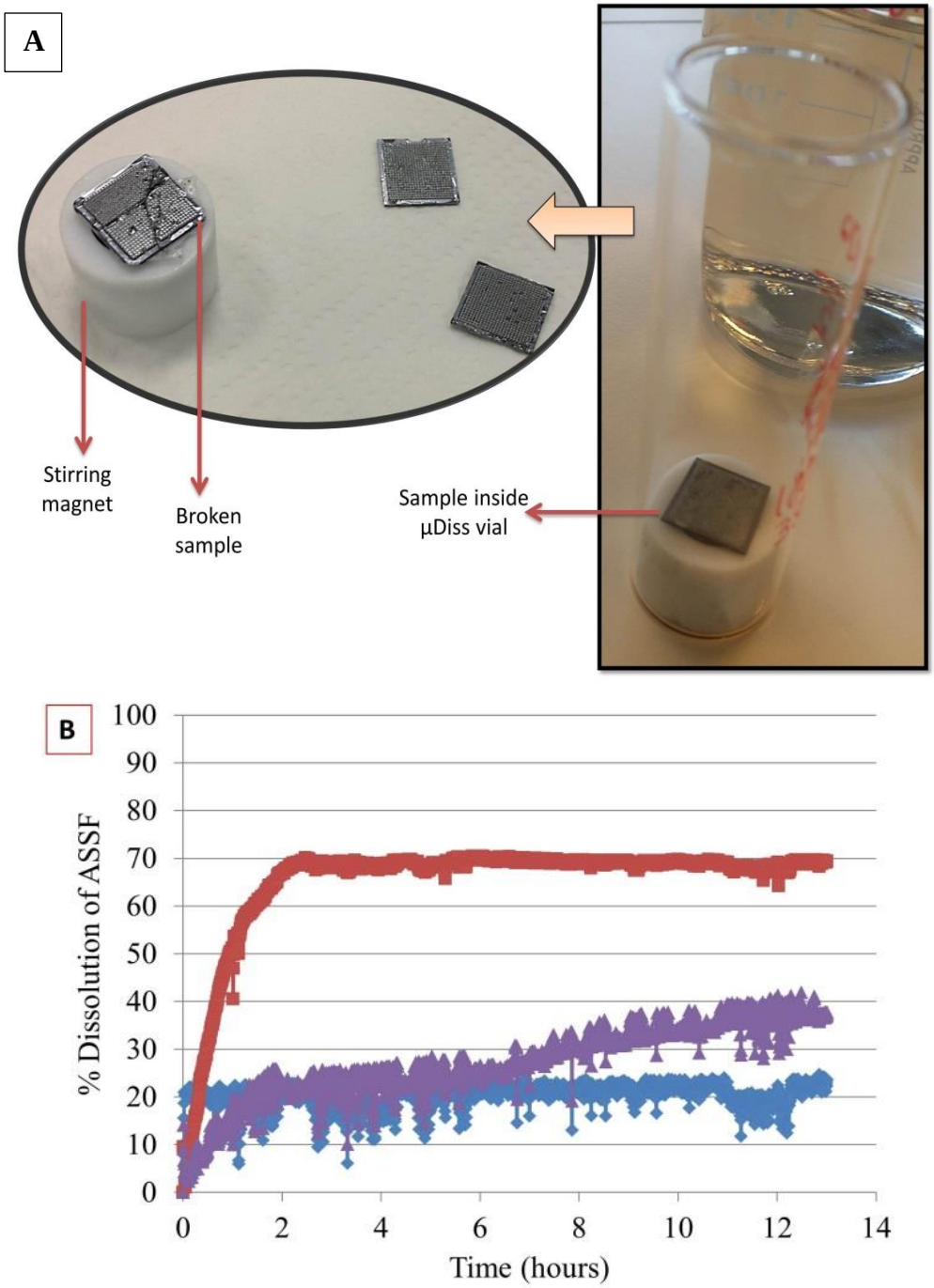

Fig. G: A. *Broken drug-loaded and lid-coated sample in a µDiss vial during release experiment* ***B.*** *Broken sample resulting into unusual high drug release (red curve) compared to the intact samples (in pH 3.5 medium during a trial experiment).*